Physics – Uspekhi **50** (6) 563 – 593 (2007)

REVIEWS OF TOPICAL PROBLEMS PACS numbers: **71.27.+a**, 74.20.Fg, 74.25.Jb

Universal behavior of strongly correlated Fermi systems

V R Shaginyan, M Ya Amusia, K G Popov

DOI: 10.1070/PU2007v050n06ABEH006288

Contents

Abstract. This review discusses the construction of a theory and the analysis of phenomena occurring in strongly correlated Fermi systems such as high-T_c superconductors, heavy-fermion metals, and quasi-two-dimensional Fermi systems. It is shown that the basic properties and the universal behavior of strongly correlated Fermi systems can be described in the framework of the Fermi-condensate quantum phase transition and the well-known Landau paradigm of quasiparticles and the order parameter. The concept of fermion condensation may be fruitful in studying neutron stars, finite Fermi systems, ultracold gases in traps, and quark plasma.

V R Shaginyan Konstantinov Petersburg Nuclear Physics Institute, Russian Academy of Sciences,
Orlova Roshcha, 188300 Gatchina, Leningrad region, Russian Federation
Tel. (7-813) 714 60 96. E-mail: vrshag@thd.pnpi.spb.ru
Racah Institute of Physics, Hebrew University, Jerusalem 91904, Israel
M Ya Amusia Racah Institute of Physics, Hebrew University, Jerusalem 91904, Israel
Tel. (972) 26584348. E-mail: amusia@vms.huji.ac.il
Ioffe Physico-Technical Institute, Russian Academy of Sciences, ul. Politekhnicheskaya 4, 194021 St. Petersburg, Russian Federation
Tel. (7-812) 292 79 40
K G Popov Komi Science Center, Ural Branch of the Russian Academy of Sciences, ul. Chernova 3a, 167982 Syktyvkar, Respublika Komi, Russian Federation
Tel. (7-8212) 21 57 40. E-mail: kpopov@dm.komisc.ru

Received 31 October 2006, revised 9 January 2007
Uspekhi Fizicheskikh Nauk **177** (6) 585 – 618 (2007)
Translated by E Yankovsky; edited by A M Semikhatov

1. Introduction

The Landau theory of the Fermi liquid has a long history and remarkable results in describing a multitude of properties of the electron liquid in ordinary metals and Fermi liquids of the ^{3}He type. The theory is based on the assumption that elementary excitations determine the physics at low temperatures. These excitations behave as quasiparticles, have a certain effective mass, and, judging by their basic properties, belong to the class of quasiparticles of a weakly interacting Fermi gas. Hence, the effective mass M^* is independent of the temperature, pressure, and magnetic field strength and is a parameter of the theory.

A recently discovered new class of strongly correlated Fermi systems, such as metals with heavy fermions, high-T_c superconductors, and quasi-two-dimensional Fermi liquids, exhibit a vast variety of physical properties [1 – 5]. The properties of these materials differ dramatically from those of ordinary Fermi systems. For instance, in the case of metals with heavy fermions, the strong correlation of electrons leads to a renormalization of the effective mass of quasiparticles, which may exceed the ordinary, 'bare,' mass by several orders of magnitude or even become infinitely large. The effective mass strongly depends on the temperature, pressure, or applied magnetic field. Such metals exhibit anomalous behavior and unusual power laws of the temperature dependence of the thermodynamic properties at low temperatures similar to the laws for the Landau anomalous Fermi liquid.

The Landau Fermi-liquid theory fails to explain the results of experimental observations related to the dependence of M^* on the temperature T, magnetic field B, pressure, etc.; this has led to the conclusion that quasiparticles do not survive in strongly correlated Fermi systems and that the heavy electron does not retain its identity as a quasiparticle excitation [6 – 11].

1.1 Quantum phase transitions and the anomalous behavior of correlated Fermi systems

The unusual properties and anomalous behavior observed in high-T_c superconductors and metals with heavy fermions are assumed to be determined by various magnetic quantum phase transitions [3]. Since a quantum phase transition occurs at the temperature $T = 0$, the control parameters are the composition, the electron (hole) number density x, the pressure, the magnetic field strength B, etc. A quantum phase transition occurs at a quantum critical point, which separates the ordered phase that emerges as the result of the quantum phase transition from the disordered phase. It is usually assumed that magnetic (e.g., ferromagnetic and antiferromagnetic) quantum phase transitions are responsible for the anomalous behavior. The critical point of such a phase transition can be shifted to absolute zero by varying the above parameters.

Universal behavior can be expected only if the system under consideration is very close to a quantum critical point, e.g., when the correlation length is much longer than the microscopic length scale, and critical quantum and thermal fluctuations determine the anomalous contribution to the thermodynamic functions of the metal. Quantum phase transitions of this type are so widespread [2 – 4] that we call them ordinary quantum phase transitions. In this case, the physics of the phenomenon is determined by thermal and quantum fluctuations of the critical state, while quasiparticle excitations are destroyed by these fluctuations.

The absence of quasiparticle excitations is considered the main reason for the anomalous behavior of heavy-fermion metals and high-T_c superconductors [2 – 4]. This approach faces certain difficulties, however. Critical behavior in experiments with metals containing heavy fermions is observed at high temperatures comparable to the effective Fermi temperature T_k. For instance, the thermal expansion coefficient $\alpha(T)$, which is a linear function of temperature for the normal Landau Fermi liquid (LFL), $\alpha(T) \propto T$, demonstrates the temperature dependence $\alpha \propto \sqrt{T}$ in measurements involving $CeNi_2Ge_2$ as the temperature varies by two orders of magnitude (as it decreases from 6 K to at least 50 mK) [12]. Such behavior can hardly be explained in the framework of the critical point fluctuation theory. Obviously, such a situation is possible only as $T \to 0$, when the critical fluctuations make the leading contribution to the entropy and when the correlation length is much longer than the microscopic length scale. At a certain temperature $T \ll T_k$, this macroscopically large correlation length must be destroyed by ordinary thermal fluctuations and the corresponding universal behavior must disappear.

Another difficulty is in explaining the restoration of the Landau Fermi-liquid behavior under a magnetic field B, as observed in metals with heavy fermions and in high-temperature superconductivity [1, 13, 14]. For the Landau Fermi liquid as $T \to 0$, the electric resistivity $\rho(T) = \rho_0 + AT^2$, the heat capacity $C(T) = \gamma T$, and the magnetic susceptibility $\chi = \text{const}$. It turns out that the coefficient $A(B)$, the Sommerfield coefficient $\gamma(B)$, and the magnetic susceptibility $\chi(B)$ depend on the magnetic field strength B such that $A(B) \propto \gamma^2(B)$ and $A(B) \propto \chi^2(B)$, which implies that the Kadowaki – Woods relation $K = A(B)/\gamma^2(B)$ [15] is B-independent and is preserved [13]. Such universal behavior, quite natural with quasiparticles playing the main role, can hardly be explained in the framework of the approach that presupposes the absence of quasiparticles, which is characteristic of ordinary quantum phase transitions in the vicinity of a quantum critical point.

For instance, the Kadowaki – Woods relation does not agree with the spin density wave scenario [13] and with the results of research in quantum criticality based on the renormalization-group approach [16]. Moreover, measurements of charge and heat transfer have shown that the Wiedemann – Franz law holds in some high-T_c superconductors [14, 17] and heavy-fermion metals [18, 19]. All this suggests that quasiparticles do exist in such metals, and this conclusion is also corroborated by photoemission spectroscopy results [20, 21].

The inability to explain the behavior of heavy-fermion metals while staying within the framework of theories based on ordinary quantum phase transitions implies that another important concept introduced by Landau, the order parameter, also ceases to operate (e.g., see Refs [8 – 11]). Thus, we are left without the most fundamental principles of many-body quantum physics [22], and many interesting phenomena associated with the anomalous behavior of strongly correlated Fermi systems remain unexplained.

1.2 Limits and goals of the review

In this review, we show that diverse systems such as high-T_c superconductors, heavy-fermion metals, and quasi-two-dimensional strongly correlated Fermi liquids exhibit common universal behavior, which can be described within a single approach based on the fermion-condensation theory [23, 24]. However, in view of the lack of space, we do not discuss the specific features of strongly correlated systems in full; instead, we focus on the universal behavior of such systems. For instance, we ignore the physics of Fermi systems such as neutron stars, atomic clusters and nuclei, quark plasma, and ultracold gases in traps, in which a Fermi condensate can exist [25 – 29]. Ultracold gases in traps are interesting because the easy tuning of traps allows selecting the values of the parameters required for observations of the quantum critical point and the fermion condensate.

Experimental studies of the properties of quantum phase transitions and their critical points are very important for

understanding the physical nature of high-T_c superconductivity and heavy-fermion metals. The experimental data that refer to different strongly correlated Fermi systems complement each other. In the case of high-T_c superconductivity, no such experiments have been conducted, because the respective critical points are in the superconductivity range at low temperatures and the physical properties of the respective quantum phase transition are altered by superconductivity. But such experiments can be conducted for heavy-fermion metals. Recent experimental research has provided data on the behavior of heavy-fermion metals, shedding light on the nature of critical points and phase transitions (e.g., see Refs [13, 14, 17–21]). Hence, a key issue is the simultaneous study of high-T_c superconductivity and the anomalous behavior of heavy-fermion metals.

To avoid difficulties associated with the anisotropy generated by the crystal lattice of solids, its special features, defects, etc., we study the universal behavior of electron (hole) high-T_c superconductors, heavy-fermion metals, and quasi-two-dimensional Fermi systems at low temperatures using the model of a homogeneous heavy-electron (fermion) liquid. The model is quite meaningful because we consider the universal behavior exhibited by these materials at low temperatures, a behavior related to power-law divergences of quantities such as the effective mass, the heat capacity, the thermal expansion, etc. These divergences, or the critical exponents that characterize them, are determined by momentum transfers that are small compared to momenta of the order of the reciprocal lattice length, whose contributions have no effect on the dynamics of the systems under investigation, the dynamics related to small momentum transfer, and can therefore be ignored, as is usually done in the fluctuation theory of critical exponents [22]. Similarly, we can ignore the difficulties and specific features associated with a high-T_c superconductor or a heavy-fermion metal.

We analyze the universal properties of strongly correlated Fermi systems using the fermion-condensation theory [23, 24, 30], because the behavior of heavy-fermion metals already suggests that their unusual properties can be associated with the quantum phase transition related to the unlimited increase in the effective mass at the critical point. For instance, the effective-mass divergence has been observed at the quantum critical point induced by a magnetic field [6, 13, 18, 19, 31]. Such a quantum phase transition is a Fermi-condensate quantum phase transition, leading to a Fermi condensate. The main feature of a Fermi-condensate quantum phase transition is the divergence of the effective mass M^* at its quantum critical point [23, 24, 30]. We assume from now on that a heavy-electron liquid exists either near such a transition or already after the critical point.

2. A Fermi liquid with a Fermi condensate

One of the most complex problems of modern condensed-matter physics is the problem of the structure and properties of Fermi systems with large interparticle coupling constants. A theory of the Fermi liquid, later called 'normal,' was first proposed by Landau as a means for solving such problems by introducing the concepts of quasiparticles and amplitudes that characterize the effective quasiparticle interaction [22, 32]. The Landau theory can be regarded as an effective low-energy theory with the high-energy degrees of freedom eliminated by introducing amplitudes that determine the quasiparticle interaction instead of the strong interparticle interaction. The stability of the ground state of the Landau Fermi liquid is determined by the Pomeranchuk stability conditions: stability is violated when at least one Landau amplitude becomes negative and reaches its critical value [22, 33]. We note that the new phase in which stability is restored can also be described, in principle, by the Landau Fermi-liquid theory.

2.1 Landau theory of the Fermi liquid

We begin by recalling the main ideas of the Landau Fermi-liquid theory [22, 32]. The theory is based on the concept of quasiparticles, which are elementary weakly excited states of the Fermi liquid and are therefore specific excitations that determine the low-temperature thermodynamic and transport properties of the Fermi liquid. In the case of the electron liquid, the quasiparticles are characterized by the electron quantum numbers and the effective mass M^*. The ground-state energy of the system is a functional of the quasiparticle occupation numbers (or the quasiparticle distribution function) $n(\mathbf{p}, T)$, and the same is true of the free energy $F\big[n(\mathbf{p}, T)\big]$, the entropy $S\big[n(\mathbf{p}, T)\big]$, and other thermodynamic functions. We can find the distribution function from the minimum condition for the free energy $F = E - TS$:

$$\frac{\delta(F-\mu N)}{\delta n(\mathbf{p}, T)} = \varepsilon(\mathbf{p}, T) - \mu(T) - T \ln \frac{1-n(\mathbf{p}, T)}{n(\mathbf{p}, T)} = 0\,, \quad (2.1)$$

where μ is the chemical potential and

$$\varepsilon(\mathbf{p}, T) = \frac{\delta E\big[n(\mathbf{p}, T)\big]}{\delta n(\mathbf{p}, T)} \quad (2.2)$$

is the quasiparticle energy. This energy is a functional of $n(\mathbf{p}, T)$, in the same way as the energy E is: $E\big[n(\mathbf{p}, T)\big]$. The entropy $S\big[n(\mathbf{p}, T)\big]$ is given by the well-known expression [22, 32]

$$S\big[n(\mathbf{p}, T)\big] = -2\int \big[n(\mathbf{p}, T)\ln\big(n(\mathbf{p}, T)\big) + \big(1-n(\mathbf{p}, T)\big)\ln\big(1-n(\mathbf{p}, T)\big)\big]\,\frac{d\mathbf{p}}{(2\pi)^3}\,, \quad (2.3)$$

which follows from combinatorial reasoning.

Equation (2.1) is usually written in the standard form of the Fermi–Dirac distribution,

$$n(\mathbf{p}, T) = \left[1 + \exp\frac{\varepsilon(\mathbf{p}, T) - \mu}{T}\right]^{-1}. \quad (2.4)$$

As $T \to 0$, Eqns (2.1) and (2.4) have the standard solution $n(p, T \to 0) \to \theta(p_F - p)$, with $\theta(p_F - p)$ the step function and $\varepsilon(p \approx p_F) - \mu = p_F(p - p_F)/M_L^*$, where M_L^* is the effective mass of the Landau quasiparticle,

$$\frac{1}{M_L^*} = \frac{1}{p}\,\frac{d\varepsilon(p, T=0)}{dp}\bigg|_{p=p_F}. \quad (2.5)$$

It is assumed that M_L^* is positive and finite on the Fermi surface. As a result, the temperature-dependent corrections to M_L^*, to the quasiparticle energy $\varepsilon(\mathbf{p})$, and to other quantities begin with the term proportional to T^2. The effective mass is given by the well-known Landau equation

$$\frac{1}{M_L^*} = \frac{1}{M} + \sum_{\sigma_1}\int \frac{\mathbf{p}_F\mathbf{p}_1}{p_F^3}\,F_{\sigma,\sigma_1}(\mathbf{p}_F, \mathbf{p}_1)\,\frac{\partial n_{\sigma_1}(\mathbf{p}_1, T)}{\partial p_1}\,\frac{d\mathbf{p}_1}{(2\pi)^3}\,, \quad (2.6)$$

where $F_{\sigma,\sigma_1}(\mathbf{p}_F, \mathbf{p}_1)$ is the Landau amplitude, which depends on the momenta $\mathbf{p}$ and $\mathbf{p}_F$ and the spins σ, and M is the 'bare' electron mass. For simplicity, we ignore the spin dependence of the effective mass, because M^*_L is almost completely spin-independent in the case of a homogeneous liquid and weak magnetic fields.

Equation (2.6) at $T = 0$, combined with the fact that $n(\mathbf{p}, T = 0)$ becomes $\theta(p_F - p)$, yields the well-known result [34]

$$\frac{M^*_L}{M} = \frac{1}{1 - N_0 F^1(p_F, p_F)/3}\,,$$

where N_0 is the density of states of a free Fermi gas and $F^1(p_F, p_F)$ is the p-wave component of the Landau interaction amplitude. Because $x = p_F^3/3\pi^2$ in the Landau Fermi-liquid theory, the Landau interaction amplitude can be written as $F^1(p_F, p_F) = F^1(x)$. We assume that at a certain critical point x_{FC}, the denominator $(1 - N_0 F^1(p_F, p_F)/3)$ tends to zero, i.e.,

$$\left(1 - \frac{N_0 F^1(x)}{3}\right) \propto (x - x_{FC}) + a(x - x_{FC})^2 + \ldots \to 0\,.$$

As a result, we find that [35, 36]

$$\frac{M^*_L(x)}{M} \approx A + \frac{B}{x - x_{FC}} \propto \frac{1}{r}\,, \tag{2.7}$$

where A and B are constants and $r = (x - x_{FC})/x_{FC}$ is the 'distance' from the quantum critical point x_{FC} at which $M^*_L(x \to x_{FC}) \to \infty$.

The behavior of $M^*_L(x)$ described by formula (2.7) is in good agreement with the results of experiments [37, 38] and calculations [39–41] (see also Section 6). In the case of electron systems, Eqn (2.7) holds for $x > x_{FC}$, when $r > 0$ [24, 42]. Such behavior of the effective mass is observed in heavy-fermion metals, which have a fairly flat and narrow conductivity band corresponding to a large effective mass $M^*_L(x \approx x_{FC})$, with a strong effective correlation and the effective Fermi temperature $T_k \sim p_F^2/M^*_L(x)$ of the order of several dozen degrees kelvin or even lower (e.g., see Ref. [1]).

2.2 The Fermi-condensate quantum phase transition

It was shown recently that the Pomeranchuk stability conditions do not encompass all possible types of instability and that at least one was overlooked [23]. This type of instability corresponds to a situation where the effective mass, the most important characteristic of the Landau quasiparticles, can become infinitely large. As a result, the quasiparticle kinetic energy is infinitely small near the Fermi surface and the function $n(\mathbf{p})$ is determined by the potential energy. This leads to the formation of a new class of strongly correlated Fermi liquids with a Fermi condensate [23, 24, 43], separated from the normal Fermi liquid by a Fermi-condensate quantum phase transition [44, 45].

It follows from Eqn (27) that at $T = 0$ and as $r = (x - x_{FC}) \to 0$, the effective mass diverges, $M^*_L(r) \to \infty$. Beyond the critical point x_{FC}, the distance r becomes negative and, correspondingly, so does the effective mass. To avoid an unstable and physically meaningless state with a negative effective mass, the system must undergo a quantum phase transition at the critical point $x = x_{FC}$, which, as we see shortly, is a Fermi-condensate quantum phase transition [44, 46]. Because the kinetic energy of quasiparticles that are near the Fermi surface is proportional to the inverse effective mass, the potential energy of the quasiparticles near the Fermi surface determines the ground-state energy as $x \to x_{FC}$. Hence, a phase transition reduces the energy of the system and transforms the quasiparticle distribution function; beyond the phase transition point, the quasiparticle distribution is determined, for $x \leqslant x_{FC}$, by the ordinary equation for a minimum of the energy functional [23]:

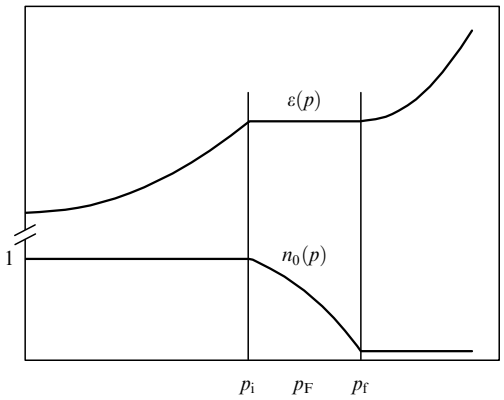

Figure 1. The quasiparticle distribution function $n_0(p)$ and the single-particle spectrum $\varepsilon(p)$. Because $n_0(p)$ is a solution of Eqn (2.8), we have $n_0(p < p_i) = 1$, $0 < n_0(p_i < p < p_f) < 1$, $n_0(p > p_f) = 0$, and $\varepsilon(p_i < p < p_f) = \mu$. The Fermi momentum p_F satisfies the condition $p_i < p_F < p_f$.

$$\frac{\delta E[n(\mathbf{p})]}{\delta n(\mathbf{p}, T = 0)} = \varepsilon(\mathbf{p}) = \mu\,, \qquad p_i \leqslant p \leqslant p_f\,. \tag{2.8}$$

Equation (2.8) yields the quasiparticle distribution function $n_0(\mathbf{p})$ that minimizes the ground-state energy E. This function found from Eqn (2.8) differs from the step function in the interval from p_i to p_f, where $0 < n_0(\mathbf{p}) < 1$, and coincides with the step function outside this interval. Equation (2.8) also suggests that the single-particle spectrum is absolutely 'flat' within this interval. A possible solution $n_0(\mathbf{p})$ of Eqn (2.8) and the corresponding single-particle spectrum $\varepsilon(\mathbf{p})$ are depicted in Fig. 1. Quasiparticles with momenta within the interval (p_i, p_f) have the same single-particle energies equal to the chemical potential μ and form a Fermi condensate, while the distribution $n_0(\mathbf{p})$ describes the new state of the Fermi liquid with a Fermi condensate [23, 24, 43]. In contrast to the Landau, marginal, or Luttinger Fermi liquids, which exhibit the same topological structure of the Green's function, in systems with a Fermi condensate, where the Fermi surface spreads into a strip, the Green's function belongs to a different topological class [28, 29, 43]. The topological class of the Fermi liquid is characterized by the invariant [43]

$$N = \mathrm{tr} \oint_C \frac{\mathrm{d}l}{2\pi i}\, G(\mathrm{i}\omega, \mathbf{p})\, \partial_l G^{-1}(\mathrm{i}\omega, \mathbf{p})\,, \tag{2.9}$$

where 'tr' denotes the trace over the spin indices of the Green's function and the integral is taken along an arbitrary contour C encircling the singularity of the Green's function. The invariant N in (2.9) takes integral values even when the singularity is not of the pole type, cannot vary continuously, and is conserved in a transition from the Landau Fermi liquid to marginal liquids and under small perturbations of

the Green's function. As shown by Volovik [28, 29, 43], the situation is quite different for systems with a Fermi condensate, where the invariant N becomes a half-integer and the system with a Fermi condensate transforms into an entirely new class of Fermi liquids with its own topological structure.

With Fermi-condensate quantum phase transitions (as well as with other phase transitions), we have to deal with strong particle interaction, and there is no way in which a theoretical investigation based on first principles can provide an absolutely reliable solution. Hence, the only way to verify that a Fermi condensate exists is to study this state by exactly solvable models and to examine the experimental facts that could be interpreted as direct confirmation of the existence of a Fermi condensate.

Exactly solvable models unambiguously suggest that Fermi systems with a Fermi condensate exist (e.g., see Refs [47–50]). Taking the results of topological investigations into account, we can state that the new class of Fermi liquids with a Fermi condensate is nonempty, actually exists, and represents an extended family of new states of Fermi systems [28, 29, 43].

We note that the solutions $n_0(\mathbf{p})$ of Eqn (2.8) are new solutions of the well-known equations of the Landau Fermi-liquid theory. Indeed, at $T = 0$, the standard solution given by a step function, $n(\mathbf{p}, T \to 0) \to \theta(p_F - p)$, is not the only possible one. Anomalous solutions $\varepsilon(\mathbf{p}) = \mu$ of Eqn (2.1) can exist if the logarithmic expression on its right-hand side is finite. This is possible if $0 < n_0(\mathbf{p}) < 1$ within a certain interval $p_i \leqslant p \leqslant p_f$. Then, this logarithmic expression remains finite within this interval as $T \to 0$, the product $T \ln\left[\left(1 - n_0(\mathbf{p})\right)/n_0(\mathbf{p})\right]\big|_{T\to 0} \to 0$, and we again arrive at Eqn (2.8).

Thus, as $T \to 0$, the quasiparticle distribution function $n_0(\mathbf{p})$, which is a solution of Eqn (2.8), does not tend to the step function $\theta(p_F - p)$ and, correspondingly, in accordance with Eqn (2.3), the entropy $S_{NFL}(T)$ of this state tends to a finite value S_0 as $T \to 0$:

$$S_{NFL}(T \to 0) \to S_0 \,. \tag{2.10}$$

The question of how the Nernst theorem works in systems with a Fermi condensate is discussed in Section 3.1, and the behavior of the entropy is considered in Section 8.

We assume that as the density decreases (or as the interaction force increases), we reach the point $x \approx x_{FC}$ at which a Fermi condensate is formed. This means that $p_i \to p_f \to p_F$ and that the deviation $\delta n(\mathbf{p}) = n_0(\mathbf{p}) - \theta(p_F - p)$ is small. Expanding the function $E\left[n(\mathbf{p})\right]$ in a Taylor series in $\delta n(\mathbf{p})$ and keeping only the leading terms, we can use Eqn (2.8) to obtain the following relation that is valid within the interval $p_i \leqslant p \leqslant p_f$:

$$\mu = \varepsilon(\mathbf{p}) = \varepsilon_0(\mathbf{p}) + \int F(\mathbf{p}, \mathbf{p}_1)\, \delta n(\mathbf{p}_1)\, \frac{d\mathbf{p}_1}{(2\pi)^2} \,, \tag{2.11}$$

where $F(\mathbf{p}, \mathbf{p}_1) = \delta^2 E/\delta n(\mathbf{p})\delta n(\mathbf{p}_1)$ is the Landau amplitude. Both quantities, the amplitude and the single-particle energy $\varepsilon_0(\mathbf{p})$, are calculated at $n(\mathbf{p}) = \theta(p_F - p)$. Equation (2.11) has nontrivial solutions for densities $x \leqslant x_{FC}$ if the corresponding Landau amplitude, which is density-dependent, is positive and sufficiently large for the potential energy to be higher than the kinetic energy. For instance, such a state is realized in a low-density electron liquid. The transformation of the Fermi step function $n(\mathbf{p}) = \theta(p_F - p)$ into a smooth function determined by Eqn (2.11) then becomes possible [23, 24, 42].

A system with a Fermi condensate can be considered a strongly correlated Fermi liquid at densities $x < x_{FC}$. It follows from Eqn (2.11) that the quasiparticles of a Fermi condensate form a collective state, because their state is determined by the macroscopic number of quasiparticles with momenta $p_i < p < p_f$. The shape of the single-particle spectrum related to the Fermi condensate is independent of the Landau interaction, which is in general determined by the properties of the system as a whole, including the collective states, irregularities of structure, the presence of impurities, and composition. The length of the interval from p_f to p_i where a Fermi condensate exists is the only characteristic determined by the Landau interaction; of course, the interaction must be strong enough for a Fermi-condensate quantum phase transition to occur. Therefore, we conclude that spectra related to a Fermi condensate have a universal shape.

In Sections 2.3 and 3.1 we show that these spectra are dependent on the temperature and the superconducting gap and that this dependence is also universal. The existence of such spectra can be considered a characteristic feature of a 'quantum protectorate,' in which the properties of the material, including the thermodynamic properties, are determined by a certain fundamental principle [51, 52]. In our case, the state of matter with a Fermi condensate is also a quantum protectorate, since the new type of quasiparticles of this state determines the special universal thermodynamic and transport properties of the Fermi liquid with a Fermi condensate.

2.3 The 'shadow' of the Fermi condensate at finite temperatures

According to Eqn (2.1), the single-particle energy $\varepsilon(\mathbf{p}, T)$ is linear in T for $T \ll T_f$ within the interval (p_i, p_f) [53]. Expanding $\ln\left[\left(1 - n(\mathbf{p})\right)/n(\mathbf{p})\right]$ in a series in $n(\mathbf{p})$ at $p \approx p_F$, we can write the expression

$$\frac{\varepsilon(\mathbf{p}, T) - \mu(T)}{T} = \ln\frac{1 - n(\mathbf{p})}{n(\mathbf{p})} \approx \frac{1 - 2n(\mathbf{p})}{n(\mathbf{p})}\bigg|_{p\approx p_F} , \tag{2.12}$$

where T_f is the temperature above which the effect of the Fermi condensate is insignificant [54]:

$$\frac{T_f}{\varepsilon_F} \sim \frac{p_f^2 - p_i^2}{2M\varepsilon_F} \sim \frac{\Omega_{FC}}{\Omega_F} \,, \tag{2.13}$$

with Ω_{FC} being the volume occupied by the Fermi condensate, ε_F being the Fermi energy, and Ω_F being the volume of the Fermi sphere. We note that for $T \ll T_f$, the occupation numbers $n(\mathbf{p})$ obtained from Eqn (2.8) are almost perfectly independent of T. At finite temperatures, according to Eqn (2.12), the dispersionless plateau $\varepsilon(\mathbf{p}) = \mu$ shown in Fig. 1 is slightly rotated counterclockwise in relation to μ. As a result, the plateau is slightly tilted and rounded off at its end points. According to Eqns (2.5) and (2.12), the effective mass M^*_{FC} that refers to the Fermi-condensate quasiparticles is given by

$$M^*_{FC} \approx p_F \frac{p_f - p_i}{4T} \,. \tag{2.14}$$

In deriving Eqn (2.14), we approximated the derivative as $dn(p)/dp \approx -1/(p_f - p_i)$.

Equation (2.14) clearly shows that for $0 < T \ll T_f$, the electron liquid with a Fermi condensate behaves as if it were placed at a quantum critical point, since the electron effective mass diverges as $T \to 0$. Actually, the system is on the quantum critical line $x < x_{FC}$, because critical behavior is observed for all $x \leqslant x_{FC}$ as $T \to 0$. In Sections 5 and 8, we show that the behavior of such a system differs dramatically from that of a system at a quantum critical point.

Recalling that $p_f - p_i \ll p_F$ and using Eqns (2.13) and (2.14), we estimate the effective mass M^*_{FC} as

$$\frac{M^*_{FC}}{M} \sim \frac{N(0)}{N_0(0)} \sim \frac{T_f}{T}\,, \tag{2.15}$$

where $N_0(0)$ is the density of states of a noninteracting electron gas and $N(0)$ is the density of states on the Fermi surface.

Equations (2.14) and (2.15) yield the temperature dependence of M^*_{FC}. Multiplying both sides of Eqn (2.14) by $p_f - p_i$, we obtain an expression for the characteristic energy,

$$E_0 \approx 4T, \tag{2.16}$$

which determines the momentum interval (p_i, p_f) with the low-energy quasiparticles characterized by the energy $|\varepsilon(\mathbf{p}) - \mu| \leqslant E_0/2$ and the effective mass M^*_{FC}. The quasiparticles that do not belong to this momentum interval have an energy $|\varepsilon(\mathbf{p}) - \mu| \geqslant E_0/2$ and an effective mass M^*_L that is weakly temperature-dependent [44, 45, 55]. Equation (2.16) shows that E_0 is independent of the condensate volume. We conclude from Eqns (2.14) and (2.16) that for $T \ll T_f$, the single-electron spectrum of Fermi-condensate quasiparticles has a universal shape and has the features of a quantum protectorate.

Thus, a system with a Fermi condensate is characterized by two effective masses, M^*_{FC} and M^*_L. This fact manifests itself in a break or an abrupt change in the quasiparticle dispersion law, which for quasiparticles with energies $\varepsilon(\mathbf{p}) \leqslant \mu$ can be approximated by two straight lines intersecting at $E_0/2 \approx 2T$. Figure 1 shows that at $T = 0$, the straight lines intersect at $p = p_i$. This break occurs at finite temperatures $T_c \leqslant T \ll T_f$, where T_c is the critical temperature of the superconducting phase transition, which agrees with the experimental data in [56] and, as we see in Section 3, this behavior agrees with the experimental data at $T \leqslant T_c$ [56, 57]. At $T > T_c$, the quasiparticles are well-defined, because their width γ is small compared to their energy and is proportional to the temperature, $\gamma \sim T$ [20, 54]. The quasiparticle excitation curve (see Section 4) can be approximately described by a simple Lorentzian [55], which also agrees with the experimental data [58].

We estimate the density x_{FC} at which the Fermi-condensate quantum phase transition occurs. We show in Section 6 that an unlimited increase in the effective mass precedes the appearance of a density wave or a charge density wave formed in electron systems at $r_s = r_{cdw}$, where $r_s = r_0/a_B$, r_0 is the average distance between electrons, and a_B is the Bohr radius. Hence, a Fermi-condensate quantum phase transition certainly occurs at $T = 0$ when r_a reaches its critical value r_{FC} corresponding to x_{FC}, with $r_{FC} < r_{cdw}$ [42]. We note that the increase in the effective mass as the electron number density decreases was observed in experiments involving 2D metallic electron systems at $r_s \approx 7.5$ [38]; the same effect was observed in experiments involving ^{3}He 2D systems as the electron number density increased [59]. On the other hand, charge density waves can also exist in lightly doped high-T_c superconductors [60, 61], leading to the formation of a Fermi condensate.

Thus, the formation of a Fermi condensate can be considered a general property of different strongly correlated systems rather than an exotic phenomenon corresponding to the anomalous solution of Eqn (2.8) [42]. Beyond the Fermi-condensate quantum phase transition point, the condensate volume is proportional to $r_s - r_{FC}$, with $T_f/\varepsilon_F \sim (r_s - r_{FC})/r_{FC}$, at least when $(r_s - r_{FC})/r_{FC} \ll 1$. This implies that

$$\frac{r_s - r_{FC}}{r_{FC}} \sim \frac{p_f - p_i}{p_F} \sim \frac{x_{FC} - x}{x_{FC}}\,. \tag{2.17}$$

Because a state of a system with a Fermi condensate is highly degenerate, the Fermi condensate serves as a stimulator of phase transitions that could lift the degeneracy of the spectrum. For instance, a Fermi condensate can stimulate the formation of spin density waves, an antiferromagnetic state, etc., thus generating new properties of the systems. The presence of a Fermi condensate strongly facilitates a transition to the superconducting state, because both phases have the same order parameter (see Section 3, in which we examine the properties of a superconducting state in the presence of a Fermi condensate). Thus, superconductivity lifts the degeneracy of the spectrum and 'wins the race' with other phase transitions at temperatures up to the critical temperature T_c.

3. The superconducting state with a Fermi condensate

In this section we discuss the superconducting state of a 2D liquid of heavy electrons, since high-T_c superconductors are represented mainly by 2D structures. On the other hand, our study can easily be generalized to the 3D case. To show that there is no fundamental difference between the 2D and 3D cases, we derive Green's functions for the 3D case in Section 3.2.

3.1 The superconducting state at $T = 0$

The ground-state energy $E_{gs}\bigl[\kappa(\mathbf{p}), n(\mathbf{p})\bigr]$ of a 2D electron liquid is a functional of the superconducting state order parameter $\kappa(\mathbf{p})$ and of the quasiparticle occupation numbers $n(\mathbf{p})$. This energy is determined by the well-known Bardeen–Cooper–Schrieffer (BCS) equations and in the weak-coupling superconductivity theory is given by [62, 63]

$$E_{gs}\bigl[\kappa(\mathbf{p}), n(\mathbf{p})\bigr] = E\bigl[n(\mathbf{p})\bigr] + \lambda_0 \int V(\mathbf{p}_1, \mathbf{p}_2)\, \kappa(\mathbf{p}_1)\, \kappa^*(\mathbf{p}_2)\, \frac{\mathrm{d}\mathbf{p}_1\, \mathrm{d}\mathbf{p}_2}{(2\pi)^4}\,, \tag{3.1}$$

where $E\bigl[n(\mathbf{p})\bigr]$ is the Landau functional that determines the energy of a normal Fermi liquid and

$$n(\mathbf{p}) = v^2(\mathbf{p})\,, \qquad \kappa(\mathbf{p}) = v(\mathbf{p})\, u(\mathbf{p})\,, \tag{3.2}$$

where $u(\mathbf{p})$ and $v(\mathbf{p})$ are normalized parameters such that $v^2(\mathbf{p}) + u^2(\mathbf{p}) = 1$ and $\kappa(\mathbf{p}) = \bigl[n(\mathbf{p})\bigl(1 - n(\mathbf{p})\bigr)\bigr]^{1/2}$. It is assumed that the constant λ_0, which determines the magnitude of the pairing interaction $\lambda_0 V(\mathbf{p}_1, \mathbf{p}_2)$, is small. We define the superconducting gap as

$$\Delta(\mathbf{p}) = -\lambda_0 \int V(\mathbf{p}, \mathbf{p}_1)\, \kappa(\mathbf{p}_1)\, \frac{\mathrm{d}\mathbf{p}_1}{4\pi^2}\,. \tag{3.3}$$

Minimizing $E_{\rm gs}$ in $v(\mathbf{p})$ and using (3.3), we arrive at equations that relate the single-particle energy $\varepsilon(\mathbf{p})$ to $\Delta(\mathbf{p})$ and $E(\mathbf{p})$:

$$\varepsilon(\mathbf{p})-\mu=\Delta(\mathbf{p})\,\frac{1-2v^2(\mathbf{p})}{2\kappa(\mathbf{p})}\,,\qquad \frac{\Delta(\mathbf{p})}{E(\mathbf{p})}=2\kappa(\mathbf{p})\,, \tag{3.4}$$

where the single-particle energy $\varepsilon(\mathbf{p})$ is determined by Landau equation (2.2):

$$E(\mathbf{p})=\sqrt{\xi^2(\mathbf{p})+\Delta^2(\mathbf{p})}\,, \tag{3.5}$$

with $\xi(\mathbf{p})=\varepsilon(\mathbf{p})-\mu$. Substituting the expression for $\kappa(\mathbf{p})$ from (3.4) in Eqn (3.3), we obtain the well-known equation of the BCS theory for $\Delta(\mathbf{p})$:

$$\Delta(\mathbf{p})=-\frac{\lambda_0}{2}\int V(\mathbf{p},\mathbf{p}_1)\,\frac{\Delta(\mathbf{p}_1)}{E(\mathbf{p}_1)}\,\frac{\mathrm{d}\mathbf{p}_1}{4\pi^2}\,. \tag{3.6}$$

As $\lambda_0\to 0$, the maximum value of Δ_1 of the superconducting gap $\Delta(\mathbf{p})$ tends to zero and each equation in (3.4) reduces to Eqn (2.8):

$$\frac{\delta E\bigl[n(\mathbf{p})\bigr]}{\delta n(\mathbf{p})}=\varepsilon(\mathbf{p})-\mu=0 \tag{3.7}$$

if $0<n(\mathbf{p})<1$, or $\kappa(\mathbf{p})\neq 0$, in the interval $p_{\rm i}\leqslant p\leqslant p_{\rm f}$. Equation (3.7) shows that for $x<x_{\rm FC}$, the function $n(\mathbf{p})$ is determined from the solution to the standard problem of finding the minimum of the functional $E\bigl[n(\mathbf{p})\bigr]$ [23, 54]. Equation (3.7) specifies the quasiparticle distribution function $n_0(\mathbf{p})$ that ensures the minimum of the ground-state energy $E_{\rm gs}\bigl[\kappa(\mathbf{p}),n(\mathbf{p})\bigr]$ as $\lambda_0\to 0$. We can now study the relations between the state specified by Eqn (3.7) or (2.8) and the superconducting state.

At $T=0$, Eqn (3.7) determines the specific state of a Fermi liquid with a Fermi condensate, the state for which the absolute value of the order parameter $\bigl|\kappa(\mathbf{p})\bigr|$ is finite in the momentum interval $p_{\rm i}\leqslant p\leqslant p_{\rm f}$ as $\Delta_1\to 0$. Such a state can be considered superconducting with an infinitely small value of Δ_1. Hence, the entropy of this state at $T=0$ is zero. Obviously, the quantum state with a Fermi condensate that emerged as a result of a Fermi-condensate quantum phase transition disappears at finite temperatures [44, 45]. Any quantum phase transition that occurs at absolute zero is controlled not by the temperature but by other parameters, such as the pressure, the magnetic field strength, or the density x of mobile charge carriers. In the case of a Fermi condensate, as shown in Section 2, the controlling parameter may be the density x of the system, which determines the value of the Landau amplitude. As we saw in Section 2, the Fermi-condensate quantum phase transition occurs at the quantum critical point $x=x_{\rm FC}$. For $x>x_{\rm FC}$, the system is on the disordered side of the Fermi-condensate quantum phase transition; for $x<x_{\rm FC}$, it is on the ordered side, and the order parameter $\kappa(\mathbf{p})$ is finite in the interval $p_{\rm i}<p_{\rm F}<p_{\rm f}$.

Solutions $n_0(\mathbf{p})$ of Eqn (3.7) constitute a new class of solutions of the BCS equations and Landau Fermi-liquid equations. In contrast to the ordinary solutions of the BCS equations [62], the new solutions are characterized by an infinitely small superconducting gap $\Delta_1\to 0$, with the order parameter $\kappa(\mathbf{p})$ remaining finite. On the other hand, in contrast to the standard solution of the Landau Fermi-liquid theory, the new solutions $n_0(\mathbf{p})$ determine the state of a heavy-electron liquid with a finite entropy S_0 as $T\to 0$ [see Eqn (2.10)].

We arrive at an important conclusion that the solutions of Eqn (3.7) can be interpreted as the general solutions of the BCS equations and the Landau Fermi-liquid theory equations, while Eqn (3.7) itself can be derived either from the BCS theory or from the Landau Fermi-liquid theory. Thus, both states of the system coexist as $T\to 0$. As the system passes into a state with an order parameter $\kappa(\mathbf{p})$, the entropy suddenly vanishes, with the system undergoing a first-order transition near which the critical quantum and thermal fluctuations are suppressed and the quasiparticles are well-defined excitations (see also Section 8). It follows from Eqn (2.9) that a Fermi-condensate quantum phase transition is related to a change in the topological structure of the Green's function and belongs to Lifshits's topological phase transitions, which occur at absolute zero [43]. This fact establishes a relation between Fermi-condensate quantum phase transitions and quantum phase transitions under which the Fermi sphere splits into a sequence of Fermi layers [64] (see Section 5). We note that in the state with the order parameter $\kappa(\mathbf{p})$, the system entropy $S=0$ and the Nernst theorem holds in systems with a Fermi condensate.

If $\lambda_0\neq 0$, the gap Δ_1 becomes finite, leading to a finite value of the effective mass $M^*_{\rm FC}$, which may be obtained from Eqn (3.4) by taking the derivative with respect to the momentum p of both sides and using Eqn (2.5) [44, 45, 55]:

$$M^*_{\rm FC}\approx p_{\rm F}\,\frac{p_{\rm f}-p_{\rm i}}{2\Delta_1}\,. \tag{3.8}$$

As regards the energy scale, it is determined by the parameter E_0:

$$E_0=\varepsilon(\mathbf{p}_{\rm f})-\varepsilon(\mathbf{p}_{\rm i})\approx p_{\rm F}\,\frac{p_{\rm f}-p_{\rm i}}{M^*_{\rm FC}}\approx 2\Delta_1\,. \tag{3.9}$$

3.2 Green's function of the superconducting state with a Fermi condensate at $T=0$

We write two equations for the 3D case, the Gor'kov equations [65], which determine the Green's functions $F^+(\mathbf{p},\omega)$ and $G(\mathbf{p},\omega)$ of a superconductor (e.g., see Ref. [22]):

$$\begin{aligned} F^+&=-\frac{\lambda_0\Xi^*}{\bigl(\omega-E(\mathbf{p})+\mathrm{i}0\bigr)\bigl(\omega+E(\mathbf{p})-\mathrm{i}0\bigr)}\,,\\ G&=\frac{u^2(\mathbf{p})}{\omega-E(\mathbf{p})+\mathrm{i}0}+\frac{v^2(\mathbf{p})}{\omega+E(\mathbf{p})-\mathrm{i}0}\,. \end{aligned} \tag{3.10}$$

The gap Δ and the function Ξ are given by

$$\Delta=\lambda_0|\Xi|\,,\qquad \mathrm{i}\Xi=\iint_{-\infty}^{\infty}F^+(\mathbf{p},\omega)\,\frac{\mathrm{d}\omega\,\mathrm{d}\mathbf{p}}{(2\pi)^4}\,. \tag{3.11}$$

We recall that the function $F^+(\mathbf{p},\omega)$ has the meaning of the wave function of Cooper pairs and Ξ is the wave function of the motion of these pairs as a whole and is just a constant in a homogeneous system [22]. It follows from Eqns (3.4) and (3.11) that

$$\mathrm{i}\Xi=\int_{-\infty}^{\infty}F_0^+(\mathbf{p},\omega)\,\frac{\mathrm{d}\omega\,\mathrm{d}\mathbf{p}}{(2\pi)^4}=\mathrm{i}\int\kappa(\mathbf{p})\,\frac{\mathrm{d}\mathbf{p}}{(2\pi)^3}\,. \tag{3.12}$$

Taking Eqns (3.11) and (3.4) into account, we can write Eqns (3.10) as

$$F^{+}=-\frac{\kappa(\mathbf{p})}{\omega-E(\mathbf{p})+\mathrm{i}0}+\frac{\kappa(\mathbf{p})}{\omega+E(\mathbf{p})-\mathrm{i}0}\,,$$
$$G=\frac{u^2(\mathbf{p})}{\omega-E(\mathbf{p})+\mathrm{i}0}+\frac{v^2(\mathbf{p})}{\omega+E(\mathbf{p})-\mathrm{i}0}\,. \tag{3.13}$$

As $\lambda_0\to 0$, the gap $\Delta\to 0$, but Ξ and $\kappa(\mathbf{p})$ remain finite if the spectrum becomes flat, $E(\mathbf{p})=0$, and Eqns (3.13) become

$$F^{+}(\mathbf{p},\omega)=-\kappa(\mathbf{p})\left[\frac{1}{\omega+\mathrm{i}0}-\frac{1}{\omega-\mathrm{i}0}\right],$$
$$G(\mathbf{p},\omega)=\frac{u^2(\mathbf{p})}{\omega+\mathrm{i}0}+\frac{v^2(\mathbf{p})}{\omega-\mathrm{i}0} \tag{3.14}$$

in the interval $p_\mathrm{i}\leqslant p\leqslant p_\mathrm{f}$. The parameters $v(\mathbf{p})$ and $u(\mathbf{p})$ are determined by the condition that the spectrum be flat: $\varepsilon(\mathbf{p})=\mu$. If we take Landau equation (2.2) into account, this condition again reduces to Eqns (2.8) and (3.7) for determining the minimum of the functional $E\big[n(\mathbf{p})\big]$.

We construct the functions $F^{+}(\mathbf{p},\omega)$ and $G(\mathbf{p},\omega)$ in the case where the constant λ_0 is finite but small, such that $v(\mathbf{p})$ and $\kappa(\mathbf{p})$ can be found on the basis of the Fermi-condensate solutions of Eqn (2.8). Then Ξ, Δ, and $E(\mathbf{p})$ are given by Eqns (3.12), (3.11), and (3.4). Substituting the functions constructed in this manner into (3.13), we obtain $F^{+}(\mathbf{p},\omega)$ and $G(\mathbf{p},\omega)$ [66]. We note that Eqns (3.11) imply that the gap Δ is a linear function of λ_0 under the adopted conditions.

3.3 The superconducting state at finite temperatures

We assume that the region occupied by the Fermi condensate is small: $(p_\mathrm{f}-p_\mathrm{i})/p_\mathrm{F}\ll 1$ and $\Delta_1\ll T_\mathrm{f}$. Then, the order parameter $\kappa(\mathbf{p})$ is determined primarily by the Fermi condensate, i.e., the distribution function $n_0(\mathbf{p})$ [44, 45]. To be able to solve Eqn (3.6) analytically, we adopt the BCS approximation for the interaction [62]: $\lambda_0 V(\mathbf{p},\mathbf{p}_1)=-\lambda_0$ if $\big|\varepsilon(\mathbf{p})-\mu\big|\leqslant\omega_\mathrm{D}$ and the interaction is zero outside this region, with ω_D being a certain characteristic energy. As a result, the superconducting gap depends only on the temperature, $\Delta(\mathbf{p})=\Delta_1(T)$, and Eqn (3.6) becomes

$$1=N_\mathrm{FC}\lambda_0\int_0^{E_0/2}\frac{\mathrm{d}\xi}{\sqrt{\xi^2+\Delta_1^2(0)}}+N_\mathrm{L}\lambda_0\int_{E_0/2}^{\omega_\mathrm{D}}\frac{\mathrm{d}\xi}{\sqrt{\xi^2+\Delta_1^2(0)}}\,, \tag{3.15}$$

where we introduce the notation $\xi=\varepsilon(\mathbf{p})-\mu$ and the density of states N_FC in the interval $(p_\mathrm{i},p_\mathrm{f})$ or in the E_0-energy interval. It follows from Eqn (3.8) that $N_\mathrm{FC}=(p_\mathrm{f}-p_\mathrm{F})\,p_\mathrm{F}/2\pi\Delta_1(0)$. Within the energy interval $(E_0/2,\omega_\mathrm{D})$, the density of states N_L has the standard form $N_\mathrm{L}=M_\mathrm{L}^{*}/2\pi$. As $E_0\to 0$, Eqn (3.15) becomes the BCS equation. On the other hand, assuming that $E_0\leqslant 2\omega_\mathrm{D}$ and discarding the second integral on the right-hand side of Eqn (3.15), we obtain

$$\Delta_1(0)=\frac{\lambda_0 p_\mathrm{F}(p_\mathrm{f}-p_\mathrm{F})}{2\pi}\ln\left(1+\sqrt{2}\right)$$
$$=2\beta\varepsilon_\mathrm{F}\,\frac{p_\mathrm{f}-p_\mathrm{F}}{p_\mathrm{F}}\ln\left(1+\sqrt{2}\right), \tag{3.16}$$

where $\varepsilon_\mathrm{F}=p_\mathrm{F}^2/2M_\mathrm{L}^{*}$ is the Fermi energy and $\beta=\lambda_0 M_\mathrm{L}^{*}/2\pi$ is the dimensionless coupling constant. Using the standard value of β for ordinary superconductors, e.g., $\beta\approx 0.3$, and assuming that $(p_\mathrm{f}-p_\mathrm{F})/p_\mathrm{F}\approx 0.2$, we obtain a large value $\Delta_1(0)\sim 0.1\varepsilon_\mathrm{F}$ from Eqn (3.16); for ordinary superconductors, this gap has a much smaller value: $\Delta_1(0)\sim 10^{-3}\varepsilon_\mathrm{F}$. With the integral discarded earlier taken into account, we find that

$$\Delta_1(0)\approx 2\beta\varepsilon_\mathrm{F}\,\frac{p_\mathrm{f}-p_\mathrm{F}}{p_\mathrm{F}}\ln\left(1+\sqrt{2}\right)+\Delta_1(0)\beta\ln\frac{2\omega_\mathrm{D}}{\Delta_1(0)}\,. \tag{3.17}$$

On the right-hand side of Eqn (3.17), the value of Δ_1 is given by (3.16). As $E_0\to 0$ and $p_\mathrm{f}\to p_\mathrm{F}$, the first term on the right-hand side of Eqn (17) is zero, and we obtain the ordinary BCS result. The correction related to the second integral in (3.15) is small because the second term on the right-hand side of Eqn (3.17) contains the additional factor β. In what follows, we show that $2T_\mathrm{c}\approx\Delta_1(0)$. The isotopic effect is small in this case, because T_c depends on ω_D logarithmically, but the effect is restored as $E_0\to 0$.

At $T\approx T_\mathrm{c}$, Eqns (3.8) and (3.9) are replaced by Eqns (2.14) and (2.16), which also hold for $T_\mathrm{c}\leqslant T\ll T_\mathrm{f}$:

$$M_\mathrm{FC}^{*}\approx p_\mathrm{F}\,\frac{p_\mathrm{f}-p_\mathrm{i}}{4T_\mathrm{c}}\,,\qquad E_0\approx 4T_\mathrm{c}\quad\text{for}\quad T\approx T_\mathrm{c}\,, \tag{3.18}$$

$$M_\mathrm{FC}^{*}\approx p_\mathrm{F}\,\frac{p_\mathrm{f}-p_\mathrm{i}}{4T}\,,\qquad E_0\approx 4T\quad\text{for}\quad T\geqslant T_\mathrm{c}\,. \tag{3.19}$$

Equation (3.15) is replaced by its standard generalization valid for finite temperatures:

$$1=N_\mathrm{FC}\lambda_0\int_0^{E_0/2}\frac{\mathrm{d}\xi}{\sqrt{\xi^2+\Delta_1^2}}\tanh\frac{\sqrt{\xi^2+\Delta_1^2}}{2T}$$
$$+N_\mathrm{L}\lambda_0\int_{E_0/2}^{\omega_\mathrm{D}}\frac{\mathrm{d}\xi}{\sqrt{\xi^2+\Delta_1^2}}\tanh\frac{\sqrt{\xi^2+\Delta_1^2}}{2T}\,. \tag{3.20}$$

Because $\Delta_1(T\to T_\mathrm{c})\to 0$, Eqn (3.20) implies a relation that closely resembles the BCS result [5],

$$2T_\mathrm{c}\approx\Delta_1(0)\,, \tag{3.21}$$

where $\Delta_1(T=0)$ is found from Eqn (3.17). Comparing (3.8) and (3.9) with (3.18) and (3.19), we see that both M_FC^{*} and E_0 are temperature-independent for $T\leqslant T_\mathrm{c}$.

3.4 Bogoliubov quasiparticles

Equation (3.6) shows that the superconducting gap depends on the single-particle spectrum $\varepsilon(\mathbf{p})$. On the other hand, it follows from (3.4) that $\varepsilon(\mathbf{p})$ depends on $\Delta(\mathbf{p})$ if (3.7) has a solution that determines the existence of a Fermi condensate as $\lambda_0\to 0$. We assume that λ_0 is so small that the pairing interaction $\lambda_0 V(\mathbf{p},\mathbf{p}_1)$ leads only to a small perturbation of the order parameter $\kappa(\mathbf{p})$. Equation (3.8) implies that the effective mass and the density of states $N(0)\propto M_\mathrm{FC}^{*}\propto 1/\Delta_1$ are finite.

Thus, in contrast to the spectrum in the standard superconductivity theory, the single-particle spectrum $\varepsilon(\mathbf{p})$ depends strongly on the superconducting gap, and Eqns (2.2) and (3.6) must be solved by a self-consistent method.

We suppose that Eqns (2.2) and (3.6) have been solved and the effective mass M_FC^{*} has been found. This means that

we can find the quasiparticle dispersion law $\varepsilon(\mathbf{p})$ by choosing the effective mass M^* equal to the obtained value of $M^*_{\rm FC}$ and then solve Eqn (3.6) without taking (2.6) into account, as is done in the standard BCS superconductivity theory [62]. Hence, the superconducting state with a Fermi condensate is characterized by Bogoliubov quasiparticles [67] with dispersion (3.5) and the normalization condition $v^2(\mathbf{p}) + u^2(\mathbf{p}) = 1$ for the coefficients $v(\mathbf{p})$ and $u(\mathbf{p})$. Moreover, quasiparticle excitations of the superconducting state in the presence of a Fermi condensate coincide with the Bogoliubov quasiparticles characteristic of the BCS theory, and superconductivity with a Fermi condensate resembles the BCS superconductivity, which points to the applicability of the BCS formalism to the description of the high-$T_{\rm c}$ superconducting state [68]. At the same time, the maximum value of the superconducting gap set by Eqn (3.17) and other exotic properties are determined by the presence of the Fermi condensate. These results are in good agreement with the experimental facts obtained for the high-$T_{\rm c}$ superconductors $Bi_2Sr_2Ca_2Cu_3O_{10+\delta}$ [69].

In constructing the superconducting state with a Fermi condensate, we returned to the foundations of the Landau Fermi-liquid theory, from which the high-energy degrees of freedom have been eliminated by the introduction of quasiparticles. The main difference between the Landau Fermi liquid, which forms the basis for constructing the superconducting state, and the Fermi liquid with a Fermi condensate is that in the latter case we must increase the number of low-energy degrees of freedom by introducing a new type of quasiparticle with the effective mass $M^*_{\rm FC}$ and the characteristic energy E_0 given by (3.9). Hence, the dispersion law $\varepsilon(\mathbf{p})$ is characterized by two types of quasiparticles with the effective masses $M^*_{\rm L}$ and $M^*_{\rm FC}$ and the scale E_0. These new quasiparticles determine the properties of the superconductor, including the lineshape of quasiparticle excitations [44, 45, 70], while the dispersion of the Bogoliubov quasiparticles has the standard form.

We note that for $T < T_{\rm c}$, the effective mass $M^*_{\rm FC}$ and the scale E_0 are temperature-independent [70]. For $T > T_{\rm c}$, the effective mass $M^*_{\rm FC}$ and the scale E_0 are given by Eqns (2.14) and (2.16). Obviously, we cannot directly relate these new quasiparticles (excitations) of the Fermi liquid with a Fermi condensate to excitations (quasiparticles) of an ideal Fermi gas, as is done in the standard Fermi-liquid theory, because the system is beyond the Fermi-condensate quantum phase transition point. Nevertheless, the main principles of the Landau Fermi-liquid theory can be applied at the Fermi-condensate quantum phase transition: the concept of the order parameter is retained and low-energy excitations of a strongly correlated liquid with a Fermi condensate are represented by quasiparticles. The properties and dynamics of these new quasiparticles are closely related to the properties of the superconducting state and are of a collective nature, formed by the Fermi-condensate quantum phase transition and determined by the macroscopic number of Fermi-condensate quasiparticles with momenta in the interval $(p_{\rm i}, p_{\rm f})$. Such a system cannot be perturbed by scattering on impurities and lattice defects and, therefore, has the features of a quantum protectorate and demonstrates universal behavior [44, 45, 51, 52].

Several remarks concerning the quantum protectorate and the universal behavior of superconductors with a Fermi condensate are in order. Similarly to the Landau Fermi liquid theory, the theory of high-$T_{\rm c}$ superconductivity based on the Fermi-condensate quantum phase transition deals with quasiparticles that are elementary low-energy excitations. The theory provides a qualitative general description of the superconducting and the normal states of a superconductor. Of course, with phenomenological parameters (e.g., the pairing coupling constant) chosen, we can obtain a quantitative description of superconductivity, in the same way as this can be done in the Landau theory when describing a normal Fermi liquid, e.g., ^{3}He. Hence, any theory capable of describing a Fermi condensate and compatible with the BCS theory gives the same qualitative picture of the superconducting and normal states as the picture based on the Fermi-condensate quantum phase transition. Obviously, both approaches may be coordinated on the level of numerical results by choosing the appropriate parameters. For instance, because the formation of a Fermi condensate is possible in the Hubbard model [50], it allows reproducing the results of the theory based on the Fermi-condensate quantum phase transition. It is appropriate to note here that the corresponding description restricted to the case $T = 0$ has been obtained in the framework of the Hubbard model [71, 72].

3.5 The pseudogap

We discuss some features of the superconducting state with a Fermi condensate [73, 74]. We consider two possible types of the superconducting gap $\Delta(\mathbf{p})$ determined by Eqn (3.6) and the interaction $\lambda_0 V(\mathbf{p}, \mathbf{p}_1)$. If the interaction is caused by attraction, occurring, for instance, as a result of an exchange of phonons or magnetic excitations, the solution of Eqn (3.6) with an s-wave or (s + d)-mixed waves has the lowest energy. If the pairing interaction $\lambda_0 V(\mathbf{p}_1, \mathbf{p}_2)$ is a combination of an attractive interaction and a strongly repulsive interaction, d-wave superconductivity may occur (e.g., see Refs [75, 76]). However, both the s- and d-wave symmetries lead to approximately the same result for the size of the gap Δ_1 in Eqn (3.17) [70]. Hence, d-wave superconductivity is not a universal and necessary property of high-$T_{\rm c}$ superconductors. This conclusion agrees with the experimental evidence described in Refs [77–81].

We can define the critical temperature T^* as the temperature at which $\Delta_1(T^*) \equiv 0$. For $T \geqslant T^*$, Eqn (3.20) has only the trivial solution $\Delta_1 \equiv 0$. On the other hand, the critical temperature $T_{\rm c}$ can be defined as the temperature at which superconductivity disappears and the gap occupies only a part of the Fermi surface. Thus, there are two different temperatures $T_{\rm c}$ and T^*, which may not coincide in the case of the d-wave symmetry of the gap. As shown in Refs [55, 73], in the presence of a Fermi condensate, Eqn (3.20) has nontrivial solutions at $T_{\rm c} \leqslant T \leqslant T^*$, when the pairing interaction $\lambda_0 V(\mathbf{p}_1, \mathbf{p}_2)$ consists of attraction and strong repulsion, which leads to d-wave superconductivity. In this case, the gap $\Delta(\mathbf{p})$ as a function of the angle ϕ, or $\Delta(\mathbf{p}) = \Delta(p_{\rm F}, \phi)$, has new nodes at $T > T_{\rm node}$, as shown in Fig. 2 [55].

Figure 2 shows the ratio $\Delta(p_{\rm F}, \phi)/T^*$ calculated for three temperatures: $0.9\,T_{\rm node}$, $T_{\rm node}$, and $1.2\,T_{\rm node}$. In contrast to curve *1*, curves *2* and *3* have flat sections. Clearly, the flattening occurs because of the two new zeros that emerge at $T = T_{\rm node}$. As the temperature increases, the region $\theta_{\rm c}$ between the zeros (indicated by arrows in Fig. 2) increases in size. It is also clear that the gap Δ is very small within the interval $\theta_{\rm c}$. It was found in [82, 83] that the magnetism and the superconductivity affect each other, which leads to suppres-

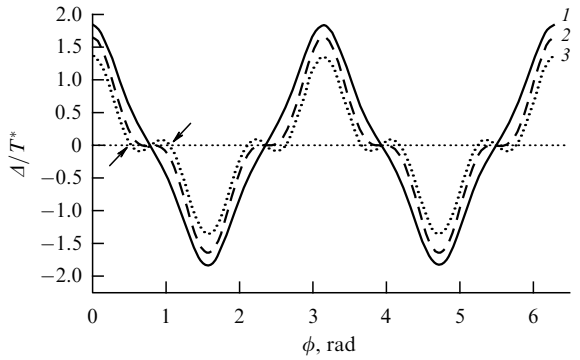

Figure 2. The gap $\Delta(p_F, \phi)$ as a function of ϕ calculated for three values of the temperature expressed in units of $T_{node} \approx T_c$. The solid curve (*1*) represents the function $\Delta(p_F, \phi)$ calculated for the temperature $0.9T_{node}$. The dashed curves (*2*) represents the same function at $T = T_{node}$, and the dotted curve (*3*) depicts the function calculated at $T = 1.2T_{node}$. The arrows indicate the region θ_c limited by the two new zeros that emerge at $T > T_{node}$.

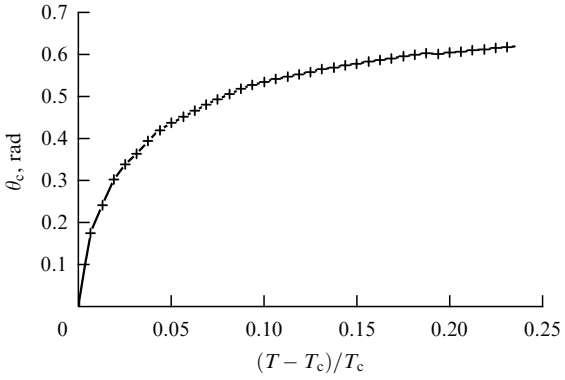

Figure 3. The result of a numerical calculation of the angle θ_c separating two zeros as a function of $(T - T_c)/T_c$.

sion of the magnetism at temperatures below T_c. In view of this, we can expect suppression of superconductivity due to magnetism.

Thus, we may conclude that the gap in the vicinity of T_c can be destroyed by strong antiferromagnetic correlations (or spin density waves), impurities, and sizable inhomogeneities existing in high-T_c superconductors [84]. Because the superconducting gap is destroyed in a macroscopic region of the phase space, θ_c, superconductivity is also destroyed, and therefore $T_c \approx T_{node}$. The exact value of T_c is determined by the competition between the antiferromagnetic state (or spin density waves) and the superconductivity in the interval θ_c. The behavior and the shape of the pseudogap closely resemble the similar characteristics of the superconducting gap, as Fig. 2 shows. The main difference is that the pseudogap disappears in the segment θ_c of the Fermi surface, while the gap disappears at isolated nodes of the d-wave. Our estimates show that for small values of the angle ψ, the function $\theta_c(\psi)$ rapidly increases, $\theta_c(\psi) \approx \sqrt{\psi}$. These estimates agree with the results of numerical calculations of the function $\theta_c\left([T - T_c]/T_c\right)$ (Fig. 3). Hence, we may conclude that T_c is close to T_{node}.

Thus, the pseudogap state appears at $T \geqslant T_c \approx T_{node}$ and disappears at temperatures $T \geqslant T^*$ at which Eqn (3.20) has only the trivial solution $\Delta_1 \equiv 0$. Obviously, Δ_1 determines T^* and not T_c, with the result that Eqn (2.15) should be rewritten as

$$2T^* \approx \Delta_1(0)\,. \tag{3.22}$$

The temperature T^* has the physical meaning of the temperature of the BCS transition between the state with an order parameter $\kappa \neq 0$ and the normal state.

At temperatures below T_c, the quasiparticle excitations of the superconducting state are characterized by the presence of sharp peaks. When the temperature becomes high ($T > T_c$) and $\Delta(\theta) \equiv 0$ in the interval θ_c, normal quasiparticle excitations with a width γ appear in the segments θ_c of the Fermi surface. A pseudogap exists outside the segments θ_c, and the Fermi surface is occupied by excitations of the BCS type in this region. Excitations of both types have widths of the same order of magnitude, transferring their energy and momenta into excitations of normal quasiparticles.

We estimate the value of γ. If the entire Fermi surface were occupied by the normal state, the width γ would be $\gamma \approx N^3(0)T^2/\varepsilon^2(T)$ with the density of states $N(0) \sim M^*(T) \sim 1/T$ [see Eqn (2.14)]. The dielectric constant $\varepsilon(T) \sim N(0)$ and, hence, $\gamma \sim T$ [54]. However, only a part of the Fermi surface within θ_c is occupied by normal excitations in our case. Therefore, the number of states accessible for quasiparticles and quasiholes is proportional to θ_c, and the factor T^2 is replaced by the factor $T^2\theta_c^2$. Taking all this into account yields $\gamma \sim \theta_c^2 T \sim T(T - T_c)/T_c \sim T - T_c$. Here, we ignored the small contribution provided by excitations of the BCS type. It is precisely for this reason that the width γ vanishes at $T = T_c$. Moreover, the resistivity of the normal state $\rho(T) \propto T$, because $\gamma \sim T - T_c$. Obviously, at temperatures above T^*, the relation $\rho(T) \propto T$ remains valid up to $T \sim T_f$, and T_f may be as high as the Fermi energy if the Fermi condensate occupies a significant part of the Fermi volume.

The temperature T_{node} is determined mainly by the repulsive interaction, which is part of the pairing interaction $\lambda_0 V(\mathbf{p}_1, \mathbf{p}_2)$. The value of the repulsive interaction, in turn, may be determined by the properties of the materials, such as composition or doping. Because superconductivity is destroyed at $T_c \approx T_{node}$, the ratio $2\Delta_1/T_c$ may vary within broad limits and strongly depends on the properties of the material [55, 73, 74]. For instance, in the case of $Bi_2Sr_2CaCu_2O_{6+\delta}$ it is assumed that superconductivity and the pseudogap are of common origin: $2\Delta_1/T_c \approx 28$, while $2\Delta_1/T^* \approx 4$, which agrees with the experimental data obtained in measurements involving other high-T_c superconductors [75].

We note that Eqn (3.22) also provides a good description of the maximum value of the gap Δ_1 in the case of d-wave superconductivity, because different regions with the maximum density of states may be considered unrelated [76]. We may also conclude that without a strong repulsion, with which s-wave pairing is possible, there can be no pseudogap. Thus, the transition from the superconducting gap to the pseudogap may proceed only in the case of d-wave pairing, when superconductivity is destroyed at $T_c \approx T_{node}$ and the superconducting gap gradually transforms into a pseudogap, which closes at a certain temperature $T^* > T_c$ [55, 73, 74]. The fact that there is no pseudogap in the case of s-wave pairing agrees with the experimental data (e.g., see Ref. [81]).

3.6 Dependence of the critical temperature T_c of the superconducting phase transition on doping

We examine the maximum value of the superconducting gap Δ_1 as a function of the number density x of mobile charge carriers, which is proportional to the degree of doping. Using Eqn (2.17), we can rewrite Eqn (3.16) as

$$\frac{\Delta_1}{\varepsilon_F} \sim \beta \frac{(x_{FC}-x)x}{x_{FC}}, \tag{3.23}$$

where we took into account that the Fermi level $\varepsilon_F \propto p_F^2$ and that the number density $x \sim p_F^2/(2M_L^*)$, with the result that $\varepsilon_F \propto x$. It is realistic to assume that $T_c \propto \Delta_1$, because the curve $T_c(x)$ obtained in experiments with high-T_c superconductors [2] must be a smooth function of x. Hence, we can approximate $T_c(x)$ by a smooth bell-shape function [85]:

$$T_c(x) \propto \beta(x_{FC}-x)x. \tag{3.24}$$

To illustrate the application of the above analysis, we examine the main features of a superconductor that can hypothetically exist at room temperature. Such a superconductor must be a two-dimensional structure, just as high-T_c superconducting cuprates are. Equation (3.16) implies that $\Delta_1 \sim \beta\varepsilon_F \propto \beta/r_s^2$. Bearing in mind that a Fermi-condensate quantum phase transition occurs at $r_s \sim 20$ in 3D systems and at $r_s \sim 8$ in 2D systems [42], we can expect that in 3D systems Δ_1 amounts to 10% of the maximum size of the superconducting gap in 2D systems, which in our case amounts to 60 mV for lightly doped cuprates with $T_c = 70$ K [86]. On the other hand, Eqn (3.16) implies that Δ_1 may be even larger, $\Delta_1 \sim 75$ mV. We can expect that $T_c \sim 300$ K in the case of s-wave pairing, as the simple relation $2T_c \approx \Delta_1$ implies. Indeed, we can take $\varepsilon_F \sim 500$ mV, $\beta \sim 0.3$, and $(p_f - p_i)/p_F \sim 0.5$.

Thus, the hypothetical superconductor at room temperature must be an s-wave superconductor in order to eliminate the pseudogap effect, which dramatically decreases the temperature T_c at which superconductivity is destroyed. We note that the number density x of mobile charge carriers must satisfy the condition $x \leqslant x_{FC}$ and must be varied to reach the optimum degree of doping $x_{opt} \approx x_{FC}/2$.

3.7 The gap and heat capacity near T_c

We now calculate the gap and heat capacity at temperatures $T \to T_c$. Our analysis is valid if $T^* \approx T_c$, since otherwise the discontinuities in the heat capacity considered below are smeared over the temperature interval between T^* and T_c. To simplify matters, we calculate the leading contribution to the gap and heat capacity related to the Fermi condensate. We use Eqn (3.20) to find the function $\Delta_1(T \to T_c)$ simply by expanding the first integral on its right-hand side in powers of Δ_1 and dropping the contribution from the second integral. This procedure leads to the equation [70]

$$\Delta_1(T) \approx 3.4T_c\sqrt{1-\frac{T}{T_c}}. \tag{3.25}$$

Therefore, the gap in the spectrum of single-particle excitations behaves in the ordinary manner.

To calculate the heat capacity, we can use the standard expression for the entropy S [62]:

$$S(T) = -2\int\left[f(\mathbf{p})\ln f(\mathbf{p}) + \left(1-f(\mathbf{p})\right)\ln\left(1-f(\mathbf{p})\right)\right]\frac{d\mathbf{p}}{(2\pi)^2}, \tag{3.26}$$

where

$$f(\mathbf{p}) = \left(1+\exp\frac{E(\mathbf{p})}{T}\right)^{-1},$$

$$E(\mathbf{p}) = \sqrt{\left(\varepsilon(\mathbf{p})-\mu\right)^2 + \Delta_1^2(T)}.$$

The heat capacity C is given by

$$C(T) = T\frac{dS}{dT} \approx 4\frac{N_{FC}}{T^2}\int_0^{E_0} f(E)\left(1-f(E)\right) \times\left[E^2 + T\Delta_1(T)\frac{d\Delta_1(T)}{dT}\right]d\xi + 4\frac{N_L}{T^2}\int_{E_0}^{\omega_D} f(E)\left(1-f(E)\right)\left[E^2 + T\Delta_1(T)\frac{d\Delta_1(T)}{dT}\right]d\xi. \tag{3.27}$$

In deriving Eqn (3.27), we again used the variable ξ, the above notation for the density of states, N_{FC} and N_L, and the notation $E = \left[\xi^2 + \Delta_1^2(T)\right]^{1/2}$. Equation (3.27) describes a jump in heat capacity, $\delta C(T) = C_s(T) - C_n(T)$, where $C_s(T)$ and $C_n(T)$ are the heat capacities of the superconducting and normal states at T_c; the jump is determined by the last two terms in the square brackets on the right-hand side of this equation. Using Eqn (3.25) to calculate the first term on the right-hand side of Eqn (3.27), we find [70]

$$\delta C(T_c) \approx \frac{3}{2\pi^2}(p_f - p_i)p_F^n, \tag{3.28}$$

where $n = 1$ in the 2D case and $n = 2$ in the 3D case. This result differs from the ordinary BCS result, according to which the discontinuity in the heat capacity is a linear function of T_c. The jump $\delta C(T_c)$ is independent of T_c because, as Eqn (3.19) shows, the density of state varies in inverse proportion to T_c. We note that in deriving Eqn (3.28) we took the leading contribution of the Fermi condensate into account. This contribution disappears as $E_0 \to 0$, and the second integral on the right-hand side of Eqn (27) yields the standard result.

As we show in Section 8 [see Eqn (8.4)], the heat capacity of a system with a Fermi condensate behaves as $C_n(T) \propto \sqrt{T/T_f}$. The jump in the heat capacity given by Eqn (3.28) is temperature-independent. As a result, we find that

$$\frac{\delta C(T_c)}{C_n(T_c)} \sim \sqrt{\frac{T_f}{T_c}}\frac{p_f - p_i}{p_F}. \tag{3.29}$$

In contrast to the case of normal superconductors, in which $\delta C(T_c)/C_n(T_c) = 1.43$ [22], in our case Eqn (3.29) implies that the ratio $\delta C(T_c)/C_n(T_c)$ is not constant and may be very large when $T_f/T_c \gg 1$.

4. The dispersion law and lineshape of single-particle excitations

The recently discovered break in the dispersion of quasiparticles at energies between 40 and 70 mV, resulting in a change in the quasiparticle speed at this energy [56–58], can hardly be explained by the marginal Fermi-liquid theory, because this theory contains no additional energy scales or parameters that would allow taking the break into account [67, 88]. We could assume that the break, which leads to a new energy

scale, occurs because of the interaction of electrons and collective excitations, but then we would have to discard the idea of a quantum protectorate, which would contradict the experimental data [51, 52].

As shown in Sections 2 and 3, a system with a Fermi condensate has two effective masses: $M^*_{\rm FC}$, which determines the single-particle spectrum at low energies, and $M^*_{\rm L}$, which determines the spectrum at high energies. The fact that there are two effective masses manifests itself in the form of a break in the quasiparticle dispersion law. The dispersion law can be approximated by two straight lines intersecting at a binding energy $E_0/2$ [see Eqns (2.16) and (3.9)]. The break in the dispersion law occurs at temperatures much lower than $T_{\rm f}$, when the system is in the superconducting or normal state. Such behavior is in good agreement with the experimental data [56]. It is pertinent to note that at temperatures below $T_{\rm c}$, the effective mass $M^*_{\rm FC}$ is independent of the momenta $p_{\rm F}$, $p_{\rm f}$, and $p_{\rm i}$, as shown by Eqns (3.8) and (3.16):

$$M^*_{\rm FC} \sim \frac{2\pi}{\lambda_0}\,. \tag{4.1}$$

This formula implies that $M^*_{\rm FC}$ is only weakly dependent on x if a dependence of λ_0 on x is allowed. This result is in good agreement with the experimental facts [89 – 91]. The same is true of the dependence of the Fermi velocity $v_{\rm F} = p_{\rm F}/M^*_{\rm FC}$ on x because the Fermi momentum $p_{\rm F} \sim \sqrt{n}$ is weakly dependent on the electron number density $n = n_0(1-x)$ [89, 90]; here, n_0 is the single-particle electron number density at half-filling.

Because λ_0 is the coupling constant that determines the magnitude of the pairing interaction, e.g., the electron – phonon interaction, we can expect the break in the quasiparticle dispersion law to be caused by the electron – phonon interaction. The phonon scenario could explain the constancy of the break at $T > T_{\rm c}$ because phonons are temperature-independent. On the other hand, it was found that the quasiparticle dispersion law distorted by the interaction with phonons has a tendency to restore itself to the ordinary single-particle dispersion law when the quasiparticle energy becomes higher than the phonon energy [92]. However, there is no experimental evidence that such restoration of the dispersion law actually takes place [56].

The quasiparticle excitation curve $L(q,\omega)$ is a function of two variables. Measurements at a constant energy $\omega = \omega_0$, where ω_0 is the single-particle excitation energy, determine the curve $L(q, \omega = \omega_0)$ as a function of the momentum q. We established above that $M^*_{\rm FC}$ is finite and constant at temperatures not exceeding $T_{\rm c}$. Hence, at excitation energies $\omega \leqslant E_0$, the system behaves as an ordinary superconducting Fermi liquid with the effective mass determined by Eqn (3.8) [44, 45, 55]. At $T_{\rm c} \leqslant T$, the effective mass $M^*_{\rm FC}$ is also finite and is given by Eqn (2.14). In other words, at energies $\omega < E_0$, the system behaves as a Fermi liquid whose single-particle spectrum is well defined and the width of the single-particle excitations is of the order of T [44, 45, 55]. Such behavior has been observed in experiments in measuring the quasiparticle excitation curve at a fixed energy [20, 58, 93].

The quasiparticle excitation curve can also be described as a function of ω, $L(q = q_0, \omega)$, at a constant momentum $q = q_0$. For small values of ω, the behavior of this function is similar to that described above, with $L(q = q_0, \omega)$ having a characteristic maximum and width. For $\omega \geqslant E_0$, the contribution provided by quasiparticles of mass $M^*_{\rm L}$ becomes significant and leads to an increase in the function $L(q = q_0, \omega)$. Thus, $L(q = q_0, \omega)$ has a certain structure of maxima and minima [94] directly determined by the existence of two effective masses, $M^*_{\rm FC}$ and $M^*_{\rm L}$ [44, 45, 55]. We conclude that, in contrast to Landau quasiparticles, these quasiparticles have a more complicated spectral lineshape.

We use the Kramers – Kronig transformation to calculate the imaginary part of the self-energy part $\Sigma(\mathbf{p}, \varepsilon)$. But we begin with the real part $\mathrm{Re}\,\Sigma(\mathbf{p}, \varepsilon)$, which determines the effective mass M^* [95],

$$\frac{1}{M^*} = \left(\frac{1}{M} + \frac{1}{p_{\rm F}}\frac{\partial\,\mathrm{Re}\,\Sigma}{\partial p}\right)\left(1 - \frac{\partial\,\mathrm{Re}\,\Sigma}{\partial\varepsilon}\right)^{-1}, \tag{4.2}$$

where M is the 'bare' mass. The corresponding momenta p and energies ε satisfy the inequalities $|p - p_{\rm F}|/p_{\rm F} \ll 1$ and $\varepsilon/\varepsilon_{\rm F} \ll 1$. We take $\mathrm{Re}\,\Sigma(\mathbf{p}, \varepsilon)$ in the simplest form possible that ensures the variation of the effective mass at the energy $E_0/2$,

$$\mathrm{Re}\,\Sigma(\mathbf{p}, \varepsilon) = -\varepsilon\,\frac{M^*_{\rm FC}}{M} + \left(\varepsilon - \frac{E_0}{2}\right)\frac{M^*_{\rm FC} - M^*_{\rm L}}{M} \times \left[\theta\left(\varepsilon - \frac{E_0}{2}\right) + \theta\left(-\varepsilon - \frac{E_0}{2}\right)\right], \tag{4.3}$$

where $\theta(\varepsilon)$ is the step function. To ensure a smooth transition from the single-particle spectrum characterized by $M^*_{\rm FC}$ to the spectrum characterized by $M^*_{\rm L}$, we must replace the step function with a smoother function. Substituting (4.3) in Eqn (4.2), we see that $M^* \approx M^*_{\rm FC}$ within the interval $(-E_0/2, E_0/2)$, while $M^* \approx M^*_{\rm L}$ outside this interval. Applying the Kramers – Kronig transformation to $\mathrm{Re}\,\Sigma(\mathbf{p}, \varepsilon)$, we express the imaginary part of the self-energy as [70]

$$\mathrm{Im}\,\Sigma(\mathbf{p}, \varepsilon) \sim \varepsilon^2\,\frac{M^*_{\rm FC}}{\varepsilon_{\rm F} M} + \frac{M^*_{\rm FC} - M^*_{\rm L}}{M} \times \left[\varepsilon \ln\left|\frac{2\varepsilon + E_0}{2\varepsilon - E_0}\right| + \frac{E_0}{2}\ln\left|\frac{4\varepsilon^2 - E_0^2}{E_0^2}\right|\right]. \tag{4.4}$$

Clearly, with $\varepsilon/E_0 \ll 1$, the imaginary part is proportional to ε^2; at $2\varepsilon/E_0 \approx 1$, we have $\mathrm{Im}\,\Sigma \sim \varepsilon$, and for $E_0/\varepsilon \ll 1$, the main contribution to the imaginary part is approximately constant.

It follows from Eqn (4.4) that as $E_0 \to 0$, the second term on its right-hand side tends to zero and the single-particle excitations become well-defined, which resembles the situation with a normal Fermi liquid, while the pattern of minima and maxima eventually disappears. On the other hand, the quasiparticle renormalization factor $a(\mathbf{p})$ is given by the equation [95]

$$\frac{1}{a(\mathbf{p})} = 1 - \frac{\partial\,\mathrm{Re}\,\Sigma(\mathbf{p}, \varepsilon)}{\partial\varepsilon}\,. \tag{4.5}$$

It follows from Eqns (4.4) and (4.5) that for $T \leqslant T_{\rm c}$, the amplitude of a quasiparticle on the Fermi surface increases as the characteristic energy E_0 decreases. Equations (3.9) and (3.24) imply that $E_0 \sim (x_{\rm FC} - x)/x_{\rm FC}$. When $T > T_{\rm c}$, it follows from (4.3) and (4.5) that the quasiparticle amplitude increases as the effective mass $M^*_{\rm FC}$ decreases. It follows from Eqns (2.14) and (2.17) that $M^*_{\rm FC} \sim (p_{\rm f} - p_{\rm i})/p_{\rm F} \sim (x_{\rm FC} - x)/x_{\rm FC}$. As a result, we conclude that the amplitude increases with the doping level and the single-particle

excitations are better defined in heavily doped samples. As $x \to x_{FC}$, the characteristic energy $E_0 \to 0$ and the quasiparticles become normal excitations of the Landau Fermi liquid. We note that such behavior has been observed in experiments with heavily doped Bi2212, which demonstrates high-T_c superconductivity with a gap of about 10 mV [96]. The size of the gap suggests that the region occupied by a Fermi condensate is small because $E_0/2 \approx \Delta_1$. For $x > x_{FC}$ and low temperatures, the heavy-electron liquid behaves as the Landau Fermi liquid (see Section 7). Experimental data show that, as expected, the Landau Fermi liquid exists in super-heavily doped nonsuperconducting $La_{1.7}Sr_{0.3}CuO_4$ [97, 98].

5. An electron liquid with a Fermi condensate in magnetic fields

In this section, we discuss the behavior of a heavy-electron liquid with a Fermi condensate in a magnetic field.

We assume that the coupling constant is nonzero, $\lambda_0 \neq 0$, but is infinitely small. We found in Section 3 that at $T = 0$ the superconducting order parameter $\kappa(\mathbf{p})$ is finite in the region occupied by the Fermi condensate and that the maximum value of the superconducting gap $\Delta_1 \propto \lambda_0$ is infinitely small. Hence, any weak magnetic field $B \neq 0$ is critical and destroys $\kappa(\mathbf{p})$ and the Fermi condensate. Simple energy arguments suffice to determine the type of rearrangement of the Fermi-condensate state. On the one hand, because the Fermi-condensate state is destroyed, the gain in energy $\Delta E_B \propto B^2$ tends to zero as $B \to 0$. On the other hand, the function $n_0(\mathbf{p})$, which occupies the finite interval (p_i, p_f) in the momentum space and is specified by Eqn (2.8) or (3.9), leads to a finite gain in the ground-state energy compared to the ground-state energy of a normal Fermi liquid [23].

Thus, in weak magnetic fields, the new ground state without a Fermi condensate must have almost the same energy as the state with a Fermi condensate. Such a state is formed by multiply connected Fermi spheres resembling an onion, for which a smooth distribution function of quasiparticles, $n_0(\mathbf{p})$, is replaced in the interval (p_i, p_f) with the distribution function [64, 99]

$$v(\mathbf{p}) = \sum_{k=1}^{n} \theta(p - p_{2k-1})\,\theta(p_{2k} - p)\,, \tag{5.1}$$

where the parameters $p_i \leqslant p_1 < p_2 < \ldots < p_{2n} \leqslant p_f$ are chosen such that they satisfy the normalization condition and the condition needed for the conservation of the number of particles:

$$\int_{p_{2k-1}}^{p_{2k+3}} v(\mathbf{p})\,\frac{d\mathbf{p}}{(2\pi)^3} = \int_{p_{2k-1}}^{p_{2k+3}} n_0(\mathbf{p})\,\frac{d\mathbf{p}}{(2\pi)^3}\,.$$

Figure 4 shows the corresponding multiply connected distribution. For definiteness, we present the most interesting case of a three-dimensional system. The two-dimensional case can be examined similarly. We note that the possibility of the existence of multiply connected Fermi spheres was noted in [100, 101].

We assume that the thickness of each inner slice of the Fermi sphere, $\delta p \approx p_{2k+1} - p_{2k}$, is determined by the magnetic field B. Using the well-known rule for estimating errors in calculating integrals, we find that the minimum loss of the ground-state energy due to slice formation is approximately $(\delta p)^4$. This becomes especially clear if we account for the fact that the continuous Fermi-condensate functions $n_0(\mathbf{p})$ ensure the minimum value of the energy functional $E[n(\mathbf{p})]$, while the approximation of $v(\mathbf{p})$ by steps of width δp leads to a minimal error of the order of $(\delta p)^4$. Recalling that the gain due to the magnetic field is proportional to B^2 and equating the two contributions, we obtain

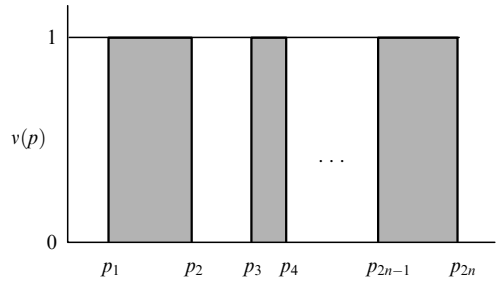

Figure 4. The function $v(\mathbf{p})$ for the multiply connected distribution that replaces the function $n_0(\mathbf{p})$ in the region (p_i, p_f) occupied by the Fermi condensate. The momenta satisfy the inequalities $p_i < p_F < p_f$, where p_F is the momentum of the Landau normal Fermi liquid. The outer Fermi surface at $p \approx p_{2n} \approx p_f$ has the shape of a Fermi step, and therefore the system behaves like a Landau Fermi liquid at $T < T^*(B)$.

$$\delta p \propto \sqrt{B}\,. \tag{5.2}$$

Therefore, as $T \to 0$, with $B \to 0$, the slice thickness δp also tends to zero and the behavior of a Fermi liquid with a Fermi condensate is replaced with that of the Landau Fermi liquid with the Fermi momentum p_f. Equation (3.7) implies that $p_f > p_F$ and the electron number density x remains constant, with the Fermi momentum of the multiply connected Fermi sphere $p_{2n} \approx p_f > p_F$ (see Fig. 4). We see in what follows that these observations play an important role in studying the behavior of the Hall coefficients $R_H(B)$ as a function of B in heavy-fermion metals at low temperatures.

To calculate the effective mass $M^*(B)$ as a function of the applied magnetic field B, we first note that at $T = 0$ the field B splits the Fermi-condensate state into Landau levels, suppresses the superconducting order parameter $\kappa(\mathbf{p})$, and destroys the Fermi-condensate state, which leads to restoration of the state characteristic of a Landau Fermi liquid [30, 102]. The Landau levels near the Fermi surface can be approximated by separate slices whose thickness in momentum space is δp. Approximating the quasiparticle dispersion law within a single slice, $\varepsilon(p) - \mu \sim (p - p_f + \delta p)(p - p_f)/M$, we find the effective mass $M^*(B) \sim M/(\delta p/p_f)$. The energy increment ΔE_{FC} caused by the transformation of the Fermi-condensate state can be estimated based on the Landau formula [22]

$$\Delta E_{FC} = \int \big(\varepsilon(\mathbf{p}) - \mu\big)\,\delta n(\mathbf{p})\,\frac{d\mathbf{p}}{(2\pi)^3}\,. \tag{5.3}$$

The region occupied by the variation $\delta n(\mathbf{p})$ has the thickness δp, with $\varepsilon(\mathbf{p}) - \mu \sim (p - p_f)\,p_f/M^*(B) \sim \delta p\,p_f/M^*(B)$. As a result, we find that $\Delta E_{FC} \sim p_f^3 \delta p^2/M^*(B)$. On the other hand, there is the addition $\Delta E_B \sim (B\mu_B)^2 M^*(B)\,p_f$ caused by the applied magnetic field, which decreases the energy and is related to the Zeeman splitting. Equating ΔE_B and ΔE_{FC} and recalling that $M^*(B) \propto 1/\delta p$ in this case, we obtain the

chain of relations

$$\frac{\delta p^2}{M^*(B)} \propto \frac{1}{\left(M^*(B)\right)^3} \propto B^2 M^*(B)\,, \tag{5.4}$$

which implies that the effective mass $M^*(B)$ diverges as

$$M^*(B) \propto \frac{1}{\sqrt{B - B_{c0}}}\,, \tag{5.5}$$

where B_{c0} is the critical magnetic field, which places the heavy-fermion metal at the magnetic-field-tuned quantum critical point and nullifies the respective Néel temperature, $T_N(B_{c0}) = 0$ [30]. In our simple model of a heavy-electron liquid with a Fermi condensate, the quantity B_{c0} is a parameter determined by the properties of the specific metal with heavy fermions. We note that in some cases $B_{c0} = 0$, e.g., the heavy-fermion metal $CeRu_2Si_2$ has no magnetic order, exhibits no superconductivity, and does not behave like a Landau Fermi liquid even at the lowest temperatures [103].

Formula (5.5) and Fig. 4 show that application of a magnetic field $B > B_{c0}$ brings the Fermi-condensate system back to the Landau Fermi-liquid state with the effective mass $M^*(B)$ that depends on the magnetic field. This means that the following dependences characteristic of the Landau Fermi liquid are restored: $C/T = \gamma_0(B) \propto M^*(B)$ for the heat capacity and $\chi_0(B) \propto M^*(B)$ for the magnetic susceptibility. The coefficient $A(B)$ determines the temperature-dependent part of the resistivity, $\rho(T) = \rho_0 + \Delta\rho$, where ρ_0 is the residual resistivity and $\Delta\rho = A(B)T^2$. Because this coefficient is directly determined by the effective mass, $A(B) \propto \left(M^*(B)\right)^2$ [104], Eqn (5.5) yields

$$A(B) \propto \frac{1}{B - B_{c0}}\,. \tag{5.6}$$

We note that the empirical Kadowaki – Woods relation [15] $K = A/\gamma_0^2 \approx \text{const}$ is valid in our case. Furthermore, K may depend on the degree of degeneracy of the quasiparticles. With this degeneration, the Kadowaki – Woods relation provides a good description of the experimental data for a broad class of heavy-fermion metals [105]. In the simplest case, where the heavy-electron liquid is formed by spin-1/2 quasiparticles with the degeneracy degree 2, the value of K turns out to be close to the empirical value [104] known as the Kadowaki – Woods ratio [15]. Hence, under a magnetic field, the system returns to the state of a Landau Fermi liquid and the constancy of the Kadowaki – Woods relation holds.

At finite temperatures, the system remains in the Landau Fermi liquid state, but when $T > T^*(B)$, the behavior of a heavy Fermi liquid with a Fermi condensate and entropy S_0 [see (2.10)] is restored. As regards finding the function $T^*(B)$, we note that the effective mass M^* characterizing the single-particle spectrum cannot change at $T^*(B)$ because no phase transition occurs at this temperature. To calculate $T^*(B)$, we equate the effective mass $M^*(T)$ in Eqn (2.14) to $M^*(B)$ in (5.5), $M^*(T) \sim M^*(B)$,

$$\frac{1}{M^*(T)} \propto T^*(B) \propto \frac{1}{M^*(B)} \propto \sqrt{B - B_{c0}}\,, \tag{5.7}$$

whence

$$T^*(B) \propto \sqrt{B - B_{c0}}\,. \tag{5.8}$$

At temperatures $T \geqslant T^*(B)$, the system returns to the behavior of a heavy Fermi liquid with the entropy S_0 and the effective mass M^* specified by Eqn (2.14). Thus, expression (5.8) determines the line in the T vs. B phase diagram that separates the region where the effective mass depends on B and the heavy Fermi liquid behaves like a Landau Fermi liquid from the region where the effective mass is temperature-dependent. At $T^*(B)$, the temperature dependence of the resistivity ceases to be quadratic and becomes linear.

It follows from (5.8) that at a certain temperature $T^*(B) \ll T_f$, the heavy-electron liquid acquires the properties of a Landau Fermi liquid in strong magnetic fields, $B - B_{c0} \propto \left(T^*(B)\right)^2$. At temperatures below $T^*(B)$, the heavy-electron liquid demonstrates an increasingly metallic behavior as the magnetic field B increases, because the effective mass decreases [see Eqn (5.5)]. Such behavior of the effective mass can be observed, for instance, in measurements of the heat capacity, magnetic susceptibility, resistivity, and Shubnikov – de Haas oscillations. From the T vs. B phase diagram constructed in this manner, it follows that a unique possibility emerges where a magnetic field can be used to control the variations in the physical nature and type of behavior of the electron liquid with a Fermi condensate.

We briefly discuss the case where the system is extremely close to a Fermi-condensate quantum phase transition on the ordered size of this transition, and hence $\delta p_{FC} = (p_f - p_i)/p_F \ll 1$. Because $\delta p \propto M^*(B)$, it follows from Eqns (5.2) and (5.5) that

$$\frac{\delta p}{p_F} \sim a_c \sqrt{\frac{B - B_{c0}}{B_{c0}}}\,, \tag{5.9}$$

where a_c is a constant of the order of unity, $a_c \sim 1$. As the magnetic field B increases, $\delta p/p_F$ becomes comparable to δp_{FC}, and the distribution function $\nu(\mathbf{p})$ disappears, being absorbed by the ordinary Zeeman splitting. As a result, we are dealing with a heavy-electron liquid 'located' on the disordered side of the Fermi-condensate quantum phase transition. We show in Section 8 that the behavior of such a system differs markedly from that of a system with a Fermi condensate. Equation (5.9) implies that the relatively weak magnetic field

$$B_{cr} \sim (\delta p_{FC})^2 = \frac{B - B_{c0}}{B_{c0}} \equiv B_{red}\,, \tag{5.10}$$

where B_{red} is the reduced field, takes the system from the ordered side of the phase transition to the disordered if $\delta p_{FC} \ll 1$.

5.1 The Landau Fermi liquid in high-T_c superconductors

Observations have shown that in the normal state obtained by applying a magnetic field whose strength is higher than the maximum critical field B_c that destroys superconductivity, the heavily doped cuprate $Tl_2Ba_2CuO_{6+\delta}$ [14] and the optimally doped cuprate $Bi_2Sr_2CuO_{6+\delta}$ [17] exhibit no significant violations of the Wiedemann – Franz law. Studies of the electron-doped superconductor $Pr_{0.91}LaCe_{0.09}CuO_{4-y}$ ($T_c = 24$ K) revealed that when a magnetic field destroyed superconductivity in this material, the spin – lattice relaxation constant $1/T_1$ obeyed the relation $T_1 T = \text{const}$, known as the Korringa law, down to temperatures about 0.2 K [106, 107]. At higher temperatures and in magnetic fields up to 15.3 T

perpendicular to the CuO_2 plane, the ratio $1/T_1T$ remains constant as a function of T for $T \leqslant 55$ K. In the temperature range from 50 to 300 K, the ratio $1/T_1T$ decreases as the temperature increases [107]. Measurements involving the heavily doped nonsuperconducting material $La_{1.7}Sr_{0.3}CuO_4$ have shown that ρ varies with T as T^2 and that the Wiedemann – Franz law holds [97, 98].

Because the Korringa and Wiedemann – Franz laws strongly indicate the presence of a Landau Fermi liquid, experiments show that the observed elementary excitations cannot be distinguished from Landau quasiparticles in high-T_c superconductors. This places severe restrictions on models describing hole- or electron-doped high-T_c superconductors. For instance, for a Luttinger liquid [108], for spin – charge separation [7], and in some $t-J$ models [109], a violation of the Wiedemann – Franz law was predicted, which contradicts experimental evidence and points to limited applicability of these models.

If the constant λ_0 is finite, then the heavy-electron liquid with a Fermi condensate is in the superconducting state. We examine the behavior of the system in magnetic fields $B > B_c$. In this case, the system becomes the Landau Fermi liquid induced by the magnetic field, and the elementary excitations become quasiparticles that cannot be distinguished from Landau quasiparticles, with the effective mass $M^*(B)$ given by Eqn (5.5). As a result, the Wiedemann – Franz law holds as $T \to 0$, which agrees with the experimental facts [14, 17]. The low-temperature properties of the system depend on the effective mass; in particular, the resistivity $\rho(T)$ behaves as $\rho(T) = \rho_0 + A(B)T^2$, with $A(B) \propto \left(M^*(B)\right)^2$. Assuming that $B_{c0} \approx 0$ in the case of high-T_c superconductors, we deduce from Eqn (5.5) that

$$\gamma_0\sqrt{B} = \text{const}\,, \tag{5.11}$$

where $\gamma_0 = C/T$, with C being the heat capacity. Taking Eqns (5.6) and (5.11) into account, we find that

$$\gamma_0 \sim A(B)\sqrt{B}\,. \tag{5.12}$$

At finite temperatures, the system remains a Landau Fermi liquid, but for $T > T^*(B)$ the effective mass becomes temperature-dependent, $M^* \propto 1/T$, and the resistivity becomes a linear function of the temperature, $\rho(T) \propto T$ [44, 45, 99]. Such behavior of the resistivity has been observed in the high-T_c superconductor $Tl_2Ba_2CuO_{6+\delta}$ ($T_c < 15$ K) [110]. At $B = 10$ T, $\rho(T)$ is a linear function of the temperature in the range from 120 mK to 1.2 K, and at $B = 18$ T the temperature dependence of the resistivity can be written in the form $\rho(T) \propto AT^2$ in the same temperature range [110].

In a Landau Fermi liquid, the spin – lattice relaxation parameter $1/T_1$ is determined by the quasiparticles near the Fermi level, whose population is proportional to M^*T, whence $1/T_1T \propto M^*$, and is a constant quantity [106, 107]. When the superconducting state disappears as a magnetic field is applied, the ground state can be regarded as a field-induced Landau Fermi liquid with a field-dependent effective mass. As a result, $T_1T = \text{const}$, which implies that the Korringa law holds. According to Eqn (5.5), the ratio $1/T_1T \propto M^*(B)$ decreases as the magnetic field increases at $T < T^*(B)$, whereas in the case of a Landau Fermi liquid it remains constant, as noted above. On the other hand, at $T > T^*(B)$, the ratio $1/T_1T$ is a decreasing function of the temperature, $1/T_1T \propto M^* \propto 1/T$. These results are in good agreement with the experimental facts [107]. Because $T^*(B)$ is an increasing function of the magnetic field [see Eqn (5.8)], the Korringa law remains valid even at higher temperatures and in stronger magnetic fields. Hence, at $T_0 \leqslant T^*(B_0)$ and high magnetic fields $B > B_0$, the system demonstrates distinct metallic behavior, because the effective mass decreases as B increases [see Eqn (5.5)] [111].

The existence of a Fermi-condensate quantum phase transition can also be verified in experiments, because at number densities $x > x_{FC}$ or beyond the Fermi-condensate quantum phase transition point, the system must become a Landau Fermi liquid at sufficiently low temperatures [102]. Experiments have shown that such a liquid indeed exists in the heavily doped nonsuperconducting compound $La_{1.7}Sr_{0.3}CuO_4$ [97, 98]. It is remarkable that for $T < 55$ K, the resistivity exhibits a T^2-behavior without an additional linear term and the Wiedemann – Franz law holds [97, 98]. At temperatures above 55 K, experimenters have observed significant deviations from the behavior of the Landau Fermi liquid. We predict that the system can again be returned to a state with the Landau Fermi-liquid behavior by applying sufficiently strong magnetic fields (see Section 7).

6. Emergence of a Fermi-condensate quantum phase transition in Fermi systems

We say that Fermi systems that approach the Fermi-condensate quantum transition point from a disordered state are highly correlated systems in order to distinguish them from strongly correlated systems (or liquids) that are already beyond the Fermi-condensate quantum transition point. A detailed description of the properties of a highly correlated electron liquid is given in Section 7, and the properties of a strongly correlated electron liquid are discussed in Section 8. In the present section, we discuss the behavior of the effective mass M^* as a function of the density x of the system as $x \to x_{FC}$.

The experimental facts for high-density 2D ^{3}He [37, 59, 112] show that the effective mass becomes divergent when the value of the density at which the 2D liquid ^{3}He begins to solidify is reached [59]. Also observed was a sharp increase in the effective mass in the metallic 2D electron system as the density x decreases and tends to the critical density of the metal – insulator transition [38]. We note that there is no ferromagnetic instability in the Fermi systems under consideration and the corresponding Landau amplitude $F_0^a > -1$ [38, 59], which agrees with the model of nearly localized fermions [34].

We examine the divergence of the effective mass in 2D and 3D highly correlated Fermi liquids at $T = 0$ as the density x approaches the Fermi-condensate quantum phase transition point of the disordered phase. We begin by calculating M^* as a function of the difference $x - x_{FC}$ for a 2D Fermi liquid. For this, we use the equation for M^* derived in [42], where the divergence of M^* related to the generation of a density wave in various Fermi liquids was predicted. As $x \to x_{FC}$, the effective mass M^* can be approximately written as

$$\frac{1}{M^*} \approx \frac{1}{M} + \frac{1}{4\pi^2}\int_{-1}^{1}\int_{0}^{g_0} \frac{y\,\mathrm{d}y\,\mathrm{d}g}{\sqrt{1-y^2}} \frac{v\big(q(y)\big)}{\big[1 - R\big(q(y),g\big)\,\chi_0\big(q(y)\big)\big]^2}\,. \tag{6.1}$$

We here use the notation $p_F\sqrt{2(1-y)} = q(y)$, where $q(y)$ is the momentum transfer, $v(q)$ is the pair interaction, the integral with respect to the coupling constant g is taken from zero to the actual value g_0, $\chi_0(q,\omega)$ is the linear response function for the noninteracting Fermi liquid, and $R(q,\omega)$ is the effective interaction, with both functions taken at $\omega = 0$. The quantities R and χ_0 determine the response function for the system,

$$\chi(q,\omega,g) = \frac{\chi_0(q,\omega)}{1 - R(q,\omega,g)\,\chi_0(q,\omega)}\,. \tag{6.2}$$

Near the instability related to the generation of a density wave at the density x_{cdw}, the singular part of the response function χ has the well-known form (e.g., see Ref. [2])

$$\chi^{-1}(q,\omega,g) \approx a(x_{cdw} - x) + b(q - q_c)^2 + c(g_0 - g)\,, \tag{6.3}$$

where a, b, and c are constants and $q_c \approx 2p_F$ is the density-wave momentum. Substituting Eqn (6.3) in (6.1) and integrating, we can represent the equation for the effective mass M^* as [35, 36]

$$\frac{1}{M^*(x)} = \frac{1}{M} - \frac{C}{\sqrt{x - x_{cdw}}}\,, \tag{6.4}$$

where C is a positive constant. It follows from Eqn (6.4) that $M^*(x)$ diverges as a function of the difference $x - x_{FC}$ and $M^*(x) \to \infty$ as $x \to x_{FC}$ [35, 36]:

$$\frac{M^*(x)}{M} \approx A + \frac{B}{x - x_{FC}}\,, \tag{6.5}$$

where A and B are constants. We note that Eqns (6.4) and (6.5) do not explicitly contain the interaction $v(q)$, although $v(q)$ affects A, B, and x_{FC}. This result agrees with Eqn (2.7), which determines the same universal type of divergence (i.e., a divergence that is independent of the interaction). Hence, both equations (6.4) and (6.5) can be applied to 2D ^{3}He, the electron liquid, and other Fermi liquids. We also see that the Fermi-condensate quantum phase transition precedes the formation of density waves (or charge-density waves) in Fermi systems.

We note that the difference $x - x_{FC}$ must be positive in both cases, since the density x approaches x_{FC} when the system is on the disordered side of the Fermi-condensed quantum phase transition with an effective mass $M^*(x) > 0$. In the case of ^{3}He, the Fermi-condensate quantum phase transition occurs as the density increases, when the potential energy begins to contribute to the ground-state energy. Thus, for the 2D ^{3}He liquid, the difference $x - x_{FC}$ on the right-hand side of Eqn (6.5) must be replaced with $x_{FC} - x$. Experiments have shown that the effective mass indeed diverges at high densities in the case of 2D ^{3}He and at low densities in the case of 2D electron systems [38, 59].

The effective mass as a function of the electron density x in a silicon MOSFET (Metal Oxide Semiconductor Field Effect Transistor), approximated by Eqn (6.4), is shown in Fig. 5. The approximation parameters are $x_{cdw} = 0.7 \times 10^{-11}$ cm^{-2}, $C = 2.14 \times 10^{-6}$ cm^{-1}, and $x_{FC} = 0.9 \times 10^{-11}$ cm^{-2} [35]. We see that Eqn (6.4) provides a good description of the experimental results. The divergence of the effective mass $M^*(x)$ discovered in measurements involving 2D ^{3}He [37, 59] is illustrated by Fig. 6. Figures 5 and 6 show that the description provided by Eqns (6.4), (6.5), and (2.7) is in good agreement with the experimental data.

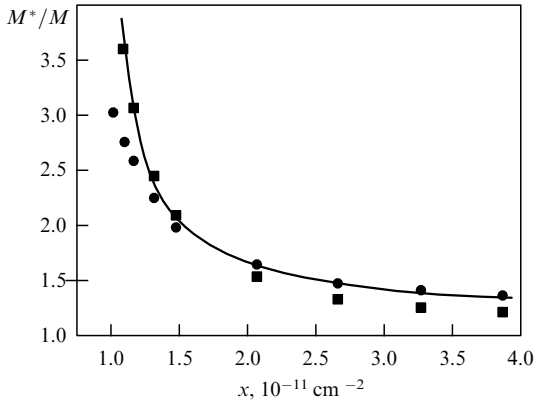

Figure 5. The ratio M^*/M in a silicon MOSFET as a function of the electron number density x. The black squares mark the experimental data on the Shubnikov – de Haas oscillations. The data obtained by applying a parallel magnetic field are marked by black circles [38, 113]. The solid line represents the function (6.4).

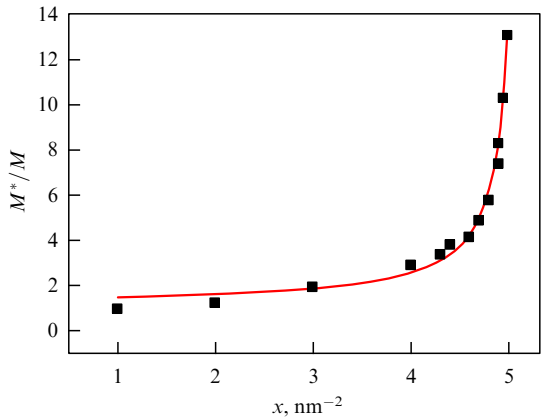

Figure 6. The ratio M^*/M in 2D ^{3}He as a function of the density x of the liquid, obtained from heat capacity and magnetization measurements. The experimental data are marked by black squares [37, 59], and the solid line represents the function $M^*(x)/M = A + B/(x_{FC} - x)$, where $A = 1.09$, $B = 1.68$ nm^{-2}, and $x_{FC} = 5.11$ nm^{-2}.

In the case of 3D systems, as $x \to x_{FC}$, the effective mass is given by the expression [42]

$$\frac{1}{M^*} \approx \frac{1}{M} + \frac{p_F}{4\pi^2}\int_{-1}^{1}\int_{0}^{g_0} \frac{v\big(q(y)\big)\,y\,dy\,dg}{\big[1 - R\big(q(y),g\big)\,\chi_0\big(q(y)\big)\big]^2}\,. \tag{6.6}$$

Comparison of Eqns (6.1) and (6.6) shows that there is no essential difference between them, although they describe different cases, 2D and 3D. In the 3D case, we can derive equations similar to (6.4) and (6.5) just as we did in the 2D case, but the numerical coefficients are different, because they depend on the number of dimensions. The only difference between 2D and 3D electron systems is that the Fermi-condensate quantum phase transition occurs in 3D systems at densities much lower than those corresponding to 2D systems. No such transition occurs in massive 3D ^{3}He because the transition is absorbed by the first-order liquid – solid phase transition [37, 59].

7. A highly correlated Fermi liquid in heavy-fermion metals

As noted in the introduction, universal behavior becomes observable in ordinary quantum phase transitions only when the electron system of a heavy-fermion metal is very close to the quantum critical point, e.g., when the correlation length is much larger than the microscopic length scale. Under this condition, the physics of the phenomenon is determined by the thermal and quantum fluctuations of the critical state, characterized by the absence of quasiparticles. But theories based on ordinary quantum phase transitions cannot explain the results of experimental observations related to the divergence of the effective mass M^* in a magnetic field, the specific behavior of the spin susceptibility and its scale properties, the behavior of thermal expansion, the constancy of the Kadowaki–Woods relation, etc. [6, 8, 9, 12, 13, 18, 31, 103, 114–120].

7.1 Dependence of the effective mass M^* on the magnetic field

When a Fermi system approaches a Fermi-condensate quantum phase transition from the disordered side, it remains a Landau Fermi liquid with an effective mass M^* that strongly depends on the distance $r = (x - x_{\rm FC})/x_{\rm FC}$, the temperature T, and the magnetic field B. This state of the system with M^* that strongly depends on T, r, and B resembles the state of a strongly correlated liquid described in Section 2. But in contrast to a strongly correlated liquid, the system in question involves no energy scale E_0 specified by Eqn (2.16) and at low temperatures becomes a Landau Fermi liquid with an effective mass $M^* \propto 1/r$ [see Eqns (2.7) and (6.5)]. Such a liquid can be called a highly correlated liquid; as we see shortly, it exhibits unusual properties that differ from those of strongly correlated Fermi systems [36, 121].

We use the Landau equation to study the behavior of the effective mass $M^*(T, B)$ as a function of the temperature and the magnetic field. For a homogeneous liquid at finite temperatures and magnetic fields, this equation acquires the form [22]

$$\frac{1}{M^*(T,B)} = \frac{1}{M} + \sum_{\sigma_1} \int \frac{\mathbf{p}_{\rm F}\mathbf{p}}{p_{\rm F}^3} F_{\sigma,\sigma_1}(\mathbf{p}_{\rm F},\mathbf{p}) \frac{\partial n_{\sigma_1}(\mathbf{p},T,B)}{\partial p} \frac{{\rm d}\mathbf{p}}{(2\pi)^3}\,, \tag{7.1}$$

where $F_{\sigma,\sigma_1}(\mathbf{p}_{\rm F},\mathbf{p})$ is the Landau amplitude dependent on the momenta $p_{\rm F}$ and p and spin σ. Because heavy-fermion metals are predominantly three-dimensional, we assume that the heavy-electron liquid is also a 3D liquid. To simplify matters, we ignore the spin dependence of the effective mass, because $M^*(T, B)$ is nearly independent of the spin in weak fields. The quasiparticle distribution function can be expressed as

$$n_\sigma(\mathbf{p},T) = \left[1 + \exp\frac{\varepsilon(\mathbf{p},T) - \mu_\sigma}{T}\right]^{-1}, \tag{7.2}$$

where $\varepsilon(\mathbf{p}, T)$ is determined by Eqn (2.2). In our case, the single-particle spectrum depends on the spin only weakly, but the chemical potential may depend on spin due to the Zeeman splitting. When this is important, we specifically indicate the spin dependence of physical quantities. We write the quasiparticle distribution function as

$$n_\sigma(\mathbf{p},T,B) \equiv \delta n_\sigma(\mathbf{p},T,B) + n_\sigma(\mathbf{p},T=0,B=0)\,.$$

Equation (7.1) then becomes

$$\frac{M}{M^*(T,B)} = \frac{M}{M^*(x)} + \frac{M}{p_{\rm F}^2}\sum_{\sigma_1}\int \frac{\mathbf{p}_{\rm F}\mathbf{p}_1}{p_{\rm F}} \times F_{\sigma,\sigma_1}(\mathbf{p}_{\rm F},\mathbf{p}_1)\frac{\partial\delta n_{\sigma_1}(\mathbf{p}_1,T,B)}{\partial p_1}\frac{{\rm d}\mathbf{p}_1}{(2\pi)^3}\,. \tag{7.3}$$

We assume that the highly correlated electron liquid is close to the Fermi-condensate quantum phase transition and the distance r is small, and therefore $M/M^*(x) \ll 1$, as follows from Eqn (2.7). For normal metals, where the electron liquid behaves like a Landau Fermi liquid with the effective mass of several 'bare' electron masses $M/M^*(x) \sim 1$, at temperatures near 1000 K, the second term on the right-hand side of Eqn (7.3) is of the order of T^2/μ^2 and is much smaller than the first term. The same is true, as can be verified, when a magnetic field $B \lesssim 100$ T is applied. Thus, at $M/M^*(x) \sim 1$, the system behaves like a Landau Fermi liquid with an effective mass that is actually independent of the temperature or magnetic field, while $\rho(T) \propto T^2$. This means that the corrections to the effective mass determined by the second term on the right-hand side of Eqn (7.3) are proportional to $(T/\mu)^2$ or $(\mu_{\rm B}B/\mu)^2$, where $\mu_{\rm B}$ is the Bohr magneton.

Near the critical point $x_{\rm FC}$, with $M/M^*(x \to x_{\rm FC}) \to 0$, the behavior of the effective mass changes dramatically because the first term on the right-hand side of Eqn (7.3) vanishes, the second term becomes dominant, and the effective mass is determined by the homogeneous version of (7.3) as a function of B and T.

We now qualitatively analyze the solutions of Eqn (7.3) at $x \approx x_{\rm FC}$ and $T = 0$. Application of a magnetic field leads to Zeeman splitting of the Fermi surface, and the distance δp between the Fermi surfaces with spin up and spin down becomes $\delta p = p_{\rm F}^{\uparrow} - p_{\rm F}^{\downarrow} \sim \mu_{\rm B}BM^*(B)/p_{\rm F}$. We note that the second term on the right-hand side of Eqn (7.3) is proportional to $(\delta p)^2 \propto \left(\mu_{\rm B}BM^*(B)/p_{\rm F}\right)^2$, and therefore Eqn (7.3) reduces to [30, 102, 122]

$$\frac{M}{M^*(B)} = \frac{M}{M^*(x)} + c\,\frac{\left(\mu_{\rm B}BM^*(B)\right)^2}{p_{\rm F}^4}\,, \tag{7.4}$$

where c is a constant. We also note that $M^*(B)$ depends on x and that this dependence disappears at $x = x_{\rm FC}$. At this point, the term $M/M^*(x)$ vanishes and Eqn (7.4) becomes homogeneous and can be solved analytically [36, 102, 122]:

$$M^*(B) \propto \frac{1}{(B - B_{\rm c0})^{2/3}}\,, \tag{7.5}$$

where $B_{\rm c0}$ is the critical magnetic field, regarded as a parameter [see the remarks after Eqn (5.5)].

Equation (7.5) specifies the universal power-law behavior of the effective mass, irrespective of the interaction type. For densities $x > x_{\rm FC}$, the effective mass $M^*(x)$ is finite and we deal with ordinary Landau quasiparticles if the magnetic field is so weak that

$$\frac{M^*(x)}{M^*(B)} \ll 1\,,$$

with $M^*(B)$ given by (7.5). The second term on the right-hand side of Eqn (7.4), which is proportional to $\left(BM^*(x)\right)^2$, is only

a small correction. In the opposite case, where

$$\frac{M^*(x)}{M^*(B)} \gg 1\,,$$

the electron liquid behaves as if it were at the quantum critical point. In the Landau Fermi-liquid mode, the main thermodynamic and transport properties of the system are determined by the effective mass, and it therefore follows from Eqn (7.5) that we have the unique possibility of controlling this mass by varying the magnetoresistance, resistivity, heat capacity, magnetization, thermal bulk expansion, etc. It must be noted that a large effective mass leads to a high density of states, which causes the emergence of a large number of competing states and phase transitions [123]. We believe that such states can be suppressed by applying an external magnetic field, and we examine the thermodynamic properties of the system without considering such competition.

7.2 Dependence of the effective mass M^* on the temperature and the damping of quasiparticles

For a qualitative examination of the behavior of $M^*(T)$ as the temperature increases, we simplify Eqn (7.3) by dropping the variable B and by imitating the effect of an external magnetic field by a finite effective mass in the denominator of the first term on the right-hand side of Eqn (7.3). Then the effective mass becomes a function of the distance r, $M^*(r)$, determined also by the magnitude of the magnetic field B. In a zero magnetic field, $r = (x - x_{\rm FC})/x_{\rm FC}$. We integrate the second term on the right-hand side of Eqn (7.3) with respect to the angular variables, then integrate by parts with respect to p, and replace p with $z = \big(\varepsilon(p) - \mu\big)/T$. In the case of a flat and narrow band, we can use the approximation where $\varepsilon(p) - \mu \approx p_{\rm F}(p - p_{\rm F})/M^*(T)$. The result is

$$\frac{M}{M^*(T)} = \frac{M}{M^*(r)} + \alpha\int_0^\infty \frac{F\big(p_{\rm F}, p_{\rm F}(1+\alpha z)\big)\,{\rm d}z}{1+\exp z} - \alpha\int_0^{1/\alpha} F\big(p_{\rm F}, p_{\rm F}(1-\alpha z)\big)\,\frac{{\rm d}z}{1+\exp z}\,, \tag{7.6}$$

where we use the notation $F \sim M\,{\rm d}(F^1 p^2)/{\rm d}p$, $\alpha = TM^*(T)/p_{\rm F}^2 = TM^*(T)/\big(T_{\rm k}M^*(r)\big)$, and $T_{\rm k} = p_{\rm F}^2/M^*(r)$, and the Fermi momentum is defined by the condition $\varepsilon(p_{\rm F}) = \mu$.

We first consider the case where $\alpha \ll 1$. Then, discarding terms of the order $\exp(-1/\alpha)$, we can set the upper limit in the second integral on the right-hand side of Eqn (7.6) to infinity, with the result that the sum of the second and third terms is an even function of α. The resulting integrals are typical expressions involving the Fermi–Dirac function in the integrand and can be evaluated by a standard procedure (e.g., see Ref. [124]). Because we need only an estimate of the integrals, we write Eqn (7.6) as

$$\frac{M}{M^*(T)} \approx \frac{M}{M^*(r)} + a_1\left(\frac{TM^*(T)}{T_{\rm k}M^*(r)}\right)^2 + a_2\left(\frac{TM^*(T)}{T_{\rm k}M^*(r)}\right)^4 + \ldots, \tag{7.7}$$

where a_1 and a_2 are constants of the order of unity.

Equation (7.7) is a typical equation of the Landau Fermi-liquid theory. The only exception is the effective mass $M^*(r)$, which depends strongly on the distance r and diverges as $r \to 0$. Nevertheless, Eqn (7.7) implies that as $T \to 0$, the corrections to $M^*(r)$ begin with terms of the order T^2 if

$$\frac{M}{M^*(r)} \gg \left(\frac{TM^*(T)}{T_{\rm k}M^*(r)}\right)^2 \approx \frac{T^2}{T_{\rm k}^2} \tag{7.8}$$

and the system behaves like a Landau Fermi liquid. Condition (7.8) implies that the behavior inherent in the Landau Fermi liquid disappears as $r \to 0$ and $M^*(r) \to \infty$. Then the free term on the right-hand side of Eqn (7.6) is negligible, $M/M^*(r) \to 0$, and Eqn (7.6) becomes homogeneous and determines the universal behavior of the effective mass $M^*(T)$.

At a certain temperature $T_1 \ll T_{\rm k}$, the value of the sum on the right-hand side of Eqn (7.7) is determined by the second term and relation (7.8) becomes invalid. Keeping only the second term in Eqn (7.7), we arrive at an equation for determining $M^*(T)$ in the transition region [122, 125]:

$$M^*(T) \propto \frac{1}{T^{2/3}}\,. \tag{7.9}$$

The temperature dependence of the $T^{-2/3}$ type in (7.9) merits a remark. Equation (7.9) holds if the second term in Eqn (7.7) is much larger than the first,

$$\frac{T^2}{T_{\rm k}^2} \gg \frac{M}{M^*(r)}\,, \tag{7.10}$$

and, at the same time, much larger than the third,

$$\frac{T}{T_{\rm k}} \ll \frac{M^*(r)}{M^*(T)} \approx 1\,. \tag{7.11}$$

Obviously, both inequalities (7.10) and (7.11) are satisfied if $M/M^*(r) \ll 1$ and T is finite. The temperature range within which Eqn (7.9) is valid collapses to zero as $r \to 0$ because $T_{\rm k} \to 0$.

Thus, if the system is very close to the quantum critical point, $x \to x_{\rm FC}$, the behavior of the effective mass specified by Eqn (7.9) is possible within a broad temperature range only if $M^*(r)$ is significantly reduced due to a magnetic field applied to the system. We can say that the distance r becomes large because of the magnetic field B. When B is finite, the $T^{-2/3}$-dependence may be observed at a relatively high temperature $T > T_1(B)$.

As regards an estimate of the transition temperature $T_1(B)$ at which the effective mass becomes temperature-dependent, we note that the effective mass is a continuous function of the temperature and the magnetic field: $M^*(B) \sim M^*(T_1)$. With Eqns (7.5) and (7.9), we obtain $T_1(B) \propto B$.

As the temperature increases, the system transfers into another mode. The coefficient α is then of the order of unity, $\alpha \sim 1$, the upper limit in the second integral in Eqn (7.6) cannot be set to infinity, and odd terms begin to play a significant role. As a result, Eqn (7.7) breaks down and the sum of the first and second integrals on the right-hand side of Eqn (7.6) becomes proportional to $M^*(T)T$. Ignoring the first term $M/M^*(r)$ and approximating the sum of integrals by $M^*(T)T$, we obtain from (7.6) that

$$M^*(T) \propto \frac{1}{\sqrt{T}}\,. \tag{7.12}$$

We therefore conclude that as the temperature increases and the condition $x \approx x_{\rm FC}$ is satisfied, the system demon-

strates regimes of three types: (i) the behavior of the Landau Fermi liquid at $\alpha \ll 1$, when Eqn (7.8) is valid and the behavior of the effective mass is described by Eqn (7.5); (ii) the behavior defined by Eqn (7.9), when $M^*(T) \propto T^{-2/3}$ and $S(T) \propto M^*(T)T \propto T^{1/3}$; and (iii) the behavior at $\alpha \sim 1$, when Eqn (7.12) is valid, $M^*(T) \propto 1/\sqrt{T}$, the entropy $S(T) \propto M^*(T)T \propto \sqrt{T}$, and the heat capacity $C(T) = T\big(\partial S(T)/\partial T\big) \propto \sqrt{T}$.

We illustrate the behavior of $S(T)$ by calculations based on the model Landau functional [24, 123]

$$E\big[n(p)\big] = \int \frac{\mathbf{p}^2 n(\mathbf{p})}{2M}\,\frac{\mathrm{d}\mathbf{p}}{(2\pi)^3} + \frac{1}{2}\int V(\mathbf{p}_1 - \mathbf{p}_2)n(\mathbf{p}_1)n(\mathbf{p}_2)\,\frac{\mathrm{d}\mathbf{p}_1\,\mathrm{d}\mathbf{p}_2}{(2\pi)^6} \tag{7.13}$$

with the interparticle interaction

$$V(\mathbf{p}) = g_0\,\frac{\exp\big(-\beta_0|\mathbf{p}|\big)}{|\mathbf{p}|}\,. \tag{7.14}$$

We normalize the effective mass to M, i.e., $M^* = M^*/M$, and the temperature T_0 to the Fermi energy $\varepsilon_{\mathrm{F}}^0$, i.e., $T = T_0/\varepsilon_{\mathrm{F}}^0$, and use the dimensionless coupling constant $g = g_0 M/(2\pi^2)$ and also $\beta = \beta_0 p_{\mathrm{F}}$. The Fermi-condensate quantum phase transition occurs when these parameters reach the critical values $\beta = b_{\mathrm{c}}$ and $g = g_{\mathrm{c}}$. On the other hand, a transition of this kind occurs as $M^* \to \infty$. This condition allows deriving a relation between b_{c} and g_{c} [24, 123]:

$$\frac{g_{\mathrm{c}}}{b_{\mathrm{c}}^3}\,(1 + b_{\mathrm{c}})\exp(-b_{\mathrm{c}})(b_{\mathrm{c}}\cosh b_{\mathrm{c}} - \sinh b_{\mathrm{c}}) = 1\,.$$

This relation implies that the critical point of the Fermi-condensate quantum phase transition can be reached by varying g_0 if β_0 and p_{F} are fixed, by varying p_{F} if β_0 and g_0 are fixed, etc. For definiteness, we vary g to reach the Fermi-condensate quantum phase transition or to study the properties of the system beyond the critical point. Calculations of $M^*(T)$, $S(T)$, and $C(T)$ based on model functional (7.13) with the parameters $g = g_{\mathrm{c}} = 6.7167$ and $\beta = b_{\mathrm{c}} = 3$ show that $M^*(T) \propto 1/\sqrt{T}$, $S(T) \propto \sqrt{T}$, and $C(T) \propto \sqrt{T}$. The temperature dependence of the entropy in this case is depicted in Fig. 7.

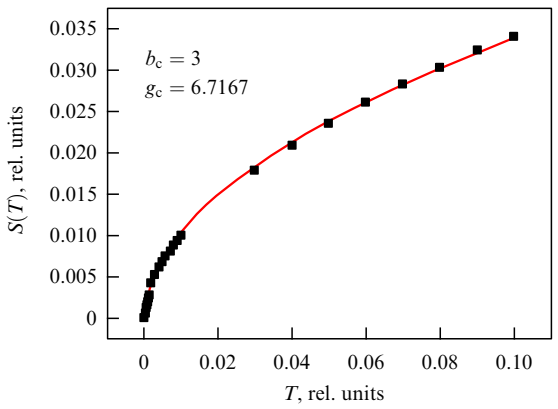

Figure 7. The entropy $S(T)$ of a highly correlated Fermi liquid at the critical point of the Fermi-condensate quantum phase transition. The solid line represents the function $S(T) \propto \sqrt{T}$, and the squares mark the results of calculations.

We now estimate the quasiparticle damping $\gamma(T)$. In the Landau Fermi-liquid theory, γ is given by [22]

$$\gamma \sim |\Gamma|^2 (M^*)^3 T^2\,, \tag{7.15}$$

where Γ is the particle–hole amplitude. In the case of a highly correlated system with a high density of states caused by the enormous effective mass, Γ cannot be approximated by the 'bare' interaction between particles but can be estimated within the 'ladder' approximation, which yields $|\Gamma| \sim 1/\big(p_{\mathrm{F}} M^*(T)\big)$ [54]. As a result, we find that $\gamma(T) \propto T^2$ in the Landau Fermi-liquid regime, $\gamma(T) \propto T^{4/3}$ in the $T^{-2/3}$-regime, and $\gamma(T) \propto T^{3/2}$ in the $1/\sqrt{T}$-regime. We note that in all these cases, the width is small compared to the characteristic quasiparticle energy, which is assumed to be of the order of T, and hence the quasiparticle concept is meaningful.

The conclusion that can be drawn here is that when the electron liquid is localized near the quantum critical point of the Fermi-condensate quantum phase transition and is on the disordered side, its low-energy excitations are quasiparticles with the effective mass $M^*(B, T)$.

We note that as $x \to x_{\mathrm{FC}}$, the quasiparticle renormalization factor $a(\mathbf{p})$ remains approximately constant and the divergence of the effective mass that follows from Eqn (2.7) is not related to the fact that $a(\mathbf{p}) \to 0$ [126]. Therefore, the quasiparticle concept remains valid and it is these quasiparticles that determine the transport and thermodynamic properties of the highly correlated electron liquid.

7.3 Electric resistivity of metals with heavy fermions

The electric resistivity

$$\rho(T) = \rho_0 + \Delta\rho_1(B, T)$$

is directly determined by the effective mass, because $\Delta\rho_1(B, T) = A(B, T)T^2 \propto \big(M^*(B, T)T\big)^2$ [104], and therefore the temperature dependences of the effective mass discussed above can be observed in measurements of the resistivity of heavy-fermion metals. At temperatures $T \ll T_1(B)$, the system is in the Landau Fermi-liquid regime, the behavior of the effective mass as $x \to x_{\mathrm{FC}}$ is described by Eqn (7.5), and the coefficient $A(B)$ can be represented as

$$A(B) \propto \frac{1}{(B - B_{\mathrm{c}0})^{4/3}}\,. \tag{7.16}$$

In this regime, the resistivity behaves as $\Delta\rho_1 = c_1 T^2/(B - B_{\mathrm{c}0})^{4/3} \propto T^2$. The second regime, a highly correlated Fermi liquid determined by Eqn (7.9), is characterized by the resistivity dependence $\Delta\rho_2 = c_2 T^2/(T^{2/3})^2 \propto T^{2/3}$. The third regime at $T > T_1(B)$ is determined by Eqn (7.12) and $\Delta\rho_3 = c_3 T^2/(\sqrt{T})^2 \propto T$. Here, c_1, c_2, and c_3 are constants.

We note that all temperature dependences corresponding to these regimes have been observed in measurements involving the heavy-fermion metals $CeCoIn_5$ and YbAgGe [18, 31, 116, 118]. By examining the ratio $\Delta\rho_2/\Delta\rho_1 \propto \big[(B - B_{\mathrm{c}0})/T\big]^{4/3}$, we can arrive at the very interesting conclusion that this ratio is a function of only one variable, $(B - B_{\mathrm{c}0})/T$, which agrees with the experimental facts [31].

7.4 Magnetic susceptibility

The magnetic susceptibility is proportional to the effective mass, $\chi \propto M^*$, where M^* is given by Eqns (7.5), (7.9), and (7.12). When $T \ll T_1$, the effective mass is given by (7.5) and

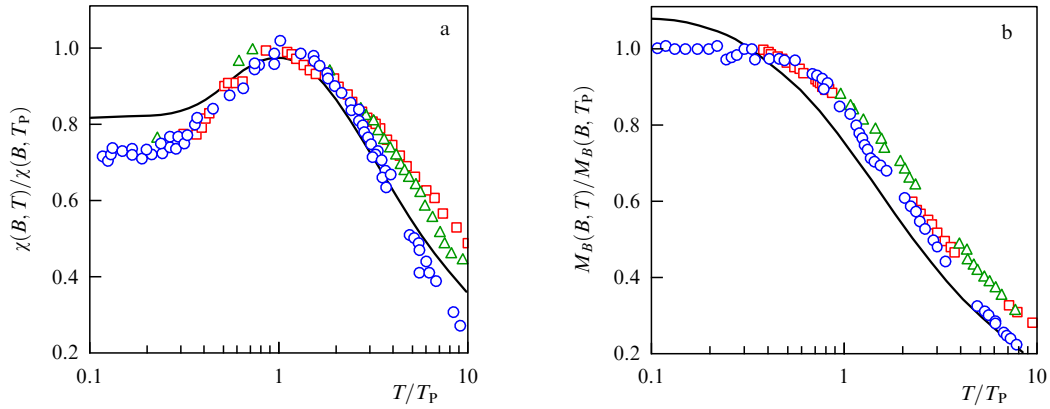

Figure 8. The normalized magnetic susceptibility $\chi(B,T)/\chi(B,T_P)$ (a) and normalized magnetization $M_B(B,T)/M_B(B,T_P)$ (b) for $CeRu_2Si_2$ in magnetic fields 0.20 mT (squares), 0.39 mT (triangles), and 0.94 mT (circles) as functions of the normalized temperature T/T_P [103]. The solid lines depict the calculated universal behavior [122].

the susceptibility is

$$\chi(B) \propto M^*(B) \propto (B - B_{c0})^{-2/3}. \tag{7.17}$$

The static magnetization is

$$M_B(B) \propto BM^*(B) \propto (B - B_{c0})^{1/3}. \tag{7.18}$$

At $T \sim T_1(B)$, as Eqn (7.9) shows, (7.17) becomes

$$\chi(T) \propto M^*(T) \propto T^{-2/3}. \tag{7.19}$$

For the temperature $T \gg T_1(B)$, as Eqn (7.12) shows, (7.17) becomes

$$\chi(T) \propto M^*(T) \propto T^{-1/2}. \tag{7.20}$$

The behavior of $\chi(B)$, $M_B(B)$, and $\chi(B,T)$ obtained by solving (7.3) (Fig. 8) is in good agreement with the results of measurements involving $CeRu_2Si_2$ with the critical field $B_{c0} = 0$ [103]. In Fig. 8, the temperature is normalized to T_P (the temperature at which the susceptibility reaches its peak value), the susceptibility is normalized to the peak value $\chi(B,T_P)$, and the magnetization is normalized to $M_B(B, T \to 0)$, for each value of the field.

We examine the state of the system as $r \to 0$. The properties of this state are determined by the magnetic field B and the temperature T. At the transition temperature $T \approx T_1(B)$, the effective mass depends on T and B; at $T \ll T_1(B)$, the system is a Landau Fermi liquid with the effective mass determined by Eqn (7.5); and at $T \gtrsim T_1(B)$, the effective mass is given by Eqn (7.9). Instead of solving Eqn (7.3), we can construct a simple interpolation formula describing the behavior of the effective mass for $T \lesssim T_1$:

$$M^*(B,T) = \frac{c_1(B - B_{c0})^2 + c_2T^2}{c_3(B - B_{c0})^{8/3} + c_4T^{8/3}}, \tag{7.21}$$

where c_1, c_2, c_3, and c_4 are certain constants. Dividing both sides of Eqn (7.21) by $M^*(B, T = 0)$ and introducing the notation $y = T/(B - B_{c0})$, we obtain

$$\frac{M^*(B,T)}{M^*(B)} = \frac{1 + (c_2/c_1)y^2}{1 + (c_4/c_3)y^{8/3}}. \tag{7.22}$$

Equation (7.22) shows that the behavior of the effective mass can be described by a universal function of a single variable, y. If we use (7.22) and the definition of susceptibility $\chi(B,T) = \partial M_B(B,T)/\partial B$, we can conclude that the susceptibility and magnetization also demonstrate scaling behavior and can be represented by a universal function of the single variable y, if they are respectively normalized to susceptibility (7.17) and magnetization (7.18). We note that the susceptibility $\chi(y)$ has a peak, while the magnetization has no peak [30, 122, 125]. It follows from Eqn (7.21) that the scaling behavior of the normalized susceptibility and magnetization is destroyed when $T \gg T_1(B)$, because the behavior of the effective mass at such temperatures is given by formula (7.12). Figure 8 shows that the above scaling behavior of the normalized susceptibility and magnetization agrees with the experiments involving $CeRu_2Si_2$, with the scaling behavior of the experimental points disappearing at $T \gg 1$, which corresponds to temperatures $T \gg T_P \approx T_1(B)$ [103].

We see from Fig. 8 that at finite field strengths B, the curve describing $\chi(B,T)/\chi(B,T_P)$ has a peak (more like a hump) at a certain temperature T_P, while $M_B(B,T)/M_B(B,T_P)$ has no such peak. This behavior agrees well with experimental results [103]. We note that such behavior of susceptibility is not typical of ordinary metals and cannot be explained within the scope of theories that take only ordinary quantum phase transitions into account [103].

7.5 Magnetoresistance

We now examine the behavior of the magnetoresistance

$$\rho_{mr}(B,T) = \frac{\rho(B,T) - \rho(0,T)}{\rho(0,T)} \tag{7.23}$$

of a highly correlated electron liquid as a function of the magnetic field B and the temperature T [121]. The resistivity $\rho(B,T) = \rho_0 + \Delta\rho(B,T) + \Delta\rho_{mr}(B)$ is measured in a magnetic field B at a temperature T. We assume that the contribution $\Delta\rho_{mr}(B)$ determined by the magnetic field can be considered in the weak-field approximation based on the well-known Kohler rule:

$$\frac{\Delta\rho_{mr}(B)}{\rho(0,T)} \approx \lambda_\perp \left(\frac{B\rho(0,\Theta_D)}{B_0\rho(0,T)}\right)^2, \tag{7.24}$$

where Θ_D is the Debye temperature, B_0 the characteristic magnetic field strength, and $\lambda_\perp$ a constant. We note that $\Delta\rho_{mr}(B) \ll \rho(0,T) \equiv \rho(T)$ is assumed in the weak-field approximation.

We suppose that the temperature is not very low, $\rho_0 \leqslant \Delta\rho(B=0,T)$, and $B \geqslant B_{c0}$. Substituting (7.24) in (7.23), we find that

$$\rho_{mr}(B,T) \approx \frac{\Delta\rho_{mr}(B)}{\rho(0,T)} + cT^2\,\frac{\left(M^*(B,T)\right)^2 - \left(M^*(0,T)\right)^2}{\rho(0,T)}\,, \tag{7.25}$$

where c is a constant determined by the temperature dependence of the resistivity: $c\left(M^*(B,T)\right)^2T^2 = \Delta\rho(B,T)$.

We examine the magnetoresistance described by Eqn (7.25) as a function of B at a certain temperature $T = T_0$. In weak magnetic fields, when $T_0 > T_1(B) \propto B$, the leading contribution to the magnetoresistance is made by the term $\Delta\rho_{mr}(B)$, because the effective mass is temperature-independent. Hence, $\left|M^*(B,T) - M^*(0,T)\right|/M^*(0,T) \ll 1$ and the leading contribution is made by $\Delta\rho_{mr}(B)$. As a result, the magnetoresistance is an increasing function of B. When B becomes so high that $T_1(B) \sim T_0$, the difference $M^*(B,T) - M^*(0,T)$ becomes negative and the magnetoresistance as a function of B reaches its maximum value at $T_1(B) > T_0$. As B increases still further, when $T_1(B) > T_0$, the effective mass $M^*(B,T)$ becomes a decreasing function of the magnetic field, as follows from Eqn (7.5). As B increases,

$$\frac{M^*(B,T) - M^*(0,T)}{M^*(0,T)} \to -1$$

and the magnetoresistance, being a decreasing function of B, is negative.

We now study the behavior of magnetoresistance as a function of T at a certain value B_0 of the magnetic field strength. At low temperatures $T \ll T_1(B_0)$, it follows from Eqns (7.5) and (7.12) that

$$\frac{M^*(B_0)}{M^*(T)} \ll 1\,,$$

and the magnetoresistance is determined by $\rho(0,T)$. We note that B_0 must be relatively high to guarantee that $M^*(B_0)/M^*(T) \ll 1$. Hence, $\rho_{mr}(B_0,T) \sim -1$, because $\Delta\rho_{mr}(B)/\rho(0,T) \ll 1$. As the temperature increases, the magnetoresistance increases, remaining negative. At $T \approx T_1(B_0)$, the magnetoresistance is approximately zero, because $M^*(B_0) \approx M^*(T)$ and $\rho(B_0,T) \approx \rho(0,T)$ at this point. This allows concluding that the change of the temperature dependence of resistivity $\rho(T)$ from quadratic to linear manifests itself in the transition from negative magnetoresistance to positive. At $T \geqslant T_1(B_0)$, the leading contribution to the magnetoresistance is made by $\Delta\rho_{mr}(B_0)$ and the magnetoresistance reaches its maximum. At $T_1(B_0) \ll T$, the magnetoresistance is a decreasing function of the temperature, because

$$\frac{\left|M^*(B,T) - M^*(0,T)\right|}{M^*(0,T)} \ll 1$$

and $\Delta\rho_{mr}(B_0)/\rho(T) \ll 1$ is a decreasing function of T.

Both transitions (from positive magnetoresistance to negative magnetoresistance with increasing B at a fixed temperature T and from negative magnetoresistance to positive magnetoresistance with increasing T at a fixed value of B) have been detected in measurements of the resistivity of $CeCoIn_5$ in a magnetic field [31]. Thus, the described behavior of magnetoresistance is in good agreement with the experimental results.

8. Metals with a strongly correlated electron liquid

At $T \ll T_f$, the function $n_0(\mathbf{p})$ given by Eqn (2.8) determines the entropy $S_{NFL}(T)$ of a heavy-electron liquid on the ordered side of the Fermi-condensate quantum phase transition. As follows from Eqn (2.10), the entropy contains a temperature-independent contribution,

$$S_0 \sim \frac{p_f - p_i}{p_F} \sim |r|\,,$$

where $r = (x - x_{FC})/x_{FC}$. Another specific contribution is related to the spectrum $\varepsilon(\mathbf{p})$, which ensures a link between the dispersionless region (p_i, p_f) occupied by the Fermi condensate and the normal quasiparticles in the regions $p < p_i$ and $p > p_f$. This spectrum has the form $\varepsilon(\mathbf{p}) \propto (p - p_f)^2 \sim (p_i - p)^2$. Such a shape of the spectrum, corroborated in exactly solvable models for systems with a Fermi condensate, leads to a contribution to the heat capacity $C \sim \sqrt{T/T_f}$ [23]. Therefore, for $0 < T \ll T_f$, the entropy can be approximated by the function

$$S_{NFL}(T) \approx S_0 + a\sqrt{\frac{T}{T_f}} + b\,\frac{T}{T_f}\,, \tag{8.1}$$

where a and b are constants. The third term on the right-hand side of Eqn (8.1), which emerges because of the contribution of the temperature-independent part of the spectrum $\varepsilon(\mathbf{p})$, yields a relatively small addition to the entropy. As we see shortly, the temperature-independent term S_0 determines the universal transport and thermodynamic properties of a heavy-electron liquid with a Fermi condensate, which we call a strongly correlated Fermi liquid. The properties of this liquid differ dramatically from those of highly correlated systems. As a result, we can think of the Fermi-condensate quantum phase transition as a phase transition that separates highly correlated and strongly correlated Fermi liquids. Because a highly correlated liquid behaves like a Landau Fermi liquid as $T \to 0$, the Fermi-correlated quantum phase transition separates the Landau Fermi liquid from a strongly correlated Fermi liquid.

Figure 9 shows the temperature dependence $S(T)$ calculated on the basis of model functional (7.13). The calculations were done with $g = 7$, 8, and 12 and $\beta = b_c = 3$. We recall that the critical value of g is $g_c = 6.7167$. We see in Fig. 9 that S_0 increases as the system moves away from the Fermi-condensate quantum phase transition. Obviously, the term S_0 on the right-hand side of Eqn (8.1), which is temperature-independent, contributes nothing to the heat capacity, but the second term in (8.1) makes a contribution, and the heat capacity behaves anomalously, $C(T) \propto \sqrt{T}$, a fact corroborated by our calculations.

8.1 Entropy, linear expansion, and Grüneisen's law

The unusual temperature dependence of the entropy of a strongly correlated electron liquid specified by Eqn (8.1) determines the unusual behavior of the liquid. The existence of a temperature-independent term S_0 can be illustrated by

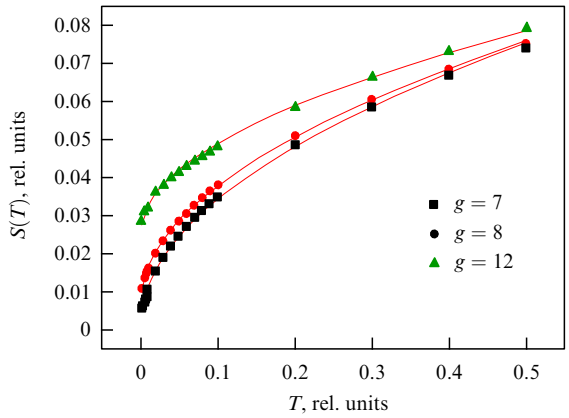

Figure 9. Entropy $S(T)$ as a function of temperature. The lines represent the approximation for $S(T)$ calculated based on Eqn (8.1), the symbols mark the results of calculations based on (7.13).

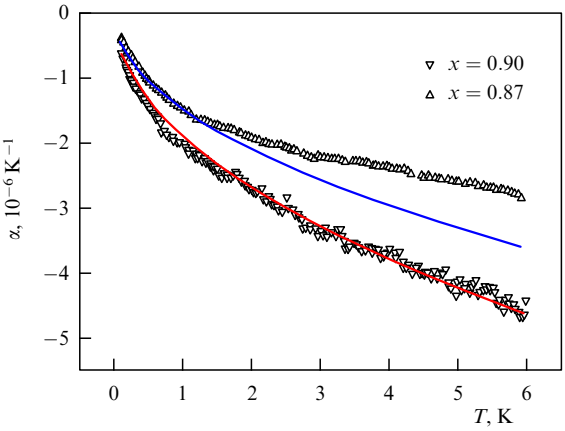

Figure 10. Thermal expansion coefficient $\alpha(T)$ as a function of temperature in the interval $0.1 \leqslant T \leqslant 6$ K. The experimental values for doping levels $x = 0.90$ and 0.87 are taken from Ref. [130]. The solid lines represent approximations of the experimental values of $\alpha(T) = c_1\sqrt{T}$, where c_1 is a fitting parameter.

calculating the thermal expansion coefficient $\alpha(T)$ [127, 128], which is given by [22]

$$\alpha(T) = \frac{1}{3}\left(\frac{\partial(\log V)}{\partial T}\right)_P = -\frac{1}{3V}\left(\frac{\partial(S/x)}{\partial P}\right)_T, \tag{8.2}$$

where P is the pressure and V is the volume. We note that the compressibility $K = \mathrm{d}\mu/\mathrm{d}(Vx)$ does not develop a singularity at the Fermi-condensate quantum phase transition and is approximately constant in systems with a Fermi condensate [129]. Substituting (8.1) in Eqn (8.2), we find that

$$\alpha_{\mathrm{FC}}(T) \approx a_0 \sim \frac{M^*_{\mathrm{FC}} T}{p_{\mathrm{F}}^2 K}, \tag{8.3}$$

where $a_0 \sim \partial S_0/\partial P$ is temperature-independent. In (8.3), we took only the leading contribution related to S_0 into account. We recall that

$$C(T) = T\frac{\partial S(T)}{\partial T} \approx \frac{a}{2}\sqrt{\frac{T}{T_{\mathrm{f}}}}. \tag{8.4}$$

As a result, the Grüneisen ratio $\Gamma(T)$ diverges as

$$\Gamma(T) = \frac{\alpha(T)}{C(T)} \approx 2\,\frac{a_0}{a}\sqrt{\frac{T_{\mathrm{f}}}{T}}, \tag{8.5}$$

from which we conclude that Grüneisen's law does not hold in strongly correlated Fermi systems.

We now see how the behavior of the effective mass described by Eqns (2.14) and (7.12) is related to the results of experimental observation. The thermal expansion coefficient $\alpha(T)$ measured for the paramagnet $CeNi_2Ge_2$ behaves as $\sqrt{T}$ as the temperature varies from 6 K to 50 mK [12]. The same behavior $\alpha(T) \propto \sqrt{T}$ was detected in measurements involving the ferromagnet $CePd_{1-x}Rh_x$ [130] (Fig. 10).

Figure 10 shows that at the critical point $x = 0.90$ at which the critical temperature of the ferromagnetic phase transition vanishes, the thermal expansion coefficient is well approximated by the dependence $\alpha(T) \propto \sqrt{T}$ as the temperature varies by almost two orders of magnitude, but even a small deviation of the system from the critical point destroys the correspondence between this approximation and the experimental data.

We note that it is possible to describe the critical behavior of two entirely different heavy-fermion metals (one is a paramagnet and the other a ferromagnet) by the function $\alpha(T) = c_1\sqrt{T}$ with only one fitting parameter c_1. This fact vividly shows that fluctuations do not determine the behavior of $\alpha(T)$. Heat-capacity measurements for $CePd_{1-x}Rh_x$ with $x = 0.90$ have shown that $C(T) \propto \sqrt{T}$ [130]. Thus, the electron systems of both metals can be interpreted as being highly correlated electron liquids.

Measurements that have been conducted with $YbRh_2(Si_{0.95}Ge_{0.05})_2$ show that $\alpha/T \propto 1/T$ and that the Grüneisen ratio diverges as $\Gamma(T) \approx T^{-q}$, with $q \approx 0.33$, which allows classifying the electron system of this compound as a strongly correlated liquid [12]. Our estimate $q = 0.5$, which follows from Eqn (8.5), is in satisfactory agreement with this experimental value. Both types of behavior of $\alpha(T)$ contradict the Landau Fermi-liquid theory, according to which the thermal expansion coefficient $\alpha(T)/T = M^* = \text{const}$ as $T \to 0$. In our case, the effective mass depends on T, and the $1/\sqrt{T}$-dependence that follows from Eqn (7.12) is in good agreement with the results for the first system [127], while the $1/T$-dependence of the effective mass, which follows from Eqn (2.14) and was predicted in Ref. [128], corresponds to the second result.

Equation (2.14) implies that $M^*(T \to 0) \to \infty$ and that a strongly correlated electron system behaves as if it were placed at the quantum critical point. Actually, the liquid is on the quantum critical curve $x < x_{\mathrm{FC}}$, and critical behavior is observed for all $x \leqslant x_{\mathrm{FC}}$ as $T \to 0$. It was shown in Section 3 that as $T \to 0$, the strongly correlated electron liquid undergoes a first-order quantum phase transition, because the entropy becomes a discontinuous function of the temperature: at finite temperatures, the entropy is given by Eqn (8.1), while $S(T = 0) = 0$. Hence, the entropy has a discontinuity $\delta S = S_0$ as $T \to 0$. This implies that, as a result of a first-order phase transition, all critical fluctuations are suppressed along the quantum critical curve and the respective divergences, e.g., the divergence of $\Gamma(T)$, are determined by quasiparticles and not critical fluctuations, as could be expected in the case of an ordinary quantum phase transition [4]. We note that according to the well-known inequality [124] $\delta Q \leqslant T\delta S$, the heat δQ of the transition from the disordered phase to the ordered phase is zero, because $\delta Q \leqslant S_0 T$ tends to zero as $T \to 0$.

8.2 The $T-B$ phase diagram, the Hall coefficient, and the magnetic susceptibility

To study the $T-B$ phase diagram of a strongly correlated electron liquid, we examine the case where non-Fermi-liquid (NFL) behavior emerges when the antiferromagnetic (AF) phase is suppressed by an external magnetic field B, e.g., as it is in the heavy-fermion metals $YbRh_2Si_2$ and $YbRh_2(Si_{0.95}Ge_{0.05})_2$ [12, 13].

The antiferromagnetic phase is a Landau electron Fermi liquid with the entropy vanishing as $T \to 0$. For magnetic fields higher than the critical value B_{c0} at which the Néel temperature $T_N(B \to B_{c0}) \to 0$, the antiferromagnetic phase transforms into a weakly polarized paramagnetic strongly correlated electron liquid. As shown in Section 5, a magnetic field applied to the system with $T = 0$ splits the Fermi-condensate state occupying the interval (p_i, p_f) into Landau levels and suppresses the superconducting order parameter $\kappa(\mathbf{p})$. The new state is specified by a multiply connected Fermi sphere, on which a smooth quasiparticle distribution function $n_0(\mathbf{p})$ in the interval (p_i, p_f) is replaced with a distribution $\nu(\mathbf{p})$ (see Fig. 4). Hence, the behavior of the Landau Fermi liquid is restored and is characterized by quasiparticles with the effective mass $M^*(B)$ given by Eqn (5.5). When the temperature increases so high that

$$T > T^*(B - B_{c0}) \propto \sqrt{B - B_{c0}}\,,$$

the entropy of the electron liquid is determined by Eqn (8.1). The described behavior of the strongly correlated liquid is shown in the $T-B$ diagram in Fig. 11.

In accordance with the experimental data, we assume that at relatively high temperatures, such that $T/T_{NO} \sim 1$, where T_{NO} is the Néel temperature in a zero magnetic field, the antiferromagnetic phase transition is a second-order one [13]. In this case, the entropy and other thermodynamic functions at the transition temperature $T_N(B)$ are continuous. This means that the entropy S_{AF} of the antiferromagnetic phase coincides with the entropy S_{NFL} of the strongly correlated liquid given by Eqn (8.1):

$$S_{AF}\big(T \to T_N(B)\big) = S_{NFL}\big(T \to T_N(B)\big)\,. \tag{8.6}$$

Since the antiferromagnetic phase behaves like a Landau Fermi liquid, i.e., $S_{AF}(T \to 0) \to 0$, Eqn (8.6) is not valid at low temperatures $T \leqslant T_{crit}$ because of the temperature-independent term S_0. Hence, the second-order antiferromagnetic phase transition becomes a first-order one at $T = T_{crit}$ (see Fig. 11).

At $T = 0$, the critical magnetic field B_{c0} in which the antiferromagnetic phase becomes a Landau Fermi liquid is determined by the condition that the ground-state energy of the antiferromagnetic phase be equal to the ground-state energy $E\big[n_0(\mathbf{p})\big]$ of the Landau electron Fermi liquid. This means that the ground state of the antiferromagnetic phase is degenerate at $B = B_{c0}$. Hence, the Néel temperature $T_N(B \to B_{c0}) \to 0$, the behavior of the effective mass $M^*(B \geqslant B_{c0})$ is determined by Eqn (5.5), and $M^*(B)$ diverges as $B \to B_{c0}$.

The phase transition separating the antiferromagnetic phase existing at $B \leqslant B_{c0}$ from the Landau Fermi liquid existing at $B \geqslant B_{c0}$ is a first-order quantum phase transition. The driving parameter of this phase transition is the magnetic field strength B. We note that the respective quantum and thermal critical fluctuations disappear at $T < T_{crit}$ because a first-order antiferromagnetic phase transition occurs at such temperatures.

We can also conclude that the critical behavior observed as $T \to 0$ and $B \to B_{c0}$ is determined by quasiparticles and not by critical fluctuations that accompany second-order phase transitions. As $r \to 0$, the electron liquid approaches the Fermi-condensate quantum phase transition from the ordered side. Obviously, $T_{crit} \to 0$ at the point $r = 0$, and the Néel temperature is zero at the point where the second-order antiferromagnetic phase transition becomes a first-order transition. Hence, the contributions determined by critical fluctuations can be expected to result in only logarithmic corrections to the values calculated in the Landau theory of phase transitions [124], while the power laws of critical behavior are again determined by the appropriate quasiparticles.

Thus, Landau's paradigm based on the concept of quasiparticles and the order parameter can be applied in studies of the $T-B$ phase diagram of a strongly correlated electron liquid.

We now examine the jump in the Hall coefficient detected in measurements involving $YbRh_2Si_2$. The Hall coefficient $R_H(B)$ as a function of B experiences a jump as $T \to 0$ when the applied magnetic field reaches its critical value $B = B_{c0}$, and then becomes even higher than the critical value at $B = B_{c0} + \delta B$, where δB is an infinitely small magnetic field strength [131]. As shown in Fig. 5, when $T = 0$, introduction of the critical magnetic field B_{c0}, which suppresses the antiferromagnetic phase (with the Fermi momentum $p_{AF} \approx p_F$) restores the Landau Fermi liquid with a Fermi momentum $p_f > p_F$. When $B < B_{c0}$, the ground-state energy of the antiferromagnetic phase is lower than that of the Landau paramagnetic electron Fermi liquid, but for $B > B_{c0}$ we are confronted with the opposite case, where the Landau paramagnetic Fermi liquid has the lower energy. At $B = B_{c0}$ and $T = 0$, both phases have the same ground-state energy, because they are degenerate.

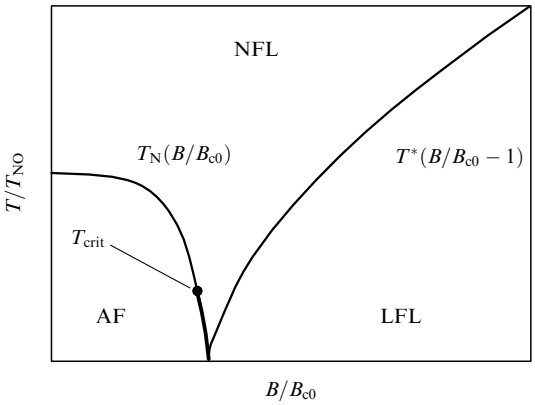

Figure 11. The $T-B$ phase diagram of a strongly correlated electron liquid. The line $T_N(B/B_{c0})$ represents the dependence of the Néel temperature on the field strength B. The black dot at $T = T_{crit}$ marks the critical temperature at which the second-order AF phase transition becomes a first-order one. For $T < T_{crit}$, the heavy solid line represents the function $T_N(B/B_{c0})$, when the AF phase transition becomes a first-order one. The strongly correlated liquid in the NFL region is characterized by the entropy S_{NFL} given by Eqn (8.1). The line separating the strongly correlated liquid (NFL) from the weakly polarized electron liquid, which behaves like the Landau Fermi liquid (LFL), is described by the function $T^*(B/B_{c0} - 1) \propto \sqrt{B/B_{c0} - 1}$ [see Eqn (5.8)].

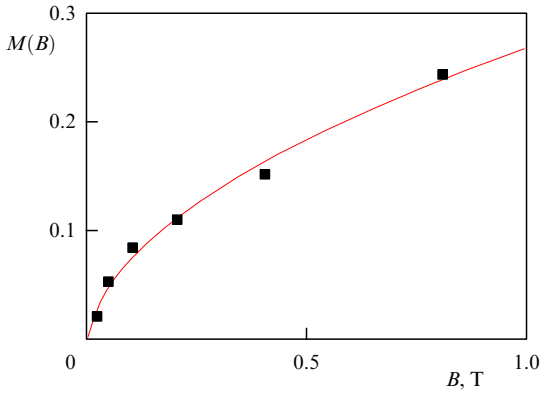

Figure 12. The values of magnetization $M(B)$ obtained in measurements involving $YbRh_2(Si_{0.95}Ge_{0.05})_2$ (black squares) [6]. The curve represents the field-dependent function $M(B) = a_M\sqrt{B}$ [see Eqn (8.9)], where a_M is a fitting parameter.

Thus, at $T = 0$ and $B = B_{c0}$, an infinitely small increase δB in the magnetic field leads to a finite discontinuity in the Fermi momentum, because the distribution function becomes multiply connected (see Fig. 4), but the number of mobile electrons does not change, As a result, the Hall coefficient experiences a sharp jump, because $R_H(B) \propto 1/p_F^3$ in the antiferromagnetic phase and $R_H(B) \propto 1/p_f^3$ in the paramagnetic phase. Assuming that $R_H(B)$ is a measure of the Fermi momentum [131] (as is the case with a simply connected Fermi volume), we obtain

$$\frac{R_H(B = B_{c0} - \delta)}{R_H(B = B_{c0} + \delta)} \approx 1 + 3\,\frac{p_f - p_F}{p_F} \approx 1 + d\,\frac{S_0}{x_{FC}}\,, \qquad (8.7)$$

where S_0/x_{FC} is the entropy per heavy electron and d is a constant ($d \sim 5$).

It follows from Eqn (8.7) that the discontinuity in the Hall coefficient is determined by the anomalous behavior of the entropy, which can be attributed to S_0. Hence, the discontinuity tends to zero as $r \to 0$ and disappears when the system is on the disordered side of the Fermi-condensate quantum phase transition, where the entropy has no temperature-independent term [132].

We turn to the magnetic susceptibility, which is proportional to the effective mass and is determined by Eqn (5.5). For $T \ll T^*(B)$, the magnetic susceptibility is given by [30]

$$\chi(B) \propto M^*(B) \propto \frac{1}{\sqrt{B - B_{c0}}}\,, \qquad (8.8)$$

and the static magnetization is

$$M(B) \propto \sqrt{B - B_{c0}}\,. \qquad (8.9)$$

Figure 12 shows that the function $M(B)$ that follows from (8.9) is in good agreement with the data of measurements involving $YbRh_2(Si_{0.95}Ge_{0.05})_2$; we note that $B_{c0} \approx 0$ in this case [6]. We also conclude that Eqns (7.21) and (7.22), which determine the scaling of the effective mass, static magnetization, and susceptibility, also hold in the case of a strongly correlated liquid, but with $y = T/\sqrt{B - B_{c0}}$. As a result, we find that the factor $d\rho/dT$ behaves as $A(B)T \propto T/(B - B_{c0})$ for $T < T^*(B)$ but behaves as $A(B)T \propto 1/T$ for $T > T^*(B)$ [30]. These observations agree with the data gathered in measurements involving $YbRh_2(Si_{0.95}Ge_{0.05})_2$ [6].

We note that as in the case of a highly correlated liquid, the susceptibility $\chi(y)$ of a strongly correlated liquid is not a monotonic function of y and has a peak. In experiments, such behavior manifests itself as the presence of a maximum in the function $\chi(B, T)$ observed at a fixed value of B with T varying. As shown in Section 5, the well-known empirical Kadowaki – Woods relation $K = A/\gamma_0^2 \approx$ const is also valid for a strongly correlated liquid [30]. These results are in good agreement with the experimental facts [6, 13, 133].

We examine the $T-B$ diagram of the heavy-fermion metal $YbRh_2Si_2$ [13] (Fig. 13). In the Landau Fermi-liquid region, the behavior of the metal is characterized by the effective mass $M^*(B)$, which diverges as $1/\sqrt{B - B_{c0}}$ [13]. It is quite evident that Eqn (5.5) provides a good description of this experimental fact: $M^*(B)$ diverges as $B \to B_{c0}$ at $T_N(B = B_{c0}) = 0$ and, as Fig. 12 shows, the calculated behavior of magnetization agrees with the experimental data. Figure 13 shows that in accordance with (5.8), the curve separating the Landau Fermi liquid region from the NFL region can be approximated by the function $c\sqrt{B - B_{c0}}$ with a fitting parameter c. Bearing in mind that the behavior of $YbRh_2Si_2$ is like that of $YbRh_2(Si_{0.95}Ge_{0.05})_2$ [6, 12, 115, 133], we conclude that the thermal expansion coefficient $\alpha(T)$ is temperature-independent and that the Grüneisen ratio diverges as a function of T in the NFL region [12]. We conclude that the entropy in the Landau Fermi-liquid region is determined by Eqn (8.1). Since the antiferromagnetic phase transition is second-order at relatively high temperatures [13], we can predict that as the temperature decreases, the phase transition becomes a first-order one. The above description of the behavior of the Hall coefficient $R_H(B)$ also agrees with the experimental facts [131].

Thus, we conclude that the universal $T-B$ phase diagram of a strongly correlated electron liquid shown in Fig. 11 agrees with the experimental $T-B$ diagram obtained from experiments involving the heavy-fermion metals $YbRh_2Si_2$ and $YbRh_2(Si_{0.95}Ge_{0.05})_2$ and shown in Fig. 13.

8.3 Heavy-fermion metals in the immediate vicinity of a Fermi-condensate quantum phase transition

We now consider the case where $\delta p_{FC} = (p_f - p_i)/p_F \ll 1$ and the electron system of a heavy-fermion metal is in a state close to the Fermi-condensate quantum phase transition while remaining on the ordered side. It follows from Eqn (5.10) that when the system is placed in a magnetic field $(B - B_{c0})/B_{c0} \geqslant B_c$, the system passes from the ordered side of the Fermi-condensate quantum phase transition to the disordered side, or the strongly correlated liquid transforms into a highly correlated one. As a result, when $T \leqslant T_1(B)$, the effective mass $M^*(B)$ is determined by Eqns (7.5) and (7.9), the Kadowaki – Woods relation and the Wiedemann – Franz law hold, and there are quasiparticles in the system. The resistivity then behaves as described in Section 7.3.

In a zero magnetic field or at temperatures $T_f \gg T > T_1(B)$, the system behaves like a strongly correlated Fermi liquid, the effective mass $M^*(T)$ is given by Eqn (2.14), and the entropy is determined by Eqn (8.1). The magnetic susceptibility $\chi(T) \propto M^*(T) \propto 1/T$, the thermal expansion coefficient $\alpha(T)$ is temperature-independent [as follows from Eqn (8.3)], and the Grüneisen ratio diverges, as follows from Eqn (8.5). We note that the heat capacity behaves as $C(T) \propto \sqrt{T}$ in either case, when the electron

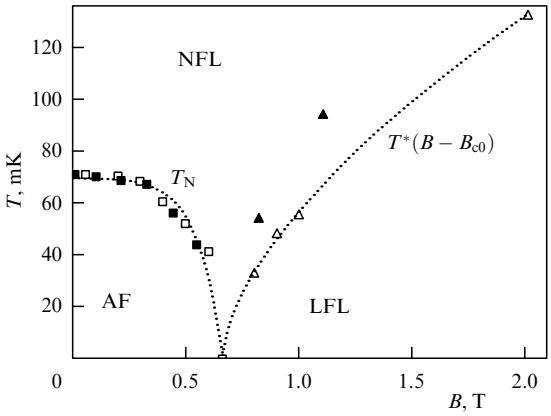

Figure 13. The $T-B$ phase diagram for $YbRh_2Si_2$; the symbols mark the experimental data [6, 13]. The line T_N depicts the field dependence of the Néel temperature. In the NFL region, the behavior of the strongly correlated liquid is characterized by the entropy S_{NFL} determined by Eqn (8.1). The line separating the NFL region from the LFL region, in which the strongly correlated liquid behaves like the Landau Fermi liquid with effective mass (5.5), was approximated by the function $T^*(B-B_{c0}) = c\sqrt{B-B_{c0}}$, where c is a fitting parameter.

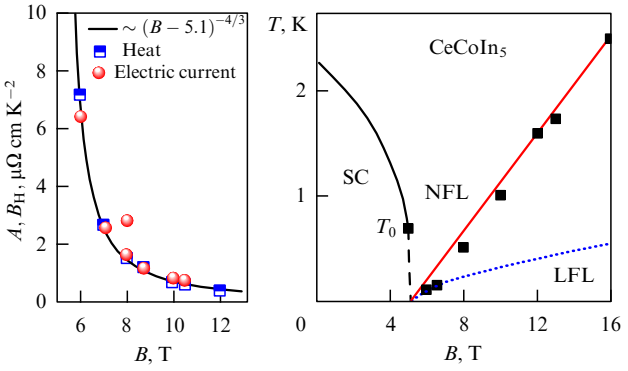

Figure 14. The $T-B$ phase diagram for $CeCoIn_5$. (a) The functions $A(B)$ and $B_H(B)$ that determine the T^2-dependence of resistance to the electric current and heat transfer in the Landau Fermi-liquid regime induced by the magnetic field; the symbols mark the experimental data. (b) The line of phase transitions in a magnetic field; the line separates the normal (NFL) state from the superconducting (SC) state [14]; the heavy solid curve corresponds to second-order phase transitions, the dashed curve corresponds to first-order phase transitions, the black square (at T_0) is the point where second-order transitions become first-order transitions. The dotted line represents the function $T^*(B)$ calculated in accordance with (8.10) for the transition region between the LFL and the strongly correlated liquid (NFL). The light solid line represents the function $T^*(B)$ calculated in accordance with (8.11) for the transition region (when $B \gg B_{cr}$) between the highly correlated and strongly correlated liquids; the black squares mark the experimental results obtained from resistivity measurements [18, 31].

system is on the ordered or disordered side of the Fermi-condensate quantum phase transition. It follows from Eqn (2.14) that $\gamma(T) \propto T$ (see also Section 3.5). Hence, at $T \gg T_1(B)$, the temperature-dependent part of the resistivity behaves as $\Delta\rho(T) \propto \gamma(T) \propto T$ in either case, when the electron system is in the highly correlated state or in the strongly correlated state.

We assume that the system becomes superconducting at a certain temperature T_c. In contrast to the jump $\delta C(T_c)$ of the heat capacity at T_c in ordinary superconductors, which is a linear function of T_c, the value of $\delta C(T_c)$ is independent of T_c in our case. Equations (3.28) and (3.29) show that both $\delta C(T_c)$ and the ratio $\delta C(T_c)/C_n(T_c)$ can be very large compared to the corresponding quantities in the ordinary BCS case [70, 134, 135].

Experiments show that the electron system in the heavy-fermion metal $CeCoIn_5$ can be considered a strongly correlated electron liquid. Indeed, for $T > T_1(B)$, the linear thermal expansion coefficient $\alpha(T) \propto$ const and the Grüneisen ratio diverges [136] [see Eqns (8.3) and (8.5)], and we may assume that the entropy is given by (8.1).

A finite magnetic field takes the system to the disordered side of the Fermi-condensate quantum phase transition; for $T < T_1(B)$, the system behaves like a highly correlated liquid with the effective mass given by (7.5). Estimates of δp_{FC} based on calculations of the magnetic susceptibility show that $\delta p_{FC} \approx 0.044$ [134]. We conclude that $B_{cr} \sim 0.01$, as follows from Eqn (5.10), and the electron system of the heavy-fermion metal $CeCoIn_5$ passes, in relatively weak magnetic fields, to the disordered side of the Fermi-condensate quantum phase transition and acquires a behavior characteristic of a highly correlated liquid. We note that the estimated value of δp_{FC} provides an explanation for the relatively large jump $\delta C(T_c)$ [134] observed at $T_c = 2.3$ K in experiments with $CeCoIn_5$ [135].

As Fig. 14a shows, the behavior $A(B) \propto B_H(B) \propto M^*(B) \propto (B-B_{c0})^{-4/3}$ specified by Eqn (7.16) is in good agreement with the experimental results [18, 31]. The coefficient $B_H(B)$ determines the T^2-dependence of the thermal resistance, and the ratio $A(B)/B_H(B)$ is field-independent, with $A/B_H \approx 0.47$ [18, 31]. In the Landau Fermi-liquid regime, the Kadowaki–Woods relation and the Wiedemann–Franz law hold, and the system contains quasiparticles [18, 31, 114, 118]. Thus, we may conclude that our description is in good agreement with the experimental facts.

At low temperatures and in a magnetic field $B_{red} \sim B_{cr}$ [see Eqn (7.16)], the electron system is a Landau Fermi liquid. As the temperature increases, the behavior of the strongly correlated liquid determined by the entropy S_0 is restored at $T^*(B)$, and the effective mass becomes temperature-dependent, according to Eqn (2.14). To calculate $T^*(B)$, we use the fact that the behavior of the effective mass is given by (7.5) for $T < T^*(B)$ and by Eqn (2.14) for $T > T^*(B)$. Since the effective mass cannot change at $T = T^*(B)$, we can estimate $T^*(B)$ by equating these two values of the effective mass, As a result, we obtain

$$T^*(B) \propto (B-B_{c0})^{2/3}\,. \tag{8.10}$$

The function $T^*(B)$ in (8.10) is shown by a dotted line in Fig. 14b. As the magnetic field becomes stronger, $B \gg B_{cr}$, the system becomes a highly correlated liquid in which the behavior of $M^*(T)$ is given by (7.9) and that of $M^*(B)$ by (7.5). Comparison of these two types of behavior yields

$$T^*(B) \propto (B-B_{c0})\,. \tag{8.11}$$

The function $T^*(B)$ in (8.11) is depicted by a light solid line in Fig. 14b. Clearly, both lines match the experimental results.

Using Eqn (8.6) to study the superconducting phase transition, we again conclude that this equation cannot be valid at sufficiently low temperatures, because the behavior of the system in the NFL region is determined by the entropy S_0. Hence, in magnetic fields, a second-order superconducting

phase transition becomes a first-order transition at a certain temperature T_0 [66]. To use Eqn (8.6) to calculate T_0, we must know the entropy of the superconductor in the magnetic field; this entropy was estimated by Volovik [137]. Using Volovik's estimate, we find that $T_0/T_c \sim 0.3$, which agrees with the experimental facts. As shown in Fig. 14, the phase diagram that we constructed agrees with the experimental data.

9. Asymmetric conductivity of strongly correlated metals

The main subjects of investigation in experiments with heavy-fermion metals are the thermodynamic properties. It seems reasonable to study the properties of correlated electron liquids that are determined by the quasiparticle distribution function $n(\mathbf{p}, T)$ and not only by the density of states or by the behavior of the effective mass M^* [138, 139]. Scanning tunnel microscopy and point-contact spectroscopy, being sensitive to the density of states and the function $n(\mathbf{p}, T)$ that determines the probability of population of quasiparticle states, and being closely related to the Andreev scattering [140, 141], are ideal tools for studying the anomalous behavior of strongly correlated Fermi systems, a behavior that is determined by the function $n_0(\mathbf{p}, T)$ and the entropy S_0.

9.1 Normal state

The tunnel current I running through a point contact of two ordinary metals is proportional to the applied voltage V and to the square of the absolute value of the quantum mechanical transition amplitude t times the difference $N_1(0)N_2(0)\big(n_1(p,T) - n_2(p,T)\big)$ [142], where $N_{1,2}(0)$ is the density of states of the respective metals. On the other hand, in the semiclassical approximation, the wave function that determines the amplitude t is proportional to $(N_1(0)N_2(0))^{-1/2}$. Therefore, the density of states drops from the final result and the tunnel current becomes independent of $N_1(0)N_2(0)$. Because the distribution $n(p, T \to 0) \to \theta(p_F - p)$ as $T \to 0$, where $\theta(p_F - p)$ is the step function, it can be verified that the differential tunnel conductivity $\sigma_d(V) = dI/dV$ is a symmetric or even function of V in the Landau Fermi-liquid theory. Actually, the symmetry of $\sigma_d(V)$ is obeyed if there is the hole–quasiparticle symmetry (which is present in the Landau Fermi-liquid theory). Hence, the fact that $\sigma_d(V)$ is symmetric is obvious and is natural in the case of metal–metal contacts for ordinary metals that are in the normal or superconducting state.

We study the tunnel current at low temperatures, which for ordinary metals is given by the expression [141, 142]

$$I(V) = 2|t|^2 \int \big[n(\varepsilon - V) - n(\varepsilon)\big]\, d\varepsilon\,, \tag{9.1}$$

where we use the atomic system of units $e = m = \hbar = 1$ and normalize the transition amplitude to unity, $|t|^2 = 1$. Because the temperatures are low, we can approximate the distribution function $n(\varepsilon)$ by the step function $\theta(\mu - \varepsilon)$; Eqn (9.1) then yields $I(V) = a_1 V$, and hence the differential conductivity $\sigma_d(V) = dI/dV = a_1 = \text{const}$ is a symmetric function of the applied voltage V.

To quantitatively examine the behavior of the asymmetric part of the conductivity $\sigma_d(V)$, we find the derivatives of both sides of Eqn (9.1) with respect to V. The result is the following equation for $\sigma_d(V)$:

$$\sigma_d = \frac{1}{T}\int n\big(\varepsilon(z) - V, T\big)\big(1 - n\big(\varepsilon(z) - V, T\big)\big)\big)\, \frac{\partial \varepsilon}{\partial z}\, dz\,. \tag{9.2}$$

In the integrand in (9.2), we took the dimensionless momentum $z = p/p_F$ instead of ε for the variable, because $n(\varepsilon)$ is no longer a function of ε in the case of a strongly correlated electron liquid; it depends on the momentum as shown in Fig. 1. Indeed, the variable ε in the interval (p_i, p_f) is equal to μ, and the quasiparticle distribution function varies within this interval.

After performing fairly simple transformations in Eqn (9.2), we find that the asymmetric part

$$\Delta\sigma_d(V) = \frac{\sigma_d(V) - \sigma_d(-V)}{2}$$

of the differential conductivity can be expressed as

$$\Delta\sigma_d(V) = \frac{1}{2}\int \frac{\alpha(1-\alpha^2)}{\big[n(z,T) + \alpha\big(1 - n(z,T)\big)\big]^2} \times \frac{\partial n(z,T)}{\partial z}\, \frac{1 - 2n(z,T)}{\big[\alpha n(z,T) + \big(1 - n(z,T)\big)\big]^2}\, dz\,, \tag{9.3}$$

where $\alpha = \exp(-V/T)$.

Asymmetric tunnel conductivity can be observed in measurements involving metals whose electron system contains a Fermi condensate. Among such metals are high-T_c superconductors and heavy-fermion metals, e.g., $YbRh_2(Si_{0.95}Ge_{0.05})_2$), $CeCoIn_5$, and $YbRh_2Si_2$. The measurements must be conducted when the heavy-fermion metal is in the superconducting or normal state. If the metal is in the normal state, measurements of $\Delta\sigma_d(V)$ can be done in a magnetic field $B > B_{c0}$ at temperatures $T^*(B) < T \leqslant T_f$ or in a zero magnetic field at temperatures higher than the corresponding critical temperature when the electron system is in the paramagnetic state and its behavior is determined by the entropy S_0. We note that at a sufficiently low temperature $T < T^*(B)$, the introduction of a magnetic field $B > B_{c0}$ leads to restoration of the Landau Fermi-liquid behavior with $M^*(B)$ determined by Eqn (4.5), and the asymmetric behavior of the differential conductivity disappears [138, 139].

Recent measurements of the differential conductivity in $CeCoIn_5$ done by the point-contact spectroscopy technique [143] have vividly revealed the asymmetry in the differential conductivity in the superconducting ($T_c = 2.3$ K) and normal states. Figure 15 shows the results of these measurements. Clearly, $\sigma_d(V)$ is nearly constant when the heavy-fermion metal is in the superconducting state, experiences no substantial variation near T_c, and then monotonically decreases as the temperature increases [143].

Figure 16 shows the results of calculations of the asymmetric part $\Delta\sigma_d(V)$ of the conductivity $\sigma_d(V)$ in accordance with Eqn (9.3). In calculating the distribution function $n(z, T)$, we used functional (7.13) (with the parameters $\beta = 3$ and $g = 8$). In this case, $(p_f - p_i)/p_F \approx 0.1$. Figure 16 also shows that the asymmetric part $\Delta\sigma_d(V)$ of the conductivity is a linear function of V for small voltages and decreases with increasing the temperature, which agrees with the behavior of the experimental curves in the inset in Fig. 16.

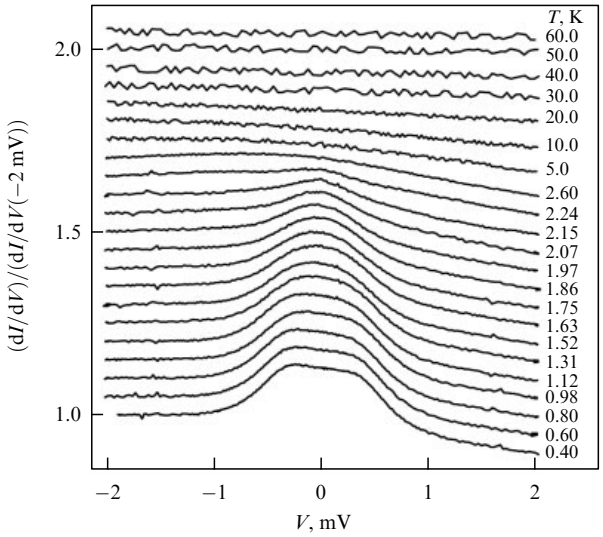

Figure 15. Differential conductivity $\sigma_{\rm d}(V)$ measured in the case of point contacts Au/$CeCoIn_5$. The curves $\sigma_{\rm d}(V)$ are displaced along the vertical axis by 0.05. The conductivity is normalized to its value at $V = -2$ mV. The asymmetry becomes noticeable at $T < 45$ K and increases as the temperature decreases [143].

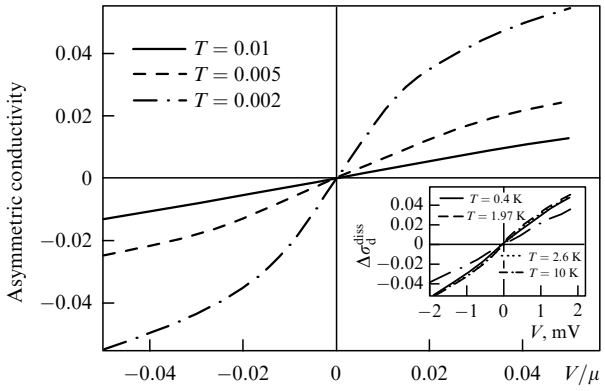

Figure 16. The asymmetric conductivity $\Delta\sigma_{\rm d}(V)$ as a function of V/μ for three values of the temperature T/μ (normalized to μ). The inset shows the behavior of the asymmetric conductivity extracted from the data in Fig. 15.

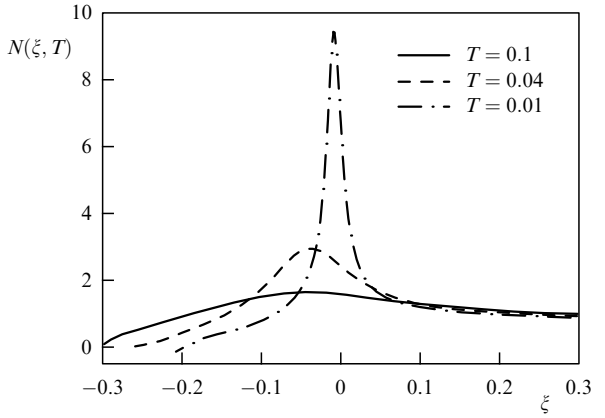

Figure 17. Density of states $N(\xi, T)$ as a function of $\varepsilon = (\varepsilon - \mu)/\mu$, calculated for three values of the temperature T (normalized to μ).

We now derive an estimation formula for analyzing the asymmetric part of the differential conductivity. It follows from Eqn (9.3) that for small values of V, the asymmetric part behaves as $\Delta\sigma_{\rm d}(V) \propto V$. Here, it is appropriate to note that the asymmetric part of the tunnel conductivity is an odd function of V, and therefore $\Delta\sigma_{\rm d}(V)$ must change sign when V changes sign. The natural unit for measuring voltage is $2T$, because this quantity determines the characteristic energy for the Fermi condensate, as shown by Eqn (2.16). Actually, the asymmetric part must be proportional to the size $(p_{\rm f} - p_{\rm i})/p_{\rm F}$ of the region occupied by the Fermi condensate:

$$\Delta\sigma_{\rm d}(V) \approx c\,\frac{V}{2T}\,\frac{p_{\rm f} - p_{\rm i}}{p_{\rm F}} \approx c\,\frac{V}{2T}\,\frac{S_0}{x_{\rm FC}}\,, \tag{9.4}$$

where $S_0/x_{\rm FC} \sim (p_{\rm f} - p_{\rm i})/p_{\rm F}$ is the temperature-independent part of the entropy [see Eqn (8.1)] and c is a constant of the order of unity. This constant can be estimated by using analytically solvable models. For instance, calculations of c in a simple model with the Landau function of the type [24]

$$E\big[n(p)\big] = \int \frac{p^2 n(\mathbf{p})}{2M}\,\frac{{\rm d}\mathbf{p}}{(2\pi)^3} + V_1 \int n(\mathbf{p}) n(\mathbf{p})\,\frac{{\rm d}\mathbf{p}}{(2\pi)^3} \tag{9.5}$$

yield $c \approx 1/2$. It follows from Eqn (9.4) that when $V \approx 2T$ and the Fermi condensate occupies a sizable part of the Fermi volume, $(p_{\rm f} - p_{\rm i})/p_{\rm F} \approx 1$, the asymmetric part becomes comparable to the differential tunnel conductivity $\Delta\sigma_{\rm d}(V) \sim V_{\rm d}(V)$.

9.2 Superconducting state

Tunnel conductivity may remain asymmetric as a high-$T_{\rm c}$ superconductor or a heavy-fermion metal passes into the superconducting state from the normal state. The reason is that the function $n_0(\mathbf{p})$ again determines the differential conductivity. As we saw in Section 3, $n_0(\mathbf{p})$ is not noticeably distorted by the pairing interaction, which is relatively weak compared to the Landau interaction, which forms the distribution function $n_0(\mathbf{p})$. Hence, the asymmetric part of the conductivity remains practically unchanged for $T \leqslant T_{\rm c}$, which agrees with the results of experiments (see Fig. 15). In calculating the conductivity by using the results of measurements done with a tunnel microscope, we must bear in mind that the density of states

$$N_{\rm s}(E) = N(\varepsilon - \mu)\,\frac{E}{\sqrt{E^2 - \Delta^2}} \tag{9.6}$$

determines the conductivity, which is zero for $E \leqslant |\Delta|$. Here, E is the quasiparticle energy given by Eqn (3.5), and $\varepsilon - \mu = \sqrt{E^2 - \Delta^2}$.

Equation (9.6) implies that the tunnel conductivity may be asymmetric if the density of states $N(\varepsilon)$ is asymmetric with respect to the Fermi level [144], as is the case with strongly correlated Fermi systems with a Fermi condensate. Our calculations of the density of states based on model functional (7.13) with the same parameters as those used in calculating $\Delta\sigma_{\rm d}(V)$ shown in Fig. 16 corroborate this conclusion.

Figure 17 shows the results of calculations of the density of states $N(\xi, T)$. Clearly, $N(\xi, T)$ is strongly asymmetric with respect to the Fermi level. If the system is in the superconducting state, the values of the normalized temperature given in the upper right corner of the diagram can be

related to Δ_1. With $\Delta_1 \approx 2T_c$, we find that $2T/\mu \approx \Delta_1/\mu$. Because $N(\xi, T)$ is asymmetric, the first derivative $\partial N(\xi, T)/\partial\xi$ is finite at the Fermi level, and the function $N(\xi, T)$ can be written as $N(\xi, T) \approx a_0 + a_1\xi$ for small values of ξ. The coefficient a_0 contributes nothing to the asymmetric part. Obviously, the value of $\Delta\sigma_d(V)$ is determined by the coefficient $a_1 \propto M^*(\xi = 0)$. In turn, $M^*(\xi = 0)$ is determined by (3.8). As a result, Eqn (9.6) yields

$$\Delta\sigma_d(V) \sim c_1 \frac{V}{|\Delta|} \frac{S_0}{x_{FC}}, \tag{9.7}$$

because $(p_f - p_i)/p_F \approx S_0/x_{FC}$, the energy E is replaced with the voltage V, and $\xi = \sqrt{V^2 - \Delta^2}$. The entropy S_0 here refers to the normal state of a heavy-fermion metal.

Actually, Eqn (9.7) coincides with Eqn (9.4) if we use the fact that the characteristic energy of the superconducting state is determined by Eqn (3.9) and is temperature-independent. In studies of the universal behavior of the asymmetric conductivity, Eqn (9.7) has proved to be more convenient than (9.6). It follows from Eqns (9.4) and (9.7) that measurements of the transport properties (the asymmetric part of the conductivity) allows determining the thermodynamic properties of the normal phase that are related to the entropy S_0. Equation (9.7) clearly shows that the asymmetric part of the differential tunnel conductivity becomes comparable to the differential tunnel conductivity at $V \sim 2|\Delta|$ if the Fermi condensate occupies a substantial part of the Fermi volume, $(p_f - p_i)/p_F \approx 1$. In the case of the d-wave symmetry of the gap, the right-hand side of Eqn (9.7) must be averaged over the gap distribution $\Delta(\phi)$, where ϕ is the angle. This simple procedure amounts to redefining the gap size or the constant c_1. As a result, Eqn (9.7) can also be applied when $V < \Delta_1$, where Δ_1 is the maximum size of the d-wave gap [138]. For the Andreev scattering, where the current is finite for any small value of V, Eqn (9.7) also holds for $V < \Delta_1$ in the case of the s-wave gap.

Low-temperature measurements with tunnel microscopy and spectroscopy techniques were used in [145] to detect an inhomogeneity in the electron density distribution in $Bi_2Sr_2CaCu_2O_{8+x}$. This inhomogeneity manifests itself as spatial variations in the local density of states in the low-energy part of the spectrum and in the size of the superconducting gap. The inhomogeneity observed in the integrated local density of states is not caused by impurities but is inherent in the system. Observation allowed relating the value of the integrated local density of states to the concentration x of local oxygen impurities.

Spatial variations in the differential tunnel conductivity spectrum are shown in Fig. 18. Clearly, the differential tunnel conductivity is highly asymmetric in the superconducting state of $Bi_2Sr_2CaCu_2O_{8+x}$. The differential tunnel conductivity shown in Fig. 18 may be interpreted as measured at different values of $\Delta_1(x)$ but at the same temperature, which allows studying the $\Delta\sigma_d(V)$ dependence on $\Delta_1(x)$.

Figure 19 shows the asymmetric conductivity diagrams obtained from the data in Fig. 18. Clearly, for small values of V, $\Delta\sigma_d(V)$ is a linear function of voltage in accordance with (9.7) and the slope of the respective straight lines $\Delta\sigma_d(V)$ is inversely proportional to the gap size Δ_1. Figure 20 shows the variation in the asymmetric part of the conductivity $\Delta\sigma_d(V)$ as the temperature increases. The measurements were done with $YBa_2Cu_3O_{7-x}/La_{0.7}Ca_{0.3}MnO_3$ at $T_c \approx 30$ K [146]. Clearly, for $T < T_c$ in the region of the linear dependence on

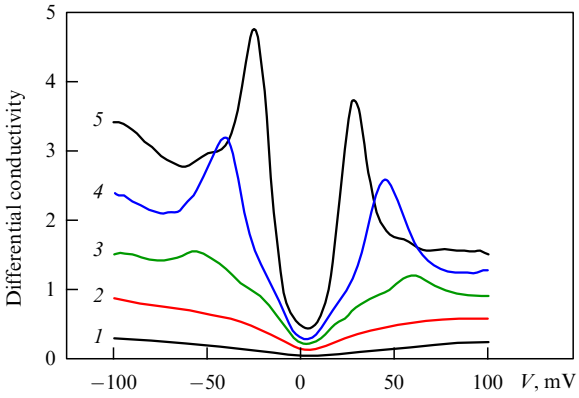

Figure 18. Spatial variation of the spectra of the differential tunnel conductivity measured in $Bi_2Sr_2CaCu_2O_{8+x}$. Lines *1* and *2* belong to regions in which the integrated local density of states is very low. Low differential conductivity and the absence of a gap are indications that we are dealing with an insulator. Line *3* corresponds to a large gap (65 meV) with mildly pronounced peaks. The integrated value of the local density of states for curve *3* is small, but is larger than for lines *1* and *2*. Line *4* corresponds to the gap about 40 meV, which is close to the average value. Line *5* corresponds to the maximum integrated local density of states and the smallest gap about 25 meV, and has two sharp coherent peaks [145].

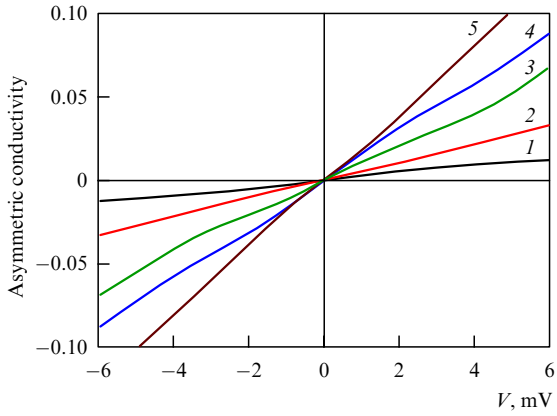

Figure 19. The asymmetric part $\Delta\sigma_d(V)$ of the differential tunnel conductivity in the high-T_c superconductor $Bi_2Sr_2CaCu_2O_{8+x}$, extracted from the data in Fig. 18, as a function of the voltage V. The lines are numbered in accordance with the numbers of the lines in Fig. 18.

V, the asymmetric part $\Delta\sigma_d(V)$ of the conductivity depends only weakly on the temperature; such behavior agrees with (9.7). When $T > T_c$, the slope of the straight lines of sections of the $\Delta\sigma_d(V)$ diagrams decreases as the temperature increases; this behavior is described by Eqn (9.4). We conclude that the description of the universal behavior of $\Delta\sigma_d(V)$ by (9.4) and (9.7) is in good agreement with the results of the experiments presented in Figs 16, 19, and 20.

10. Conclusion

In this review, we have described the effect of a Fermi-condensate quantum phase transition on the properties of various Fermi systems and presented substantial evidence in favor of the existence of such a transition. We have demonstrated that the vast body of experimental facts gathered in studies of various materials, such as high-T_c superconductors, heavy-fermion metals, and correlated 2D

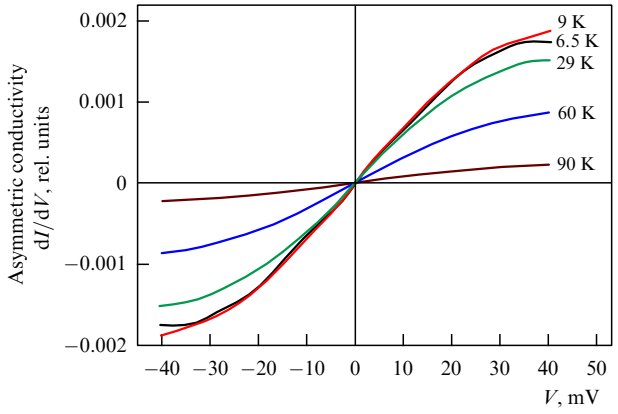

Figure 20. Temperature dependence of the asymmetric part $\Delta\sigma_d(V)$ of the conductivity spectra obtained in measurements for $YBa_2Cu_3O_{7-x}/La_{0.7}Ca_{0.3}MnO_3$ by the contact spectroscopy method; the critical temperature $T_c \approx 30$ K [146].

Fermi structures, can be explained by a theory based on the concept of a Fermi-condensate quantum phase transition. We have found that Fermi systems with a Fermi-condensate quantum phase transition exhibit all the features of a 'quantum protectorate,' while the theory of high-T_c superconductivity based on the Fermi-condensate quantum phase transition provides a description for high T_c and the maximum gap size Δ_1, which can be as large as $\Delta_1 \sim 0.1\varepsilon_F$. We have followed the transition from ordinary superconductors to high-T_c superconductors and, by a simple and yet self-consistent analysis, found that the theory explains the pseudogap state and the general features of variation in the critical temperature $T_c(x)$ as a function of the number density x of mobile charge carriers in high-T_c superconductors.

We have also found that the remarkable results of experiments with high-T_c superconductors in inducing a Landau Fermi liquid by a magnetic field, which in many respects clarified the nature of high-T_c superconductivity, can be explained by our theory. The achieved agreement between theory and experiment allows us to state that the presence of a Fermi-condensate quantum phase transition and the emergence of new quasiparticles with the effective mass strongly dependent on the magnetic field and temperature are properties inherent to the electron (hole) system of high-T_c superconductors.

We have explained the experimental results that point to a divergence of the effective mass in a 2D electron liquid and 2D ^{3}He. We have found that up to the critical point of the Fermi-condensate quantum phase transition, the heavy-fermion liquid behaves like the Landau Fermi liquid at low temperatures. However, the behavior of the heavy-fermion liquid that approaches the Fermi-condensate quantum phase transition from the disordered side may be considered that of a highly correlated liquid because the effective mass of the quasiparticles is large and strongly depends on the density, temperature, and magnetic field.

We have also studied the behavior of a highly correlated electron liquid at various temperatures and in different magnetic fields, constructed the $T-B$ phase diagram, and described the behavior of magnetoresistance. Our results are in good agreement with those of experiments involving heavy-fermion metals whose electron systems are on the disordered side of the Fermi-condensate quantum phase transition.

We have defined a strongly correlated electron liquid as a liquid on the ordered side of the Fermi-condensate quantum phase transition. In contrast to the highly correlated electron liquid, this liquid behaves anomalously at temperatures down to absolute zero, and its entropy contains a temperature-independent term. However, this liquid can be transformed into the Landau Fermi liquid by applying a magnetic field B. The resulting $T-B$ phase diagram agrees well with the experimental $T-B$ phase diagram obtained from measurements involving heavy-fermion metals.

We have shown that in finite magnetic fields, the second-order antiferromagnetic phase transition and the superconducting phase transition are replaced by a first-order phase transition as the temperature decreases. The quantum and thermal critical fluctuations corresponding to second-order phase transitions disappear and have no effect on the behavior of the system at low temperatures, and the low-temperature thermodynamics of heavy-fermion metals is determined by quasiparticles.

We have found that the Grüneisen ratio, as a function of the temperature, diverges as $T \to 0$ and provides an explanation for experiments in which a sharp jump in the Hall coefficient R_H was discovered. We have also demonstrated that the differential conductivity between a metal point contact and a heavy-fermion metal or a high-T_c superconductor can be highly asymmetric. This asymmetry is observed when a strongly correlated metal is in its normal or superconducting state. The above features determine the universal behavior of strongly correlated Fermi systems and are related to the anomalous low-temperature behavior of the entropy, which contains a temperature-independent term.

We have established that in contrast to the physics of ordinary quantum phase transitions, which is determined by the thermal and quantum fluctuations and is characterized by the absence of quasiparticles, the physics of systems with heavy fermions is determined by quasiparticles similar to the Landau quasiparticles. In contrast to the effective mass of the ordinary Landau quasiparticles, the effective mass of the new quasiparticle strongly depends on the temperature, magnetic field, pressure, and other parameters. The quasiparticles and the order parameter are well defined and can be used to describe the universal thermodynamic and transport properties of high-T_c superconductors, heavy-fermion metals, and other correlated Fermi systems. The quasiparticle system determines the conservation of the Kadowaki–Woods relation and the restoration of the Landau Fermi-liquid behavior in a magnetic field.

In the future, the realm of problems should be broadened and certain efforts should be made to describe the macroscopic features of the Fermi condensate, such as the propagation of sonic and shock waves. In addition to the already known materials whose properties not only provide information on the existence of a Fermi condensate but also almost cry aloud about such a condensate, there are other materials of enormous interest as possible objects for studying the phase transition in question. Among such objects are neutron stars, atomic clusters, ultracold gases in traps, nuclei, and quark plasma. Another possible area of research is related to the structure of the nucleon, in which the entire 'sea' of nonvalence quarks may be in the Fermi-condensate state. The combination of quarks and the gluons that hold them together is especially interesting because gluons, quite possibly, can be in the gluon-condensate phase, which could be qualitatively similar to the pion condensate proposed by

A B Migdal long ago. We believe that a Fermi condensate can be observed in traps, where there is the possibility of controlling the emergence of a quantum phase transition accompanied by the formation of a Fermi condensate by changing the particle number density.

Overall, the ideas associated with a new phase transition in one area of research stimulates intensive studies of the possible manifestation of such a transition in other areas. This has happened in the case of metal superconductivity, whose ideas were successfully used in describing atomic nuclei and in a possible explanation of the origin of the mass of elementary particles. This, quite possibly, could be the case with fermion condensation.

Finally, our general discussion shows that the Fermi-condensate quantum phase transition, the emergence of new quasiparticles, and their similarity to Landau quasiparticles constitute the properties inherent in strongly correlated fermion systems. Moreover, the Fermi-condensate quantum phase transition can be considered the universal reason for the non-Fermi-liquid behavior observed in various metals, liquids, and other Fermi systems. Thus, Landau's paradigm based on the concept of quasiparticles and the order parameter proves applicable in examining the low-temperature properties of strongly correlated Fermi systems.

This work was partly supported by the Russian Foundation for Basic Research (Project no. 05-02-16085) and INTAS (Project no. 05-02-16085). M Ya A is grateful for the financial support provided by the Israeli Science Foundation (Project no. 174/03) and the Hebrew University Intramural Funds.

References

1. Stewart G R *Rev. Mod. Phys.* **73** 797 (2001)
2. Varma C M, Nussinov Z, van Saarloos W *Phys. Rep.* **361** 267 (2002)
3. v. Löhneysen H et al. *Rev. Mod. Phys.* (to be published); cond-mat/0606317
4. Vojta M *Rep. Prog. Phys.* **66** 2069 (2003)
5. Belyavsky V I, Kopaev Yu V *Usp. Fiz. Nauk* **176** 457 (2006) [*Phys. Usp.* **49** 441 (2006)]
6. Custers J et al. *Nature* **424** 524 (2003)
7. Senthil T, Fisher M P A *Phys. Rev. B* **62** 7850 (2000)
8. Senthil T, Vojta M, Sachdev S *Phys. Rev. B* **69** 035111 (2004); Senthil T, Sachdev S, Vojta M *Physica B* **359 – 361** 9 (2005)
9. Senthil T et al. *Science* **303** 1490 (2004)
10. Coleman P, in *Lectures on the Physics of Highly Correlated Electron Systems VI* (AIP Conf. Proc., No. 629, Ed. F Mancini) (Melville, NY: American Institute of Physics, 2002) p. 79
11. Coleman P, Schofield A J *Nature* **433** 226 (2005)
12. Küchler R et al. *Phys. Rev. Lett.* **91** 066405 (2003)
13. Gegenwart P et al. *Phys. Rev. Lett.* **89** 056402 (2002)
14. Proust C et al. *Phys. Rev. Lett.* **89** 147003 (2002)
15. Kadowaki K, Woods S B *Solid State Commun.* **58** 507 (1986)
16. Millis A J et al. *Phys. Rev. Lett.* **88** 217204 (2002)
17. Bel R et al. *Phys. Rev. Lett.* **92** 177003 (2004)
18. Paglione J et al. *Phys. Rev. Lett.* **97** 106606 (2006)
19. Ronning F et al. *Phys. Rev. Lett.* **97** 067005 (2006)
20. Koralek J D et al. *Phys. Rev. Lett.* **96** 017005 (2006)
21. Fujimori S et al., cond-mat/0602296
22. Lifshitz E M, Pitaevskii L P *Statisticheskaya Fizika* (Statistical Physics) Pt. 2 (Moscow: Nauka, 1978) [Translated into English (Oxford: Pergamon Press, 1980)]
23. Khodel V A, Shaginyan V R *Pis'ma Zh. Eksp. Teor. Fiz.* **51** 488 (1990) [*JETP Lett.* **51** 553 (1990)]
24. Khodel V A, Shaginyan V R, Khodel V V *Phys. Rep.* **249** 1 (1994)
25. Khodel V A, Clark J W, Zverev M V *Phys. Rev. Lett.* **87** 031103 (2001)
26. Amusia M Ya, Msezane A Z, Shaginyan V R *Yad. Fiz.* **66** 1850 (2003) [*Phys. At. Nucl.* **66** 1802 (2003)]
27. Khodel V A et al. *Pis'ma Zh. Eksp. Teor. Fiz.* **84** 703 (2006) [*JETP Lett.* **84** 588 (2006)]
28. Volovik G E *Acta Phys. Slov.* **56** 49 (2005)
29. Volovik G E, cond-mat/0601372; in *Quantum Simulations via Analogues: From Phase Transitions to Black Holes* (Lecture Notes in Physics) (to be published)
30. Shaginyan V R *Pis'ma Zh. Eksp. Teor. Fiz.* **79** 344 (2004) [*JETP Lett.* **79** 286 (2004)]
31. Paglione J et al. *Phys. Rev. Lett.* **91** 246405 (2003); cond-mat/0405157
32. Landau L D *Zh. Eksp. Teor. Fiz.* **30** 1058 (1956) [*Sov. Phys. JETP* **3** 920 (1956)]
33. Pomeranchuk I Ya *Zh. Eksp. Teor. Fiz.* **35** 524 (1958) [*Sov. Phys. JETP* **8** 361 (1959)]
34. Pfitzner M, Wölfle P *Phys. Rev. B* **33** 2003 (1986)
35. Yakovenko V M, Khodel V A *Pis'ma Zh. Eksp. Teor. Fiz.* **78** 850 (2003) [*JETP Lett.* **78** 398 (2003)]
36. Shaginyan V R *Pis'ma Zh. Eksp. Teor. Fiz.* **77** 104 (2003) [*JETP Lett.* **77** 99 (2003)]
37. Casey A et al. *J. Low Temp. Phys.* **113** 293 (1998)
38. Shashkin A A et al. *Phys. Rev. B* **66** 073303 (2002); *Phys. Rev. Lett.* **91** 046403 (2003)
39. Boronat J et al. *Phys. Rev. Lett.* **91** 085302 (2003)
40. Zhang Y, Yakovenko V M, Das Sarma S *Phys. Rev. B* **71** 115105 (2005)
41. Zhang Y, Das Sarma S *Phys. Rev. B* **70** 035104 (2004)
42. Khodel V A, Shaginyan V R, Zverev M V *Pis'ma Zh. Eksp. Teor. Fiz.* **65** 242 (1997) [*JETP. Lett.* **65** 253 (1997)]
43. Volovik G E *Pis'ma Zh. Eksp. Teor. Fiz.* **53** 208 (1991) [*JETP Lett.* **53** 222 (1991)]
44. Amusia M Ya, Shaginyan V R *Pis'ma Zh. Eksp. Teor. Fiz.* **73** 268 (2001) [*JETP Lett.* **73** 232 (2001)]
45. Amusia M Ya, Shaginyan V R *Phys. Rev. B* **63** 224507 (2001); Shaginyan V R *Physica B* **312 – 313** 413 (2002)
46. Shaginyan V R, Han J G, Lee J *Phys. Lett. A* **329** 108 (2004)
47. Khveshchenko D V, Hlubina R, Rice T M *Phys. Rev. B* **48** 10766 (1993)
48. Dzyaloshinskii I *J. Phys. I* (France) **6** 119 (1996)
49. Lidsky D et al. *Phys. Rev. B* **57** 1340 (1998)
50. Irkhin V Yu, Katanin A A, Katsnelson M I *Phys. Rev. Lett.* **89** 076401 (2002)
51. Laughlin R B, Pines D *Proc. Natl. Acad. Sci. USA* **97** 28 (2000)
52. Anderson P W, cond-mat/0007185; cond-mat/0007287
53. Khodel V A, Clark J W, Shaginyan V R *Solid State Commun.* **96** 353 (1995)
54. Dukelsky J et al. *Z. Phys. B* **102** 245 (1997); Khodel V A, Shaginyan V R *Condens. Matter Theor.* **12** 222 (1997)
55. Artamonov S A, Shaginyan V R *Zh. Eksp. Teor. Fiz.* **119** 331 (2001) [*JETP* **92** 287 (2001)]
56. Bogdanov P V et al. *Phys. Rev. Lett.* **85** 2581 (2000)
57. Kaminski A et al. *Phys. Rev. Lett.* **86** 1070 (2001)
58. Valla T et al. *Science* **285** 2110 (1999); *Phys. Rev. Lett.* **85** 828 (2000)
59. Casey A et al. *Phys. Rev. Lett.* **90** 115301 (2003)
60. Grüner G *Density Waves in Solids* (Frontiers in Physics, Vol. 89) (Reading, Mass.: Addison-Wesley Publ. Co., 1994)
61. Tassini L et al. *Phys. Rev. Lett.* **95** 117002 (2005)
62. Bardeen J, Cooper L N, Schrieffer J R *Phys. Rev.* **108** 1175 (1957)
63. Tilley D R, Tilley J *Superfluidity and Superconductivity* 2nd ed. (Bristol: A. Hilger, 1986)
64. Artamonov S A, Pogorelov Yu G, Shaginyan V R *Pis'ma Zh. Eksp. Teor. Fiz.* **68** 893 (1998) [*JETP Lett.* **68** 942 (1998)]
65. Gor'kov L P *Zh. Eksp. Teor. Fiz.* **34** 735 (1958) [*Sov. Phys. JETP* **7** 505 (1958)]
66. Shaginyan V R et al. *Europhys. Lett.* **76** 898 (2006)
67. Bogoliubov N N *Nuovo Cimento* **7** 794 (1958)
68. Amusia M Ya, Shaginyan V R *Pis'ma Zh. Eksp. Teor. Fiz.* **77** 803 (2003) [*JETP Lett.* **77** 671 (2003)]
69. Matsui H et al. *Phys. Rev. Lett.* **90** 217002 (2003)
70. Amusia M Ya, Artamonov S A, Shaginyan V R *Pis'ma Zh. Eksp. Teor. Fiz.* **74** 435 (2001) [*JETP Lett.* **74** 396 (2001)]
71. Paramekanti A, Randeria M, Trivedi N *Phys. Rev. Lett.* **87** 217002 (2001)
72. Anderson P W et al. *J Phys.: Condens. Matter* **16** R755 (2004)

73. Shaginyan V R *Pis'ma Zh. Eksp. Teor. Fiz.* **68** 491 (1998) [*JETP Lett.* **68** 527 (1998)]
74. Amusia M Ya, Shaginyan V R *Phys. Lett. A* **298** 193 (2002)
75. Kugler M et al. *Phys. Rev. Lett.* **86** 4911 (2001)
76. Abrikosov A A *Phys. Rev. B* **52** R15738 (1995); cond-mat/9912394
77. Yeh N-C et al. *Phys. Rev. Lett.* **87** 087003 (2001)
78. Biswas A et al. *Phys. Rev. Lett.* **88** 207004 (2002)
79. Skinta J A et al. *Phys. Rev. Lett.* **88** 207005 (2002)
80. Skinta J A et al. *Phys. Rev. Lett.* **88** 207003 (2002)
81. Chen C-T et al. *Phys. Rev. Lett.* **88** 227002 (2002)
82. Metoki N et al. *Phys. Rev. Lett.* **80** 5417 (1998)
83. Honma T et al. *J. Phys. Soc. Jpn.* **68** 338 (1999)
84. Kresin V Z, Ovchinnikov Yu N, Wolf S A *Phys. Rep.* **431** 231 (2006); "Erratum" **437** 233 (2007)
85. Amusia M Ya, Shaginyan V R *Pis'ma Zh. Eksp. Teor. Fiz.* **76** 774 (2002) [*JETP Lett.* **76** 651 (2002)]
86. Miyakawa N et al. *Phys. Rev. Lett.* **83** 1018 (1999)
87. Varma C M et al. *Phys. Rev. Lett.* **63** 1996 (1989)
88. Varma C M et al. *Phys. Rev. Lett.* **64** 497 (1990)
89. Ino A et al. *Phys. Rev. B* **65** 094504 (2002)
90. Zhou X J et al. *Nature* **423** 398 (2003)
91. Padilla W J et al. *Phys. Rev. B* **72** 060511(R) (2005)
92. Valla T et al. *Phys. Rev. Lett.* **83** 2085 (1999)
93. Feng D L et al. *Phys. Rev. Lett.* **88** 107001 (2002)
94. Dessau D S et al. *Phys. Rev. Lett.* **66** 2160 (1991)
95. Migdal A B *Teoriya Konechnykh Fermi-Sistem i Svoistva Atomnykh Yader* (Theory of Finite Fermi Systems, and Applications to Atomic Nuclei) 2nd ed. (Moscow: Nauka, 1983) [Translated into English (New York: Interscience Publ., 1967)]
96. Yusof Z M et al. *Phys. Rev. Lett.* **88** 167006 (2002)
97. Nakamae S et al. *Phys. Rev. B* **68** 100502 (2003)
98. Hussey N E et al. *Nature* **425** 814 (2003)
99. Pogorelov Yu G, Shaginyan V R *Pis'ma Zh. Eksp. Teor. Fiz.* **76** 614 (2002) [*JETP Lett.* **76** 532 (2002)]
100. de Llano M, Vary J P *Phys. Rev. C* **19** 1083 (1979); de Llano M, Plastino A, Zabolitzky J G *Phys. Rev. C* **20** 2418 (1979)
101. Zverev M V, Baldo M *J. Phys.: Condens. Matter* **11** 2059 (1999)
102. Shaginyan V R, Msezane A Z, Amusia M Ya *Phys. Lett. A* **338** 393 (2005)
103. Takahashi D et al. *Phys. Rev. B* **67** 180407 (2003)
104. Khodel V A, Schuck P *Z. Phys. B* **104** 505 (1997)
105. Tsujii N, Kontani H, Yoshimura K *Phys. Rev. Lett.* **94** 057201 (2005)
106. Korringa J *Physica* **16** 601 (1950)
107. Zheng G et al. *Phys. Rev. Lett.* **90** 197005 (2003)
108. Kane C L, Fisher M P A *Phys. Rev. Lett.* **76** 3192 (1996)
109. Houghton A, Lee S, Marston J B *Phys. Rev. B* **65** 220503 (2002)
110. Mackenzie A P et al. *Phys. Rev. B* **53** 5848 (1996)
111. Amusia M Ya, Shaginyan V R *Phys. Lett. A* **315** 288 (2003)
112. Morhard K-D et al. *Phys. Rev. B* **53** 2658 (1996)
113. Kravchenko S V, Sarachik M P *Rep. Prog. Phys.* **67** 1 (2004)
114. Ronning F et al. *Phys. Rev. B* **71** 104528 (2005)
115. Pépin C *Phys. Rev. Lett.* **94** 066402 (2005)
116. Bud'ko S L, Morosan E, Canfield P C *Phys. Rev. B* **69** 014415 (2004)
117. Küchler R et al. *Phys. Rev. Lett.* **93** 096402 (2004)
118. Bianchi A et al. *Phys. Rev. Lett.* **91** 257001 (2003)
119. Zhu L et al. *Phys. Rev. Lett.* **91** 066404 (2003)
120. Ishida K et al. *Phys. Rev. Lett.* **89** 107202 (2002)
121. Shaginyan V R *Pis'ma Zh. Eksp. Teor. Fiz.* **77** 208 (2003) [*JETP Lett.* **77** 178 (2003)]
122. Clark J W, Khodel V A, Zverev M V *Phys. Rev. B* **71** 012401 (2005); Zverev M V, Khodel V A *Pis'ma Zh. Eksp. Teor. Fiz.* **79** 772 (2004) [*JETP Lett.* **79** 635 (2004)]
123. Khodel V A, Shaginyan V R *Nucl. Phys. A* **555** 33 (1993)
124. Landau L D, Lifshitz E M *Statisticheskaya Fizika* (Statistical Physics) Pt. 1 (Moscow: Nauka, 1976) [Translated into English (Oxford: Pergamon Press, 1980)]
125. Shaginyan V R *Pis'ma Zh. Eksp. Teor. Fiz.* **80** 294 (2004) [*JETP Lett.* **80** 263 (2004)]
126. Clark J W et al. *Phys. Rep.* **391** 123 (2004)
127. Amusia M Ya, Msezane A Z, Shaginyan V R *Phys. Lett. A* **320** 459 (2004)
128. Zverev M V et al. *Pis'ma Zh. Eksp. Teor. Fiz.* **65** 828 (1997) [*JETP Lett.* **65** 863 (1997)]
129. Nozières P *J. Phys. I* (France) **2** 443 (1992)
130. Sereni J G et al., cond-mat/0602588
131. Paschen S et al. *Nature* **432** 881 (2004)
132. Shaginyan V R, Popov K G, Artamonov S A *Pis'ma Zh. Eksp. Teor. Fiz.* **82** 234 (2005) [*JETP Lett.* **82** 215 (2005)]
133. Gegenwart P et al. *Phys. Rev. Lett.* **94** 076402 (2005)
134. Khodel V A, Zverev M V, Yakovenko V M *Phys. Rev. Lett.* **95** 236402 (2005)
135. Bauer E D et al. *Phys. Rev. Lett.* **93** 147005 (2004)
136. Oeschler N et al. *Phys. Rev. Lett.* **91** 076402 (2003)
137. Volovik G E *Pis'ma Zh. Eksp. Teor. Fiz.* **65** 465 (1997) [*JETP Lett.* **65** 491 (1997)]
138. Shaginyan V R *Pis'ma Zh. Eksp. Teor. Fiz.* **81** 283 (2005) [*JETP Lett.* **81** 222 (2005)]
139. Shaginyan V R, Popov K G *Phys. Lett. A* **361** 406 (2007)
140. Andreev A F *Zh. Eksp. Teor. Fiz.* **46** 1823 (1964) [*Sov. Phys. JETP* **19** 1228 (1964)]
141. Deutscher G *Rev. Mod. Phys.* **77** 109 (2005)
142. Zagoskin A M *Quantum Theory of Many-Body Systems*: *Techniques and Applications* (New York: Springer, 1998)
143. Park W K et al. *Phys. Rev. B* **72** 052509 (2005)
144. Anderson P W, Ong N P, cond-mat/0405518; Randeria M et al., cond-mat/0412096
145. Pan S H et al. *Nature* **413** 282 (2001)
146. Piano S et al. *J. Phys.: Conf. Ser.* **43** 1123 (2006)